



UNIVERSIDAD DE INVESTIGACIÓN DE TECNOLOGÍA EXPERIMENTAL YACHAY

Escuela de Ciencias Matemáticas y Computacionales

**TÍTULO: Biometric system based on electroencephalogram
analysis**

Trabajo de integración curricular presentado como requisito para
la obtención del título de Ingeniero en Tecnologías de la
Información

Autor:

Carrión Ojeda Dustin Javier

Tutor:

Ph.D. Pineda Arias Israel Gustavo

Co-tutor:

Ph.D. Fonseca Delgado Rigoberto Salomón

Urququí, agosto 2020

SECRETARÍA GENERAL
(Vicerrectorado Académico/Cancillería)
ESCUELA DE CIENCIAS MATEMÁTICAS Y COMPUTACIONALES
CARRERA DE TECNOLOGÍAS DE LA INFORMACIÓN
ACTA DE DEFENSA No. UITEY-ITE-2020-00030-AD

A los 14 días del mes de septiembre de 2020, a las 14:00 horas, de manera virtual mediante videoconferencia, y ante el Tribunal Calificador, integrado por los docentes:

Presidente Tribunal de Defensa	Dr. CUENCA PAUTA, ERICK EDUARDO , Ph.D.
Miembro No Tutor	Dr. IZA PAREDES, CRISTHIAN RENE , Ph.D.
Tutor	Dr. PINEDA ARIAS, ISRAEL GUSTAVO , Ph.D.

El(la) señor(ita) estudiante CARRION OJEDA, DUSTIN JAVIER, con cédula de identidad No. 0705786945, de la ESCUELA DE CIENCIAS MATEMÁTICAS Y COMPUTACIONALES, de la Carrera de TECNOLOGÍAS DE LA INFORMACIÓN, aprobada por el Consejo de Educación Superior (CES), mediante Resolución RPC-SO-43-No.496-2014, realiza a través de videoconferencia, la sustentación de su trabajo de titulación denominado: BYOMETRIC SYSTEM BASED ON ELECTROENCEPHALOGRAM ANALYSIS, previa a la obtención del título de INGENIERO/A EN TECNOLOGÍAS DE LA INFORMACIÓN.

El citado trabajo de titulación, fue debidamente aprobado por el(los) docente(s):

Tutor	Dr. PINEDA ARIAS, ISRAEL GUSTAVO , Ph.D.
--------------	---

Y recibió las observaciones de los otros miembros del Tribunal Calificador, las mismas que han sido incorporadas por el(la) estudiante.

Previamente cumplidos los requisitos legales y reglamentarios, el trabajo de titulación fue sustentado por el(la) estudiante y examinado por los miembros del Tribunal Calificador. Escuchada la sustentación del trabajo de titulación a través de videoconferencia, que integró la exposición de el(la) estudiante sobre el contenido de la misma y las preguntas formuladas por los miembros del Tribunal, se califica la sustentación del trabajo de titulación con las siguientes calificaciones:

Tipo	Docente	Calificación
Miembro Tribunal De Defensa	Dr. IZA PAREDES, CRISTHIAN RENE , Ph.D.	10,0
Tutor	Dr. PINEDA ARIAS, ISRAEL GUSTAVO , Ph.D.	10,0
Presidente Tribunal De Defensa	Dr. CUENCA PAUTA, ERICK EDUARDO , Ph.D.	9,0

Lo que da un promedio de: **9.7 (Nueve punto Siete)**, sobre 10 (diez), equivalente a: **APROBADO**

Para constancia de lo actuado, firman los miembros del Tribunal Calificador, el/la estudiante y el/la secretario ad-hoc.

Certifico que en cumplimiento del Decreto Ejecutivo 1017 de 16 de marzo de 2020, la defensa de trabajo de titulación (o examen de grado modalidad teórico práctica) se realizó vía virtual, por lo que las firmas de los miembros del Tribunal de Defensa de Grado, constan en forma digital.

DUSTIN JAVIER CARRION OJEDA
 Firmado digitalmente por DUSTIN JAVIER CARRION OJEDA
 Fecha: 2020.10.20 15:58:08 -05'00'

CARRION OJEDA, DUSTIN JAVIER
Estudiante

ERICK EDUARDO CUENCA PAUTA
 Signature numérique de ERICK EDUARDO CUENCA PAUTA
 Date : 2020.09.14 17:55:28 -05'00'

Dr. CUENCA PAUTA, ERICK EDUARDO , Ph.D.
Presidente Tribunal de Defensa



Firmado: «IsraelGustavo» por:

**ISRAEL
GUSTAVO
PINEDA ARIAS**

Dr. PINEDA ARIAS, ISRAEL GUSTAVO , Ph.D.

Tutor

CRISTHIAN RENE

Digitally signed by CRISTHIAN
RENE IZA PAREDES

IZA PAREDES

Date: 2020.09.14 18:08:14 -05'00'

Dr. IZA PAREDES, CRISTHIAN RENE , Ph.D.

Miembro No Tutor

**DAYSY MARGARITA
MEDINA BRITO**

Firmado digitalmente por DAYSY
MARGARITA MEDINA BRITO
Fecha: 2020.09.14 17:11:48 -05'00'

MEDINA BRITO, DAYSY MARGARITA

Secretario Ad-hoc

Autoría

Yo, **DUSTIN JAVIER CARRIÓN OJEDA**, con cédula de identidad 0705786945, declaro que las ideas, juicios, valoraciones, interpretaciones, consultas bibliográficas, definiciones y conceptualizaciones expuestas en el presente trabajo; así cómo, los procedimientos y herramientas utilizadas en la investigación, son de absoluta responsabilidad de el/la autor (a) del trabajo de integración curricular. Así mismo, me acojo a los reglamentos internos de la Universidad de Investigación de Tecnología Experimental Yachay.

Urcuquí, agosto 2020.



Dustin Javier Carrión Ojeda

CI: 0705786945

Autorización de publicación

Yo, **DUSTIN JAVIER CARRIÓN OJEDA**, con cédula de identidad 0705786945, cedo a la Universidad de Investigación de Tecnología Experimental Yachay, los derechos de publicación de la presente obra, sin que deba haber un reconocimiento económico por este concepto. Declaro además que el texto del presente trabajo de titulación no podrá ser cedido a ninguna empresa editorial para su publicación u otros fines, sin contar previamente con la autorización escrita de la Universidad.

Asimismo, autorizo a la Universidad que realice la digitalización y publicación de este trabajo de integración curricular en el repositorio virtual, de conformidad a lo dispuesto en el Art. 144 de la Ley Orgánica de Educación Superior

Urcuquí, agosto 2020.



Dustin Javier Carrión Ojeda

CI: 0705786945

Dedication

*To my parents for always support my goals and dreams and for always believe in me.
To my sister for always being there for anything I need.*

Acknowledgements

Thanks to my family for being my support during all this amazing journey. Especially my parents and sister, who, despite the distance, have always cared for and motivated me.

Thanks to Rigoberto Fonseca for being not just a professor but also a friend and mentor who guided me through all this work and for being the one who introduces me to artificial intelligence research.

Thanks to Israel Pineda for pushing me to do a better work and always being there to answer any question I had.

Thanks to all the professors who have become my friends for always being willing to help me.

Thanks to all my friends for making the university my second home, for motivating me in difficult times, for all the happy moments and for teaching me to always believe in myself.

Resumen

Actualmente la búsqueda de nuevos rasgos biométricos es una necesidad debido a que los rasgos tradicionales como huella dactilar, voz o rostro, son altamente propensos a falsificaciones. Por tal motivo, el estudio de señales bioeléctricas llama la atención por su potencial para desarrollar sistemas biométricos. Una motivación para utilizar señales electroencefalográficas es que son únicas para cada persona y son mucho más difíciles de replicar que los biométricos convencionales. El presente estudio está enfocado en el desarrollo de un sistema biométrico basado en el análisis de electroencefalogramas (EEG). Empleando seis clasificadores distintos: Clasificador ingenuo de Bayes (GNB), K-vecinos más cercanos (KNN), Bosque aleatorio (RF), AdaBoost (AB), Máquina de vectores de soporte (SVM) y Perceptrón multicapa (MLP); se realizó una comparación entre diferentes niveles de descomposición de la transformada discreta de ondícula, utilizada como método de preprocesamiento. Demostrando que el nivel de descomposición no posee un gran impacto sobre el resultado general del sistema. Posteriormente se analizó el efecto del tiempo de grabación de los EEGs sobre el desempeño del sistema, probando que este tiempo es un factor altamente influyente del desempeño general. Cabe mencionar que, durante este estudio, se utilizaron dos conjuntos de datos distintos. Finalmente, SVM y AB fueron los mejores clasificadores ya que obtuvieron valores de sensibilidad, especificidad y precisión superiores a 95%.

Palabras clave: Biométrico, electroencefalograma, nivel de descomposición, tiempo de grabación, clasificación, transformada discreta de ondícula.

Abstract

Searching for new biometric traits is currently a necessity because traditional biometrics such as fingerprint, voice, or face are highly prone to forgery. For this reason, the study of bioelectric signals is outstanding for its potential to develop biometric systems. A motivation for using EEG signals is that they are unique to each person and are much more difficult to replicate than conventional biometrics. The present study is focused on the development of a biometric system based on the analysis of electroencephalograms (EEG). Using six different classifiers: Gaussian Naïve Bayes Classifier (GNB), K-Nearest Neighbors (KNN), Random Forest (RF), AdaBoost (AB), Support Vector Machine (SVM) and Multilayer Perceptron (MLP); a comparison was made between different levels of decomposition of the discrete wavelet transform, used as a preprocessing method. This comparison proved that the level of decomposition does not have a great impact on the overall result of the system. Subsequently, the effect of the recording time of the EEGs on the performance of the system was analyzed, proving that this time is a highly influential factor in overall performance. It is worth mentioning that, during this study, two different data sets were used. Finally, SVM and AB were the best classifiers since they obtained values of sensitivity, specificity, and accuracy greater than 95%.

Keywords: Biometric, electroencephalogram, level of decomposition, recording time, classification, discrete wavelet transform.

Contents

1 INTRODUCTION	8
1.1 Problem Statement	8
1.2 Objectives	9
1.2.1 General Objective	9
1.2.2 Specific Objectives	10
1.3 Contribution	10
1.4 Document Organization	10
2 THEORETICAL FRAMEWORK.....	11
2.1 Biometric Systems	11
2.1.1 Requirements of a Biometric System	12
2.1.2 Fingerprint	13
2.1.3 Face.....	13
2.1.4 Voice.....	14
2.1.5 Signature.....	15
2.1.6 Hand Geometry	16
2.1.7 Iris.....	17
2.1.8 Palm Print	18
2.1.9 Ear.....	18
2.1.10 Bioelectrical Signals	19
2.1.10.1 Galvanic Skin Response.....	20
2.1.10.2 Electromyogram	20
2.1.10.3 Electrooculogram	21
2.1.10.4 Electrocardiogram	22
2.2 Electroencephalogram Signals.....	24
2.2.1 Preprocessing.....	27
2.2.2 Feature Extraction.....	30
2.2.3 Classification Algorithms	32
2.3 Summary.....	37
3 METHODS.....	38
3.1 General Workflow of the Proposed Biometric System	38
3.2 Data Acquisition	38
3.2.1 DEAP Dataset.....	39
3.2.2 INAOE Dataset.....	39
3.3 Data Preprocessing	40
3.4 Feature Extraction.....	42
3.5 Classification	43
3.5.1 Hyperparameter Optimization	43
3.6 Data Analysis	45

3.6.1	Performance Metrics.....	45
3.6.2	Validation of Experiments.....	46
3.6.3	Experiments Description	47
3.6.3.1	Assessment of Levels of DWT.....	47
3.6.3.2	Assessment of Different Recording Times Systematically Selected	48
3.6.3.3	Assessment of Different Recording Times Randomly Selected	49
3.7	Summary.....	50
4	RESULTS.....	51
4.1	Assessment of Levels of DWT	51
4.1.1	Results with DEAP Dataset.....	51
4.1.2	Results with INAOE Dataset.....	54
4.2	Assessment of Different Recording Times Systematically Selected.....	58
4.2.1	Results with DEAP Dataset.....	58
4.2.2	Results with INAOE Dataset.....	61
4.3	Assessment of Different Recording Times Randomly Selected.....	65
4.3.1	Results with DEAP Dataset.....	65
4.3.2	Results with INAOE Dataset.....	65
4.4	Comparison of the Proposed System	65
4.5	Summary.....	67
5	CONCLUSIONS AND FUTURE WORK.....	69
	REFERENCES	71
	APPENDICES.....	87
A	Results of the Assessment of Different Recording Times Systematically Selected	87
B	Results of the Assessment of Different Recording Times Randomly Selected ..	92

List of Figures

1	Classification of biometric systems based on their origin	12
2	Types of ridges in a fingerprint	13
3	Representation of traditional local descriptors.....	14
4	Heatmap of Mel Frequency Cepstral Coefficients extracted from an audio file ..	15
5	Representation of signature recognition systems.....	15
6	Traditional scanner and measurements for hand geometry recognition	16
7	Important features of the iris	17
8	Principal features of palm prints	18
9	Automatic ear extraction process	19
10	Bioelectrical signals	19
11	Galvanic skin response measurement	20
12	Measurement of Electromyogram.....	21
13	Electrooculogram acquisition system	22
14	Parts of electrocardiogram signal.....	23
15	The 10-20 system of electrode placement for EEG recording.....	24
16	The wave shape of brain rhythms	25
17	Workflow of the proposed biometric system.....	38
18	Example of discrete wavelet transform with five levels of decomposition	41
19	Validation process representation	47
20	General classification process	48
21	Flowchart for the assessment of levels of DWT	48
22	Flowchart for the assessment of different recording times systematically selected	49
23	Flowchart for the assessment of different recording times randomly selected.....	49
24	Sensitivity of the classifiers using different decomposition levels with the DEAP dataset.....	53
25	Specificity of the classifiers using different decomposition levels with the DEAP dataset.....	53
26	Accuracy of the classifiers using different decomposition levels with the DEAP dataset.....	53
27	Sensitivity of the classifiers using different decomposition levels with the INAOE dataset.....	56
28	Specificity of the classifiers using different decomposition levels with the INAOE dataset.....	57
29	Accuracy of the classifiers using different decomposition levels with the INAOE dataset.....	57

30	ROC curve of all classifiers using 0.25 and 60 seconds of recording time of the DEAP dataset	59
31	Sensitivity of the classifiers grouped by recording time using the DEAP dataset.	59
32	Specificity of the classifiers grouped by recording time using the DEAP dataset.	59
33	Accuracy of the classifiers grouped by recording time using the DEAP dataset...	60
34	ROC curve of all classifiers using 0.25 and 2.5 seconds of recording time of the INAOE dataset	62
35	Sensitivity of the classifiers grouped by recording time using the INAOE dataset	62
36	Specificity of the classifiers grouped by recording time using the INAOE dataset	63
37	Accuracy of the classifiers grouped by recording time using the INAOE dataset.	63

List of Tables

1	Comparison of biometric traits.....	23
2	General information of brain rhythms.....	26
3	Comparison of preprocessing techniques for EEG data	28
4	Comparison of feature extraction and classification techniques for EEG data.....	34
5	Set of values for hyperparameter optimization, and best value for each dataset ..	44
6	Results of the assessment of different levels of DWT using the DEAP dataset ...	52
7	Resulting p-values of Hotelling's T^2 tests between different levels of DWT using the DEAP dataset	54
8	Results of the assessment of different levels of DWT using the INAOE dataset .	55
9	Resulting p-values of Hotelling's T^2 tests between different levels of DWT using the INAOE dataset	57
10	Resulting p-values of Hotelling's T^2 tests between the results of each time segment and 60 seconds using the DEAP dataset	60
11	Resulting p-values of Hotelling's T^2 tests between the performance of the classifiers with 40 seconds of recording using the DEAP dataset	61
12	Resulting p-values of Hotelling's T^2 tests between the results of each time segment and 2.5 seconds using the INAOE dataset	64
13	Resulting p-values of Hotelling's T^2 tests between the performance of the classifiers with 1.75 seconds of recording using the INAOE dataset	64
14	Comparison of the present study with previous works related to biometric systems based on EEG analysis	66
15	Results of the assessment of different recording times systematically selected using DEAP dataset	87
16	Results of the assessment of different recording times systematically selected using INAOE dataset	90
17	Results of the assessment of different recording times randomly selected using DEAP dataset	92
18	Results of the assessment of different recording times randomly selected using INAOE dataset	95

List of Acronyms

AAC	Average Amplitude Change
AB	AdaBoost
ACS	Autocovariance Sequence
ANN	Artificial Neural Networks
API	Application Programming Interface
AR	Autoregressive
ARMA	Autoregressive Moving Average
ASM	Active Shape Model
BCI	Brain-Computer Interface
BSS	Blind Source Separation
CNN	Convolutional Neural Network
CSP	Common Spatial Patterns
DFA	Discriminant Function Analysis
DFT	Discrete Fourier Transform
DWT	Discrete Wavelet Transform
ECG	Electrocardiogram
EEG	Electroencephalogram
EMG	Electromyogram
EOG	Electrooculogram
FA	Fuzzy ARTMAP
FAR	False Acceptance Rate
FFT	Fast Fourier Transform
FIR	Finite Impulse Response
FRR	False Rejection Rate
FT	Fourier Transform
GBSP	Gamma-band Spectral Power
GNB	Gaussian Naive Bayes
GSR	Galvanic Skin Response
HMM	Hidden Markov Models

ICA	Independent Component Analysis
IIEG	Integrated Electroencephalogram
INAOE	Instituto Nacional de Astrofísica, Óptica y Electrónica
JADE	Joint Approximate Diagonalization of Eigen-matrices
KNN	K-Nearest Neighbors
LBP	Local Binary Patterns
LDA	Linear Discriminant Analysis
LGB	Late Gamma Band
LMS	Least Mean Square
LVQ	Learning Vector Quantizer
MANOVA	Multivariate Analysis of Variance
MAV	Mean Absolute Value
MFCC	Mel Frequency Cepstral Coefficients
MLP	Multilayer Perceptron
PCA	Principal Component Analysis
PLS	Partial Least Squares
PSD	Power Spectral Density
QDA	Quadratic Discriminant Analysis
RF	Random Forest
RMS	Root Mean Square
ROC	Receiver Operating Characteristic
SFA	Simplified Fuzzy ARTMAP
SIFT	Scale-invariant Feature Transform
SOBI	Second-order Blind Inference
SOM	Self-Organized Maps
SSI	Simple Square Integral
SVM	Support Vector Machine
VEP	Visual Evoked Potential
WPD	Wavelet Packet Decomposition
WT	Wavelet Transform

1 Introduction

With the rapid development of technologies, biometric systems are present in many daily scenarios to provide security to data [1]. Nowadays, most smartphones have at least one embedded biometric system, usually fingerprint or face recognition. However, biometrics is also applied in situations that require much more security, such as in banks, to ensure access to each account of the clients [2].

Currently, there are many types of biological traits used in the development of biometric systems. Nevertheless, many of them are susceptible to brute force attacks, forgery, or direct forcing on users [3, 4]. Also, a constant problem of most biometrics is that they cannot guarantee that the user is alive [5]. For this reason, the study of bioelectric signals used as biometric features has become a topic of interest because these signals are capable of overcoming the problem mentioned above [6, 7].

Among the bioelectric signals are electroencephalograms (EEG). Traditionally, these signals have been used mostly in medicine to make diagnoses regarding problems associated with the brain [8, 9]. One of the most important characteristics of these signals is that they are unique to each person, and any sudden change in the behavior of the person can cause significant changes in signal morphology [10]. These characteristics of EEG signals make them potential traits for the development of biometric systems.

Despite the advantages of bioelectric signals, the development of biometric systems based on them can be complex. In the case of EEGs, a preprocessing of the signals before working with them is required because they are very noisy [11-13]. After preprocessing, the state-of-the-art proposes a large number of features that can be extracted from these signals and many classification algorithms that can be used for this task [14-17]. Still, creating a functional methodology for the development of biometric systems based on EEG analysis is necessary for progress in this research area.

1.1 Problem Statement

The development of new technologies has caused the parallel development of security systems. Biometrics are of particular interest because of the need to generate systems that

are robust to possible further attacks such as those based on artificial intelligence. The research of novel biological traits helps to create biometrics that meets the security requirements of specific situations such as protecting a bank vault or blocking access to confidential documents [18]. Over the past few years, electroencephalogram signals have attracted the attention of researchers because of their properties as a biometric trait.

Despite the existence of studies on the development of biometric systems based on EEGs, it is still necessary to carry out specific analyzes to improve the future development of these biometrics. In this sense, there is a need for a comparison between classifiers based on different criteria, such as distance, statistics, decision trees, among others, using the same data for training and testing.

Moreover, there are several EEG preprocessing techniques, but finding a specific analysis of each technique is challenging. For example, it is common to use the discrete wavelet transform, but comparisons between possible variations of this technique are still lacking. One of these variations that can have a significant impact on the overall performance of the system is the level of decomposition because the lower this level is, the lower the computational cost.

Finally, a study that has not been carried out and that would be of great help for developing better biometrics is the analysis of the effect that the recording time of EEG has on the performance of classifiers. This analysis would provide a better idea of how much recording time is required to achieve a robust system. Currently, the recording time used varies from research to research, making it difficult to make comparisons between the proposed methods.

1.2 Objectives

For finding a solution to the problems described in Section 1.1, this work establishes the following general objective and specific objectives.

1.2.1 General Objective

Developing a biometric system based on the analysis of EEG signals taking into consideration some of the factors that can affect the performance of the system to helping the improvement of the future development of these systems.

1.2.2 Specific Objectives

- To compare different classification algorithms for identifying the best one for developing this kind of biometric system.
- To analyze the impact that the level of decomposition of the discrete wavelet transform has over the performance of the classifiers and selecting the best level for this specific scenario.
- To analyze the impact that the recording time of EEG has over the performance of the classifiers and proposing a standard time for future studies.
- To develop a biometric system based on EEG signals using the results obtained in the previous analyzes.

1.3 Contribution

This work presents a specific analysis of the discrete wavelet transform as a preprocessing method. Besides, it provides a first study of the impact that recording time has over the classifiers. During the whole process, a comparison is made between different classification algorithms to select the most suitable for developing these systems. The main contribution of this study is the detailed analysis of some fundamental parts in the biometric systems development process that will improve the understanding of the factors that can affect the performance of the system. Based on the results obtained in this research, the scientific article entitled "A method for studying how much time of EEG recording is needed to have a good user identification" [19] was presented in the "6th IEEE Latin American Conference on Computational Intelligence (LA-CCI)". Moreover, a scientific poster was exhibited at the conference "LatinX in AI Research at NeurIPS."

1.4 Document Organization

The organization of this document is as follows: Chapter 2 presents a review of the most commonly used biometric traits. After that, it describes all the essential concepts related to electroencephalogram signals required for this work, and in the end, it presents a brief review of the state of the art and related works. Chapter 3 presents in detailed each part of the proposed biometric system. Moreover, in this chapter, the performance metrics and the description of the experiments are presented. Chapter 4 shows the experimental results with their analysis, and finally, the conclusions and the proposed future work are presented in Chapter 5.

2 Theoretical Framework

This chapter presents the necessary background of the essential topics needed for understanding the contents of this research. First, it provides an introduction of biometric systems and those fundamental requirements of good biometric traits. Subsequently, it presents a summary of the main biometric systems. Moreover, this chapter introduces the key points related to electroencephalogram signals. These signals require a preprocessing step before working with them; therefore, this chapter also explains the most popular preprocessing techniques. Finally, the most commonly used feature extraction and classification algorithms are summarized.

2.1 Biometric Systems

For many years, humans have been used specific characteristics of the body like face or voice to distinguish each other. Even the police use body features like fingerprints to identify criminals. In this case, when the police find a fingerprint on a crime scene, they compare it with a fingerprint database until they find a match [20]. For this reason, a biometric system is a pattern recognition algorithm that extracts specific characteristics from users to identify or verify their identity, comparing these characteristics against a database [21].

A biometric system can tackle two different tasks: Identification and Verification. On the one hand, an identification system, often called a recognition system, tries to recognize to which user the extracted features belong, making a one-to-many comparison with the database [21]. For this reason, the user does not need to provide an identity.

On the other hand, the verification systems are also known as authentication systems because, as its name indicates, its purpose is to verify the users are whom they claim they are. The verification performs a one-to-one comparison with already stored templates of each user [22]. Generally, a username, a PIN, a voice recording, or any other identification is provided by a user who wants to be recognized.

By its origin, the biometric systems can be divided into biometrics based on physiological and behavioral features. Figure 1 shows this classification. Some physiological features

are fingerprints, hand geometry, DNA, and face, while behavioral are voice, keystroke, or signature [23]. Despite this classification, all biometric systems rely on something the user: *know* (e.g., PIN), *has* (e.g., credential card), *does* (e.g., signature), or *is* (e.g., face).

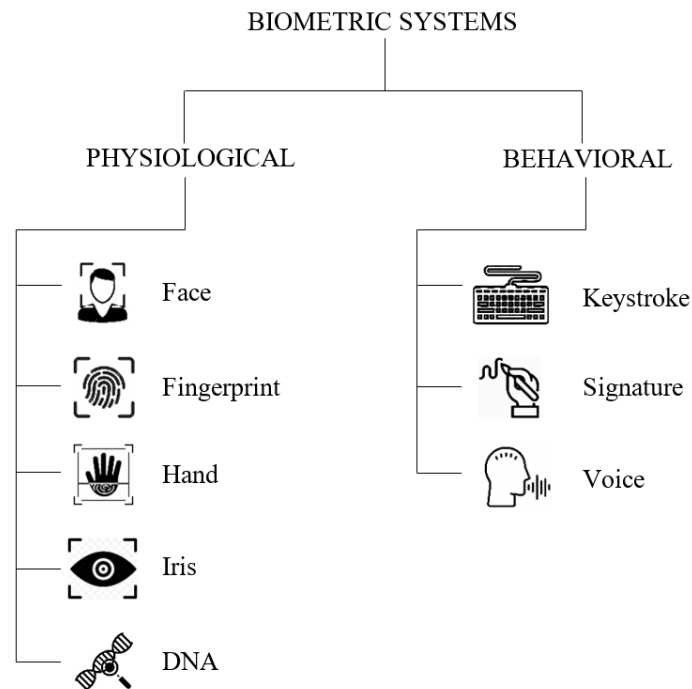


Figure 1: Classification of biometric systems based on their origin [24].

2.1.1 Requirements of a Biometric System

Although most of the biometric traits correspond to biological measurements, an ideal biometric should satisfy the following requirements [25]:

- Universality: each system user must have this biometric trait.
- Distinctiveness or uniqueness: the features of two different users must vary sufficiently to be correctly identified.
- Permanence: the time, position, and space must not affect the extracted characteristics.
- Collectability: it corresponds to how easy it is to measure the trait quantitatively.
- Performance: it refers to the recognition speed and accuracy of the system.
- Acceptability: it is related to how much the users of the system will accept the extraction of the specific biometric trait.
- Circumvention: it is related to how easy it is to fool the system.

Some of the most known traditional biometric methods are discussed below.

2.1.2 Fingerprint

Fingerprints are graphical patterns of ridges and valleys on the surface of the fingertips. Figure 2 illustrates the different types of ridges. The ridge ending and bifurcation are also known as minutiae, which is one of the most used features to develop biometric systems [26]. These features are processed and stored in a database for posterior comparisons.

Fingerprint recognition exhibits uniqueness and permanence because the fingerprints do not suffer changes over the lifetime and are unique even for identical twins [27]. Nevertheless, this technique has problems with the circumvention and universality because using some glue to copy the fingerprint of a person can fool the system [28]. Besides, people who have lost their hands or fingers cannot use this kind of system. For this reason, currently, these biometric systems are employed in applications that do not need to be extremely secure such as smartphones unblocking.

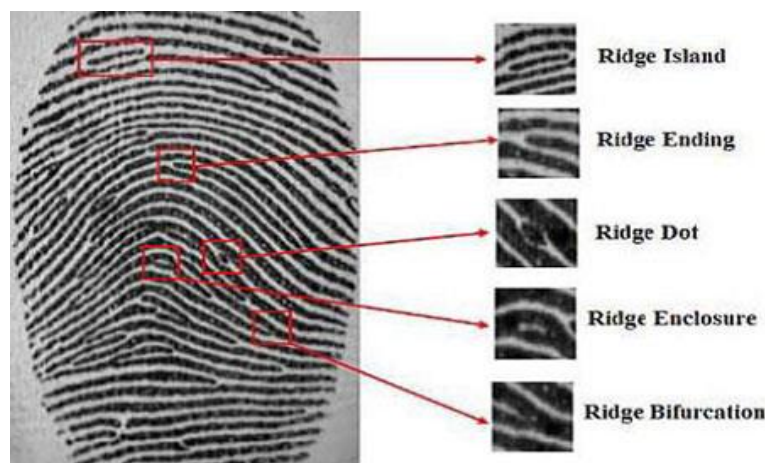


Figure 2: Types of ridges in a fingerprint [29].

2.1.3 Face

Face recognition has been one of the most extensively studied topics in computer vision. There are many applications for face recognition like the automatic classification of photographs in social networks, robotics, and digital entertainment [30]. Moreover, thanks to the quick development of smartphones, they tend to incorporate face recognition as a biometric system. However, this is not the only market for face recognition. Thanks to all the effort of researchers and the advance in deep learning [31], several applications support face recognition as a biometric system, for example, banks and other companies that require a high level of security.

The accuracy of the systems relies on the quality of the face representations. Traditional face recognition systems use local descriptors as Local Binary Patterns (LBP), Eigenfaces, Scale-invariant feature transform (SIFT), among others [32]; Figure 3 shows these conventional face representations. Researchers are currently trying to develop convolutional neural networks (CNN) that are capable of automatic feature extraction; thus, the systems are more robust [33].

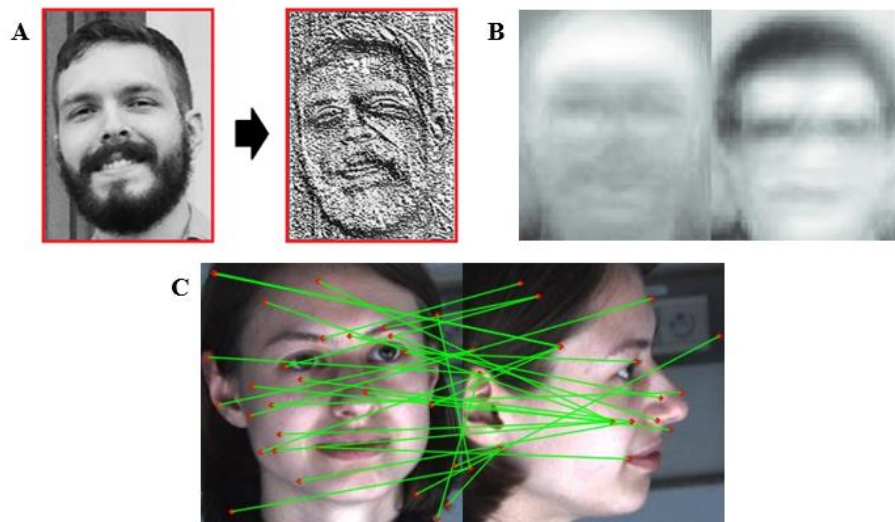


Figure 3: Representation of traditional local descriptors. (A) Local Binary Patterns [34], (B) Eigenfaces [35], and (C) Matching process of SIFT [36].

2.1.4 Voice

This biometric trait can be considered a mixture of physiological and behavioral characteristics because the mouth, lips, and vocal cords (physiological features) are responsible for its production, and it depends on the age, medical condition, and other behavioral features [37]. Generally, the human voice contains much information about the speaker, like emotion, gender, and identity [38].

In the case of voice recognition, there are two different applications: speak recognition and speaker recognition. In the first case, the system aims to understand what is saying the speaker, while in the second, it seeks to recognize who is the speaker [39]. To create biometrics based on voice recognition, the traditional extracted features used to represent the users are the Mel Frequency Cepstral Coefficients (MFCC); Figure 4 illustrates them. These features take human perception sensitivity concerning Mel frequencies [40]. Besides, another approach to this problem is using artificial neural networks; for example,

Self-Organized Maps (SOM) can help to recognize the speaker regardless of the text used [41].

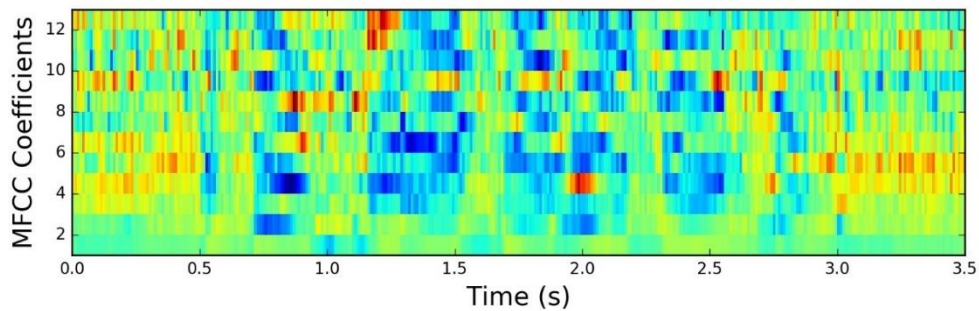


Figure 4: Heatmap of Mel Frequency Cepstral Coefficients extracted from an audio file [42].

2.1.5 Signature

The systems based on signature recognition are one of the oldest biometrics used across the world. Despite the rapid development of technology, the signature continues being one of the most socially accepted methods for verification systems [43]. The main application for this kind of system is serving as a symbol of consented authorization in scenarios such as financial transactions, land purchases, contracts, legal documents, among others. [44]. There are two groups of signature recognition systems: offline and online, also known as static and dynamic systems, respectively, Figure 5 exemplifies both of them.

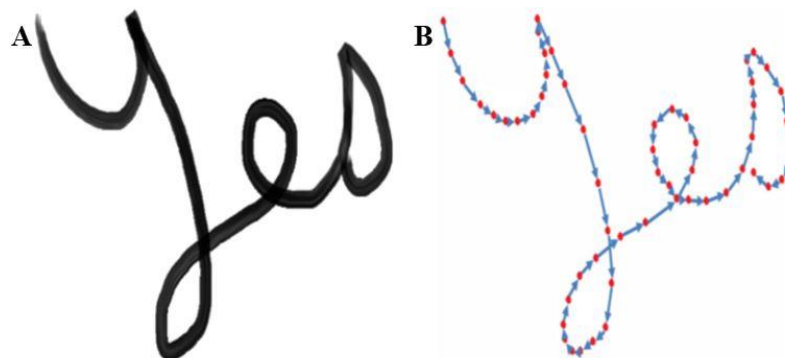


Figure 5: Representation of signature recognition systems. (A) Signature as an image (offline), and (B) Signature as a function (online) [45].

Offline systems work with hard copies of signatures, and there are two different approaches: writer-dependent and writer-independent [46]. For the first approach, the system is trained only with genuine signatures or both genuine and forged signatures. In

contrast, for the writer-independent case, the classifier is trained only once with genuine and forged signature samples of several writers [47].

Finally, an online signature is more robust than an offline one as it stores dynamic features like elevation and pressure signals. In this case, a signal over time represents the signature, and as in the offline case, there are two approaches: parametric and functional [48]. As its names indicate, the parametric approach extracts a set of parameters from the signal. On the contrary, in the functional method, a function characterizes the signature.

2.1.6 Hand Geometry

A pattern of hand shape and palm contains much information for identifying a person. Hand geometry represents the patterns of hand shape and palm lines. The most significant advantages of this biological trait are uniqueness and permanence because every person has different hand lines and shapes that do not change during the lifetime [49]. Traditional systems for hand recognition work with the length and width of fingers, the angle between them, and the surface area. Newer methods use artificial intelligence for automatic pattern recognition of complex geometric features of the hand [50]. Figure 6 presents traditional measurements for hand geometry.

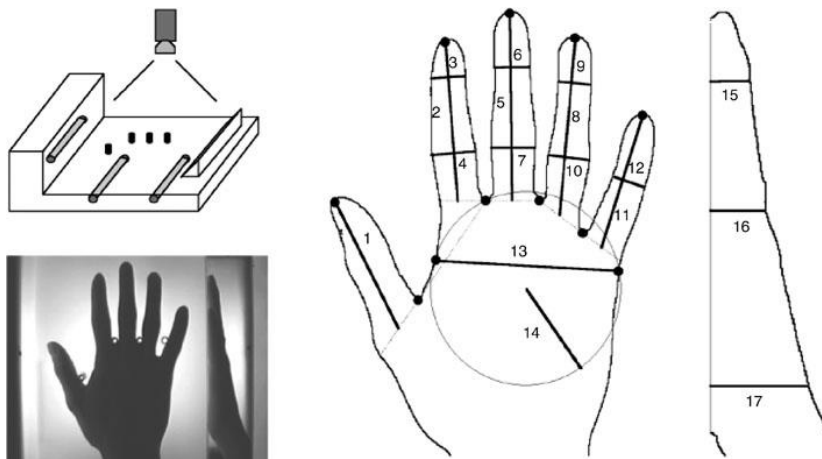


Figure 6: Traditional scanner and measurements for hand geometry recognition [51].

A hand geometry system is cheap to implement because it only needs a low-cost camera or document scanner. Also, most of the algorithms used for this recognition have low computational complexity and occupy small templates reducing the execution time and the required memory [52, 53]. Further, hand geometry is one of the best options for developing multimodal biometric systems, especially with fingerprints. For example, a

biometric system could use hand geometry for verification and fingerprints for identification [53].

2.1.7 Iris

The iris is a thin, circular diaphragm, which lies between the cornea and the lens of the human eye. The formation of the unique patterns of the iris is random and not related to any genetic factors [54]. Iris contains unique features like ridges, freckles, rings, and furrows; Figure 7 illustrates some of them. Iris recognition systems are popular these days because iris accomplishes some of the essential requirements of biometrics like uniqueness, stability, and acceptability.

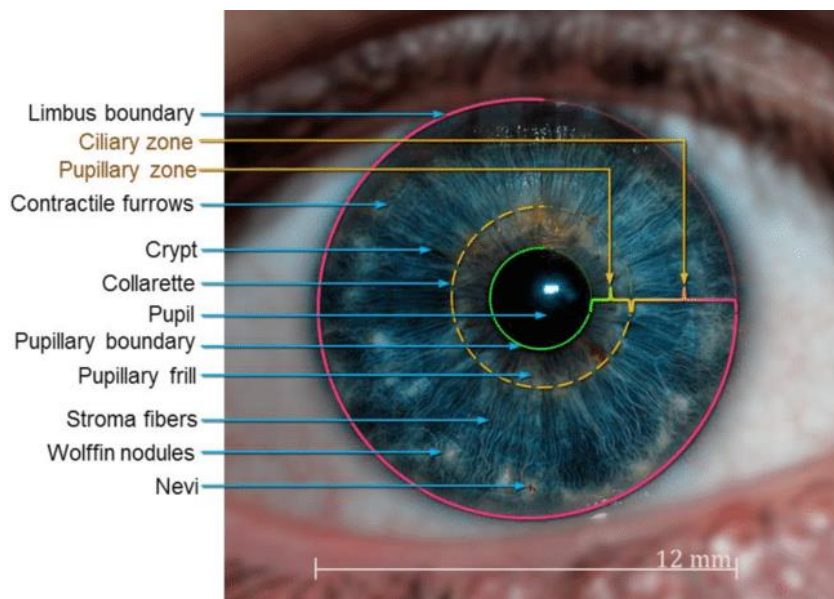


Figure 7: Important features of the iris [55].

All humans have unique iris patterns; even these patterns are different for each eye. Additionally, the iris is stable over time regardless of the age of the person [56]. Furthermore, iris recognition systems are user-friendly since an iris image can be captured from a considerable distance. Though these systems can experiment troubles with the process of iris segmentation due to it is a small area with a constantly involuntary movement, which can cause a decrease of accuracy [57].

Also, the two main problems with iris recognition systems are the liveness testing and eye contact lenses. On the one hand, with traditional methods, there is no way to verify if the user is alive. On the other hand, the contact lenses can alter the final image causing system failures [58].

2.1.8 Palm Print

Palm print contains similar patterns to fingerprint (ridges, minutiae, valleys, principal lines, and wrinkles). Figure 8 shows the principal lines that are crucial features of palm prints. They are stable over time, and they are easy to extract from low-resolution images, they are one of the biggest problems of previous biometric systems [59]. Moreover, palm prints can provide multi-spectral features which can help to avoid fake palm prints [60].

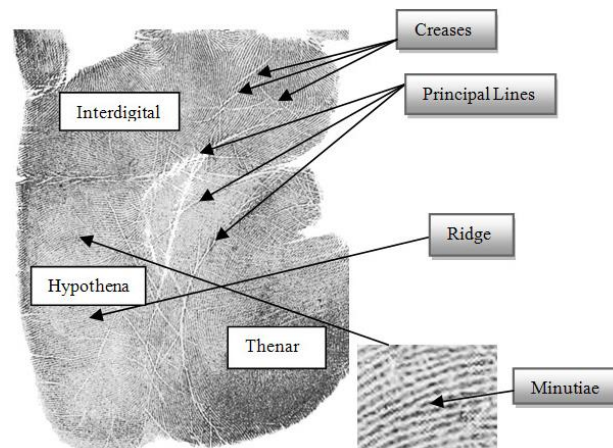


Figure 8: Principal features of palm prints [61].

Palm print recognition methods can be divided into categories based on texture, line, subspace learning, correlation filter, local descriptor, and orientation coding [62]. However, most of these methods perform a two-dimensional analysis. For this reason, recently, three-dimensional techniques have been applied to increase the accuracy and robustness of the biometric systems based on palmprint recognition [63].

2.1.9 Ear

The ear seems to be an advantageous biometric trait since, in principle, everyone has ears, their images are easy to take, they are different for each person, and its structure does not suffer radical changes over time. These features of ears satisfy the biometric characteristics of universality, collectability, distinctiveness, and permanence [64]. Additionally, the limited surface of the ear, allows faster processing, while the lack of significant changes reduces intra-class variations [65].

Despite all the benefits of ear recognition systems, slight variations in the orientation of the ear concerning the acquisition device can cause significant changes in the results. Moreover, occlusion due to hair, earrings, or headscarves can affect the correct

segmentation of the ear surface [66]. Some methods solve the problem of rotation. For example, the Active Shape Model (ASM) helps automatically extract the ear from 2D images even if the head is a little rotated [67], as shown in Figure 9.

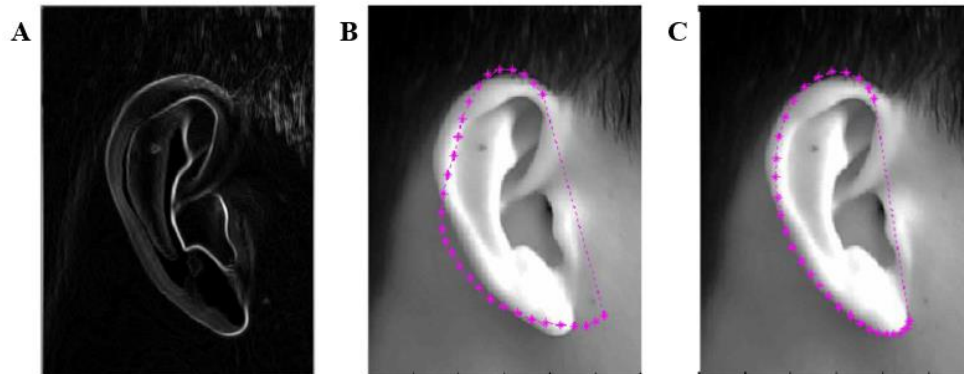


Figure 9: Automatic ear extraction process. (A) Sobel edge extraction, (B) Initial matching function, and (C) Improved matching function [67].

2.1.10 Bioelectrical Signals

Bioelectrical signals are those that are generated by the summation of electrical potential differences across a specialized tissue or an organ. The most studied bioelectrical signals are [68]:

- Galvanic skin response (GSR),
- Electromyogram (EMG),
- Electrooculogram (EOG),
- Electrocardiogram (ECG), and
- Electroencephalogram (EEG)

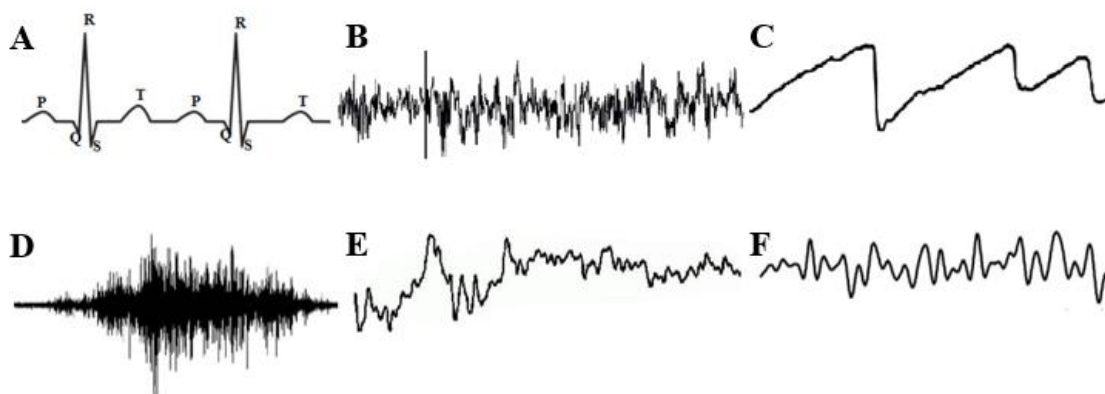


Figure 10: Bioelectrical signals. (A) Electrocardiogram, (B) Electroencephalogram, (C) Galvanic Skin Response, (D) Electromyogram, (E) Electrooculogram, and (F) Mechanomyogram [68].

Figure 10 shows a representation of each signal. A typical application of these signals is a medical diagnosis. However, recent studies have shown that the bioelectrical signals can also be applied as biological traits for biometric systems. One of the main advantages of these traits over the previous is that they guarantee that the user is alive [6].

2.1.10.1 Galvanic Skin Response

Galvanic skin response is the property of the human body that causes continuous variation in the electrical characteristics of the skin. It is a method used to measure the electrical conductance of the skin. The state of the sweat glands of the skin produces variations on the conductance. The conductivity is measured by placing the sensor into two fingers, as shown in Figure 11.



Figure 11: Galvanic skin response measurement [69].

If the individual produces a high sweating level, the conductivity increases, while if the sweating level is low, the conductivity decreases, producing an increase in the resistivity [70]. In most cases, this signal is examined in parallel with other bioelectrical signals to develop reliable biometrics because the analysis of just the galvanic skin response is more often used to sentiment analysis.

2.1.10.2 Electromyogram

Electromyography detects the electrical potential difference that activates the muscle cells. These signals can be analyzed to understand the biomechanics associated with the movement of a human or an animal [70]. Figure 12 presents the two methods for performing an electromyogram. The first one is a surface method, and the other one is an intramuscular method. Nonetheless, only the first one is suitable for developing biometrics because it is a non-invasive technique that facilitates data acquisition.

The extracted signal requires an amplification close to a thousand times because it is only a few millivolts in amplitude. Most of the developed biometric systems based on EMG place the electrodes around the wrist to use the EMG and the circumference of the wrist as biometric data. These systems can be remarkably accurate, achieving a 97.9% recognition rate [6].

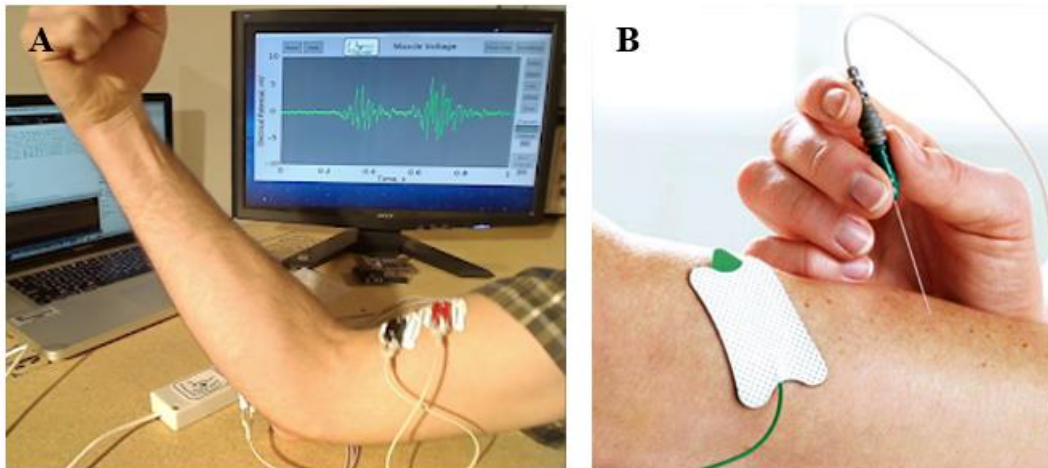


Figure 12: Measurement of Electromyogram. (A) Surface [71], and (B) Intramuscular [72].

2.1.10.3 Electrooculogram

Electrooculogram signal is the electrical recording of the eyeball and eyelid movements through an electrode placed near the eye. The advantages of EOG signals over conventional biometric traits are that these signals cannot be easily forged or captured remotely, such as the voice or face. Moreover, they are one dimensional, low-frequency signals that can be quickly processed [73]. Furthermore, these signals are unique to each person because of the different eye blinking patterns of each individual. Nonetheless, the main problem with EOG signals is the dissatisfaction of the users since, as seen in Figure 13, signal acquisition can be annoying.

Even though there are many eye movements, the most studied for developing biometrics is the saccade, which consists of rapid vertical or horizontal eye movements [6]. From this eye movement, the extracted features are generally based on amplitude, accuracy, latency, and maximum velocity [73].

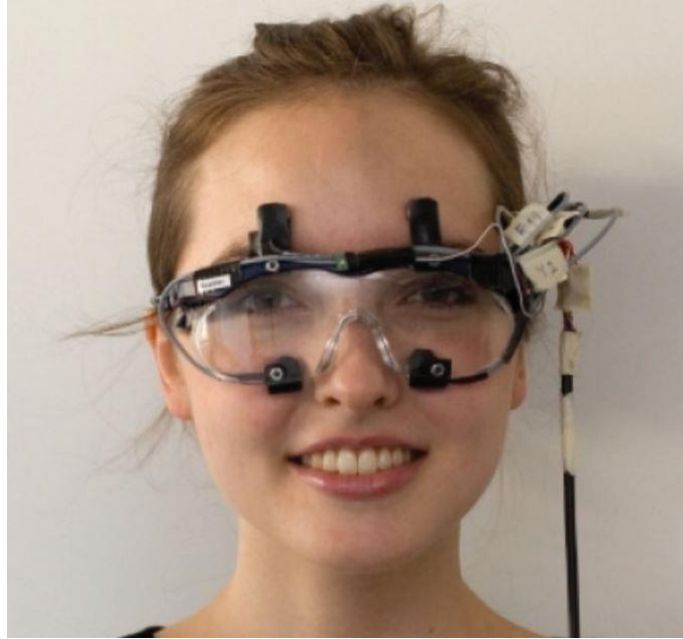


Figure 13: Electrooculogram acquisition system [74].

2.1.10.4 Electrocardiogram

Electrocardiography is a non-invasive technique that monitors the direction and magnitude of the electrical activity produced by depolarization and repolarization of the atria and ventricles of the heart. Figure 14 illustrates the components of an ECG. The primary use of electrocardiograms is related to medical applications. However, currently, researchers are investigating the benefits of these signals as a biometric trait. As heart mass, orientation, position, size, anatomy, the conductivity of cardiac muscles and the activation order, chest configuration, individual's age, sex, relative body weight, and other electrophysiological factors vary among individuals, ECG differs from person to person [75]. All these factors affect the morphology of the ECG signal satisfying the uniqueness requirement of a biometric system.

There are two types of methods for working with these signals for biometric applications, the fiducial points-based methods, and the non-fiducials-based methods. The first group relies on local features of the heartbeats, such as the temporal or amplitude difference between consecutive fiducial points. The fiducial points are extracted in the temporal domain. On the other hand, the non-fiducials-based methods generally use features based on the autocorrelation of the signals [6].

Table 1 summarizes compliance with the requirements of a biometric system, introduced in Section 2.1.1, of all the biometrics presented in this section.

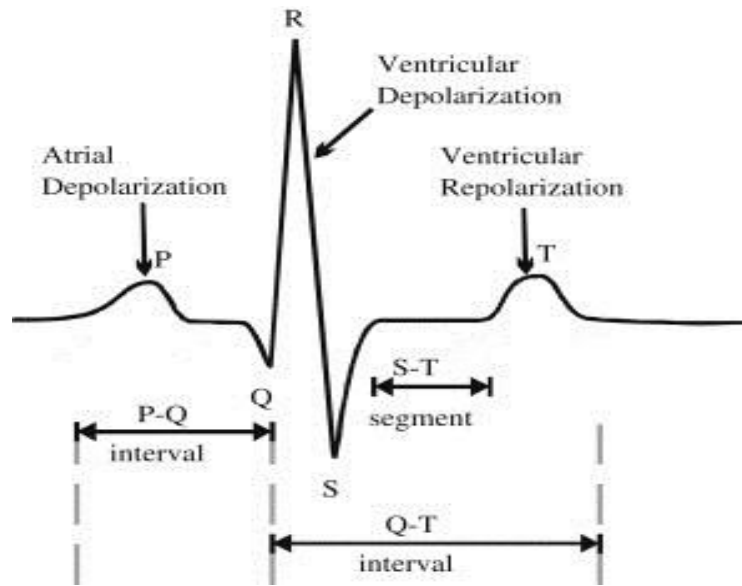


Figure 14: Parts of electrocardiogram signal [76].

Table 1: Comparison of biometric traits [1, 77].

Biometric Trait	Universality	Distinctiveness	Permanence	Ease of Collectability	Performance	Acceptability	Ease of Circumvention
Fingerprint	Medium	High	High	High	Medium	High	High
Face	High	Medium	Medium	High	High	High	Medium
Voice	Medium	High	Low	High	Medium	High	High
Signature	Medium	Medium	High	High	Medium	High	High
Hand Geometry	Medium	High	Medium	Medium	Medium	Medium	Medium
Iris	High	High	High	Medium	High	High	Medium
Palm Print	Medium	High	High	Medium	Medium	Medium	Medium
Ear	High	High	High	High	Medium	Low	Medium
GSR	High	Medium	High	Medium	Medium	Low	Low
EMG	High	Medium	High	Medium	High	Low	Low
EOG	High	High	High	Low	High	Low	Low
ECG	High	High	Medium	Low	High	Low	Low

2.2 Electroencephalogram Signals

The electric potential difference produced by a human brain has the order of a few microvolts. These voltage fluctuations are the result of ionic current that flows between the neurons. The excitatory and inhibitory postsynaptic potentials developed by cell bodies and dendrites of pyramidal neurons produce cortical potentials [78]. The electric potential generated by a single neuron is minimal; thus, it is impossible to detect. Therefore, the EEG determines the summation of the synchronous activity of a large number of neurons present in the brain [79].

Electrodes, also known as channels, are placed on the scalp of the person to record the EEG signals. The amplitude of the signal may go from 10 to 100 microvolts with a frequency between 1 and 100 Hz. There are two types of recordings, monopolar and bipolar. The first type is the measure of the potential at an active electrode, while the bipolar recording is a voltage difference between two active electrodes. The most used recording type is a monopolar recording [79].

In clinical applications, many EEG channels are recorded simultaneously from various locations on the scalp to make a comparison of the activities in different regions of the brain. The International Federation of Societies for Electroencephalography and Clinical Neurophysiology recommends the 10-20 system of electrode placement for clinical EEG recording; Figure 15 illustrates this systematic placement of electrodes [78].

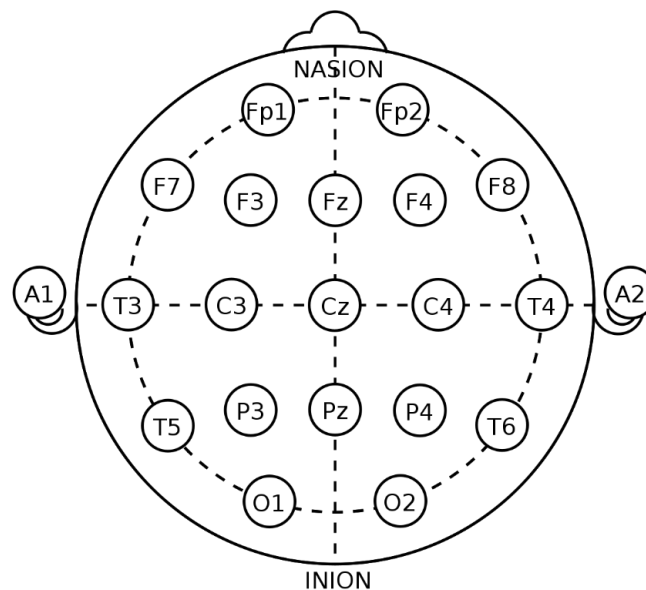


Figure 15: The 10-20 system of electrode placement for EEG recording [80].

The signal extracted from electrodes is called raw EEG signal. This signal could include some non-cerebral signals known as artifacts. There are roughly three groups of artifacts: biological, biomedical, and environmental. Some of the biological artifacts are blinking of eyes during signal acquisition procedure and muscular activities [81].

Sometimes bioelectrical signals like ECG, EMG, or EOG get mixed up with the EEG signals. These contaminations are the biomedical artifacts. These kinds of artifacts are the most difficult to remove because, most of the time, they are very similar to the actual EEG signal. Finally, the environmental artifacts are line noise, pulse, electrode stabilization, among others [79]. The elimination of the artifacts is crucial, especially from the medical point of view, because their presence can lead to a wrong diagnosis.

A highly studied application of EEG signals is the analysis of brain rhythms for medical purposes. These rhythms are the result of the classification of EEG signals into five specific frequency sub-bands: delta (δ , 0–4 Hz), theta (θ , 4–8 Hz), alpha (α , 8–13 Hz), beta (β , 13–30 Hz) and gamma (γ , 30–50 Hz) [82]. Table 2 summarizes the main characteristics of each brain rhythm, and Figure 16 shows their wave shape. All these rhythms allow the investigation of the nervous system, monitoring of sleep stages, biofeedback and control, and diagnosis of diseases like epilepsy, Parkinson, and many more [81, 83].

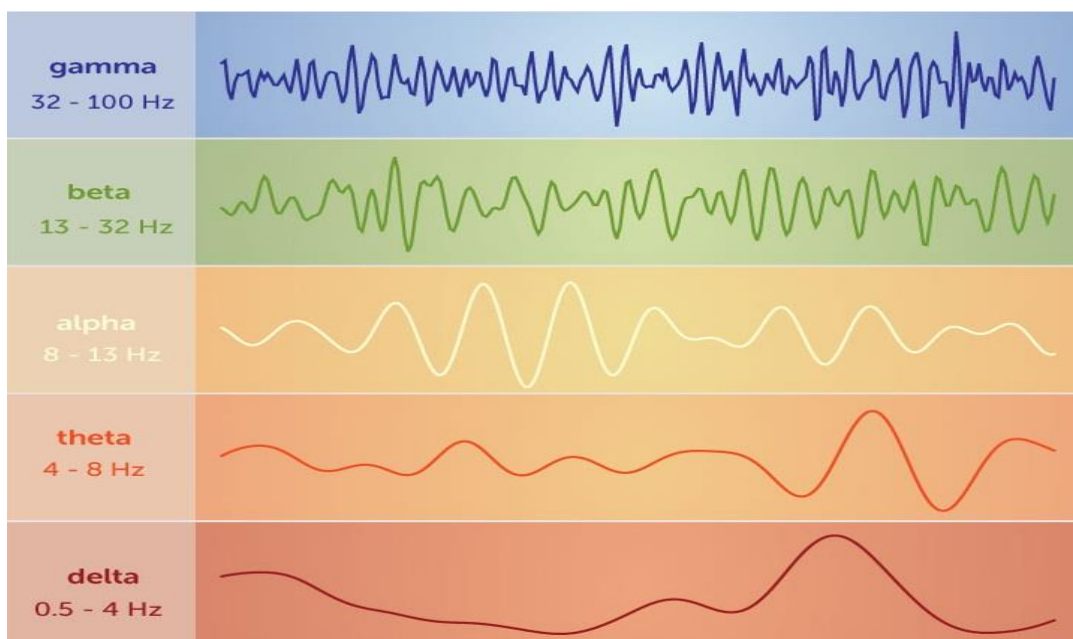


Figure 16: The wave shape of brain rhythms [84].

Table 2: General information of brain rhythms.

Rhythm	Frequency range (Hz)	Amplitude (μv)	State of mind
Delta (δ)	0 - 4	High amplitude (20 – 200)	Deep sleep, loss of bodily awareness, repair
Theta (θ)	4 – 8	More than 20	Creativity, insight, deep states, dreams, deep meditation, reduced consciousness
Alpha (α)	8 – 13	30 – 50	Physically and mentally relaxed
Beta (β)	13 – 30	5 – 30	Awake, alert consciousness, thinking, excitement
Gamma (γ)	30 - 50	Less than 5	Heightened perception, learning, problem-solving tasks, cognitive processing

Signal processing techniques can help to distinguish between the brain activity of a healthy and unhealthy person. However, the nature of EEG signals is highly non-linear, non-Gaussian, non-correlated, and non-stationary [85]. Also, EEG features depend on several factors like the age and the mental state of the subject [80]. The general experimental design for working with EEG signals include initial recording at rest (eyes open, eyes closed) as a baseline and then the recording while doing a specific task as a trial [77]. These signals are an excellent choice to employ them as biometric traits because they fulfill most of the requirements of biometric systems [18]:

- **Universality:** All human brains are composed of neurons that produce electrical activity that forms EEG signals. Moreover, individuals of any age and any mental state, including vegetative state or coma, produce these signals.
- **Distinctiveness:** The evidence from EEG-based person recognition research shows that EEG signals are sufficiently different among people so that they can be correctly classified.

- **Permanence:** Some researchers have conducted session-to-session tests to validate EEG variability over time. These studies have concluded that EEG signals maintain a significant degree of repeatability [86].
- **Collectability:** Unfortunately, the process of signal acquisition can be time-consuming and inconvenient for routine biometric procedures because it needs to place electrodes over the scalp. In some cases, it also uses a conductive paste to reduce skin impedance.
- **Performance:** The accuracy of the system depends on preprocessing and feature extraction. Two commonly used metrics for quantifying the performance of the system are the false acceptance rate (FAR) and the false rejection rate (FRR).
- **Acceptability:** The EEG signals are socially acceptable for medical purposes, but for developing biometric systems, there are some doubts concerning privacy due to the sentimental analysis or Brain-Computer Interface (BCI) systems that try to “read minds.”
- **Circumvention:** One of the crucial problems of traditional biometrics is that the features can be collected without user consent. Nonetheless, no technique allows the recording of brain waves remotely. Additionally, even if someone is forcing the user to make a recording of EEG, the negative emotions would lead to an authentication failure.

2.2.1 Preprocessing

The human head is composed of layers like the scalp, skull, and brain, so EEG signals over the scalp are relatively weak and subject to contamination from the artifacts previously discussed [87]. Therefore, after recording, EEG signals must be processed to reduce these noises as much as possible. A widely applied technique for reducing the noise is bandpass filtering, which works by analyzing the signal across a period of time.

One of the advantages of bandpass filtering is that it can work on short signal recordings. Furthermore, it has proven that this filtering technique is useful to maximize the signal-to-noise ratio [88]. In bandpass filtering, a low-pass filter removes or attenuates high-frequency noise while the high-pass filter removes or attenuates low-frequency noise. Regardless the advantages of bandpass filtering, in most of the works it is combined with other techniques such as Principal Component Analysis (PCA) [89], Support Vector Machines (SVMs) [90], Independent Component Analysis (ICA) [89, 91], Blind Source

Separation (BSS) [92], Wavelet Transform (WT) [93] and Fourier Transform (FT) [93, 94].

Most current researches employ a Discrete Fourier Transform (DFT) or Discrete Wavelet Transform (DWT). DFT transforms the time domain signal samples to frequency domain components. Also, it establishes a relationship between the time domain representation and the frequency domain representation [95]. DWT is widely used for time-frequency analysis, especially in EEG signal analysis due to its non-stationary characteristics. The efficiency of this transform depends on the levels of decomposition used. These levels are the main steps of the DWT. At each level, the signal is convoluted with a low-pass filter and a high-pass filter. These filters depend on the mother wavelet chose for the decomposition. Then, the filtered signals of each level pass through downsampling by a factor of two. This filtering process effectively reduces the noise injected by artifacts [9].

Table 3 shows a summary of preprocessing techniques. This summary contains a description of the proposed algorithm, with its contribution and challenges.

Table 3: Comparison of preprocessing techniques for EEG data.

Authors	Year	Algorithm	Contribution	Challenges
Joyce et al. [92]	2004	ICA using Second-order Blind Inference (SOBI) procedure	An automated procedure for extracting and removing ocular artifacts	Being capable of removing the muscle-related artifacts
Vallabhaneni et al. [88]	2005	None	Review on Spatial and Temporal Domain techniques for preprocessing	Lack of implementation of the presented methods
Kumar, Arumuganathan, Sivakumar, & Vimal [96]	2008	Adaptive filter with Least Mean Square (LMS) algorithm through WT	A robust technique for removing ocular artifacts	Difficulty to found correct values for the filter order and convergence factor which can lead to a bad performance on other scenarios
Li, Sun, Zhang, Wu, & Wu [97]	2009	Notchfilter, BSS and Finite Impulse Response (FIR) filtering	Artifact removal using basic filtering and BSS technique	Working with data from more subjects and with more EEG channels

Authors	Year	Algorithm	Contribution	Challenges
Guerrero-Mosquera & Navia [98]	2009	Low-pass filter and ICA based on the Joint Approximate Diagonalization of Eigen-matrices method (JADE)	Artifact removal through the implementation of ICA	Artifacts were identified and visually eliminated. Automatic removal is not implemented yet
Wang & Makeig [99]	2009	Bandpass filtering and the extended infomax ICA algorithm	Noise removal using filtering and ICA. Additionally, the used ICA technique can match efficiently the distributing of the input	The time complexity of the extended infomax ICA algorithm is not optimal
Zhou & Gotman [91]	2009	ICA based on JADE algorithm	The method works without parameter tuning	The number of sources is limited to 40 or 50 depending on the available memory of the computer
Vidaurre, Krämer, Blankertz, & Schlögl [100]	2009	Spatial Filters: Bipolar montage, Laplacian montage, 3 Laplacian channels, 11 Laplacian channels and Common Spatial Patterns (CSP)	Comparison among different spatial filters which are easy and fast to calculate and only a very low number of parameters needs to be selected	Improving the filters by adapting the bias
Azim et al. [93]	2010	Bandpass elliptic filter, DWT and Fast Fourier Transform (FFT)	Combination of different techniques for achieving better results	Improving the signal acquisition and implementation of digital filters
Kameswara, Rajyalakshmi, & Prasad [101]	2012	None	Review on the classic preprocessing techniques (Basic Bandpass filtering, Adaptive filtering and BSS)	Making a real comparison among the different type of preprocessing techniques

Authors	Year	Algorithm	Contribution	Challenges
Jirayucharoensak & Israsena [102]	2013	Infomax ICA and Lifting Wavelet Transform	Effective removal of ocular and muscular artifacts	It cannot be seen as a general procedure because the algorithm is based on fixing a threshold which can change according to the data
Kalaivani, Kalaivani, & Anusuya [103]	2014	Eight level DWT	Simple but effective denoising process and frequency band decomposition	Choosing of the level of decomposition and mother wavelet needs to be done for other applications
Oana & Anca [104]	2015	Basic Bandpass filtering	Effective isolation of the Mu rhythm frequency range	Cleaning the artifacts of the signal
Maki, Toda, Sakti, Neubig, & Nakamura [105]	2015	Multi-Channel Wiener Filter	Provides an unsupervised method for EEG event signal separation using multi-channel EEG signals	This method does not use any prior information for estimation of spatial correlation matrices and blindly separates EEG signals into individual EEG components using time-varying scaled spatial correlation matrices.
Swee & You [94]	2016	EmoEngine and FFT analysis	Comparison between an API (EmoEngine) for preprocessing the signals and a classic technique	Comparing the API with respect to more robust methods

2.2.2 Feature Extraction

Feature extraction in systems based on EEG signals is a process that translates the preprocessed brain signal (input signal) into a feature vector correlated to a neurological phenomenon [106]. Extracting the most representative features from EEG signals

constitutes a crucial step in the development of a robust biometric system because these features present different degrees of distinctiveness among people [107].

The quality of the extracted features produces a direct impact on the identification results. For this reason, there are many ways of performing this step. The most common EEG features can be extracted using the information of a single channel or from more than one channel in domains like time, time-spatial, or frequency. Generally, the feature vectors are the result of the concatenation of the extracted features from each channel. Consequently, these vectors are usually significantly shorter than the input signal. The most popular features are: Autoregressive (AR) features, Power spectral density (PSD) and features based on Wavelet Transform.

The *autoregressive modeling* of EEG signals is a generalization of the Autoregressive Moving Average (ARMA) model in time series prediction [108]. AR modeling is a parametric modeling technique in which a mathematical model is used to formulate a linear prediction to describe the signal generation system [109].

In simple words, the AR model forecasts the output based on previous input and output values. The value of each current sample $y(t)$ in an AR model is linearly related to the p most recent sample values, as shown in (1):

$$y(t) = - \sum_{k=1}^p a_k y(t-k) + x_n \quad (1)$$

where $\{a_k \mid k \in \{1, 2, \dots, p\}\}$ are the linear parameters, p is the order of the model, n corresponds to the discrete sample time, and x_n is the noise input [87].

Power spectral density is a function that represents the distribution of the average signal power over frequencies. The definition of PSD can be presented as the discrete-time Fourier transform of the autocovariance sequence (ACS) as follows [110]:

$$\phi(\omega) = \sum_{k=-\infty}^{\infty} r(k) e^{-i\omega k} \quad (2)$$

where $i = \sqrt{-1}$, ω is the radian frequency, and $r(k)$ represents the ACS that is defined as

$$r(k) = E\{y(t)y^*(t-k)\} \quad (3)$$

where $y(t)$ is the discrete-time signal $\{y(t) \mid t \in \{0,1,2, \dots\}\}$ which it is assumed to be a sequence of random variables with zero mean ($E\{y(t)\} = 0 \forall t$), and $y^*(t)$ is its complex conjugate.

For calculating the PSD, some methods in the nonparametric approach have been employed, such as Bartlett and Welch. These classic methods use a periodogram for estimating the power of a signal at different frequencies [111]. However, the Welch method is frequently applied because it can reduce more noise and frequency resolution than standard Bartlett's method.

Finally, the features based on *wavelet transform* are one of the most popular in recent research for EEG based biometrics. The main advantage of these features is that they capture the time and frequency characteristics of the input signal. Examples of these features are: Energy, Entropy, Root Mean Square (RMS), Mean Absolute Value (MAV), Integrated EEG (IEEG), Simple Square Integral (SSI), Variance of the EEG, and Average Amplitude Change (AAC) [112]. The most used version of WT is the DWT. Section 3.3 explains in detail this transformation, and Section 3.4 explains the feature extraction process of this work. For this reason, this section does not provide a formal definition of this technique.

The AR, PSD, and WT based features can be extracted from a single EEG channel separately to handle only the most significant channels. Nevertheless, in most of the applications, all the available channels are used to avoid losing important information. As it was mention before, the feature vector will be the concatenation of the features extracted from each channel into a single one-dimensional vector.

2.2.3 Classification Algorithms

A classifier is an algorithm that takes a feature vector as input and returns the corresponding class. When trained, it represents a model of the association between the extracted features and the classes [9]. In the case of biometrics, the classes are subjects, e.g., for a given feature vector from subject 1; the classifier works as a function c that takes as input the feature vector and maps it to the subject. The classifiers need to adjust their hyperparameters to the working data for maximizing their performance.

One of the most used classifiers for this application is Support Vector Machine [113]. This classifier finds a hyperplane within the features space, maximizing the margin

between the nearest data point of each class and the hyperplane [114]. Despite being initially designed for binary classification problems [115], SVMs can be extended to multiclass problems.

Additionally, with the rapid development of Artificial Neural Networks (ANN), they are frequently used for people identification in biometric systems. The inspiration of ANNs is the brain structures where the organization of the layer-wise neurons allows to achieve a high-level abstraction of the data [116]. The result of the ANN depends on the characteristics of the neurons and their associated interconnection weights. By modifying the connections between the neurons, the network can adapt to the desired outputs.

Nonetheless, classical classifiers are also employed. K-Nearest Neighbors (K-NN) is a distance-based classifier because it predicts the output class based on the k nearest training classes to the input feature vector [117]. Random Forest (RF) is an ensemble of decision tree classifiers. Each tree is constructed using a randomly selected group of features, independently sampled with an identical distribution for all trees [118]. Each tree in the forest predicts a class, and the output is the most voted class for each input feature vector. AdaBoost (AB) is additionally an ensemble classifier as RF, but in this case, the weak classifier can be any of the previous classifiers. AB is adaptive because it tweaks its weak classifiers in favor of those instances misclassified by previous classifiers [119].

It is important to know that no rule indicates which classifier is better for a specific application. For this reason, it is pertinent to make a comparison among different classifiers to obtain the best one for developing biometrics based on EEG signals. Moreover, all the classifiers have many hyperparameters that need to be adjusted. For this reason, there are many hyperparameter optimization techniques. Some techniques are quick because they do not perform a complete search, which in most cases, does not guarantee to find the best hyperparameters. Greedy search performs a complete search concerning its dictionary of parameters and always finds the best parameters inside it. Though, it takes much time because it proves all possible combinations within its dictionary [120].

Table 4 shows a comparison of different feature extraction and classification algorithms. The database column corresponds to the number of people used in the experiments, which varies a lot for each study.

Table 4: Comparison of feature extraction and classification techniques for EEG data.

Authors	Year	Database	EEG Channels	Methodology (Feature extraction + Classifier)	Results (Classification Accuracy)
Poulos, Rangoussi, Chrissikopoulos, & Evangelou [121]	1999	4	1	AR model of α -rhythm + Kohonen's Learning Vector Quantizer (LVQ) neural network	72% - 84%
Paranjape, Mahovsky, Benedicenti, & Koles [122]	2001	40	8	AR models for single EEG traces using Lattice Equivalent Model and Levinson Recursion + Discriminant Function Analysis (DFA)	49% - 82%
Poulos, Rangoussi, Alexandris, & Evangelou [123]	2001	4	18	FFT based spectral analysis of α -rhythm + LVQ neural network	80% - 100%
Palaniappan & Raveendran [124]	2002	10	61	Visual evoked potential (VEP) signals of γ -band + Fuzzy ARTMAP (FA) neural network	90.95%
Palaniappan & Paramesran [125]	2002	20	61	VEP patterns selected by genetic algorithm and FA + Multilayer Perceptron (MLP) trained by back-propagation	95.9%
Palaniappan [126]	2004	20	61	γ -band spectral power (GBSP) computed using Parseval's theorem + MLP with a single hidden layer trained by back-propagation	99.06%
Ravi & Palaniappan [127]	2005	40	61	Normalized late γ -band (LGB) spectral powers + Neural network trained by back-propagation	95.4%
				LGB spectral powers + Simplified fuzzy ARTMAP (SFA) neural network	82.44%

Authors	Year	Database	EEG Channels	Methodology (Feature extraction + Classifier)	Results (Classification Accuracy)
Palaniappan [128]	2006	5	6	Combination of six order AR coefficients, Channel Spectral Power, Inter-hemispheric Channel Spectral Power differences and Linear Complexity + Linear Discriminant Analysis (LDA)	99.83%
Mohammadi, Shoushtari, Ardekani, & Shamsollahi [129]	2006	10	100	AR parameters of each epoch + Competitive neural network with a reinforcement learning algorithm	85% - 100%
Palaniappan & Ravi [130]	2006	20	61	GBSP computed using Parseval's theorem + LDA	84.25% - 96.50%
				GBSP computed using Parseval's theorem + K-NN	62.48% - 94.18%
				GBSP computed using Parseval's theorem + SFA	66.26% - 92.84%
Palaniappan & Mandic [131]	2007	40	61	The energy of the channels reduced by Davies Bouldin index + Elman neural network trained by resilient back-propagation	98.56%
Touyama & Hirose [132]	2008	5	1	P300 evoked potentials + LDA	97.6%
Palaniappan [133]	2008	4	6	AR coefficients of order six estimated with Burg's method + LDA	92.45% - 99.9%
Yazdani, Roodaki, Rezatofghi, Misaghian, & Setarehdan [134]	2008	20	61	PSD of γ -band VEP signal + K-NN	100%

Authors	Year	Database	EEG Channels	Methodology (Feature extraction + Classifier)	Results (Classification Accuracy)
Riera, Soria-Frisch, Caparrini, Grau, & Ruffini [135]	2008	51	2	AR modelling + Classification score	98.1%
Das, Zhang, Giesbrecht, & Eckstein [136]	2009	20	20	Spatio-temporal filter + SVM	94.08%
				Spatio-temporal filter + LDA	87.78%
Palaniappan & Eswaran [137]	2009	40	61	Genetic algorithms and Min-max clustering + SFA neural network	95.42%
Gupta, Khan, Palaniappan, & Sepulveda [138]	2009	4	8	P300 and γ -band energy feature using Wavelet Packet Decomposition (WPD) + Generalized regression neural network	85%
Brigham & Kumar [139]	2010	120	64	Univariate AR model and PSD + Linear SVM	98.95%
Zúquete, Quintela, & Silva [140]	2010	70	8	Energy of VEP from γ -band + Radial SVM	98.5%
				The energy of VEP from γ -band + K-NN	95.1%
Abdullah, Subari, Loong, Loong, & Ahmad [141]	2010	10	8	WPD coefficients + ANN	81%
Hu [142]	2010	3	6	AR coefficients + MLP trained with back-propagation	92.8%
Yang et al. [143]	2011	7	2	P300 waves obtained by the oddball paradigm + LVQ neural network	92.14%
Shedeed [144]	2011	3	4	DFT and Wavelet mean, std and entropy + MLP	93%
Gui, Jin, & Xu [145]	2014	32	6	Wavelet mean, std and entropy + MLP	94.04%

Authors	Year	Database	EEG Channels	Methodology (Feature extraction + Classifier)	Results (Classification Accuracy)
Koike-Akino et al. [146]	2016	25	14	PCA and Partial Least Squares (PLS) + Quadratic Discriminant Analysis (QDA)	96.7%
Zhang et al. [116]	2017	20	64	γ -band spectral power ratio + RF	86%
				γ -band spectral power ratio + MLP	85.1%
				γ -band spectral power ratio + K-NN	78%
				γ -band spectral power ratio + AB	73.9%
				γ -band spectral power ratio + Bagging	66.7%
Saini et al. [147]	2018	70	14	γ -band features + Hidden Markov Models (HMM)	95.65%

2.3 Summary

This chapter presented the theoretical background that supports this study. The basis of biometric systems was introduced, remarking the characteristics of good biometric traits. A brief description of the main biometric traits was showed, highlighting their strengths and weaknesses. Also, this chapter presented five of the most popular bioelectrical signals. These signals are extremely significant because they introduce novel ways of developing robust biometrics.

Moreover, this chapter provided a more in-depth description of electroencephalogram signals. This description covered an explanation of how these signals fulfill each of the characteristics for good biometrics. Finally, it included a review of the state-of-the-art of preprocessing, feature extraction, and classification techniques. Chapter 3 will present the proposed methods for designing a viable biometric system based on the analysis of electroencephalogram signals.

3 Methods

This chapter explains in detail the proposed method for developing biometric systems based on EEG analysis. It begins with the general workflow of the system. After that, each step in the workflow is detailed. Furthermore, this chapter describes the performance metrics used to verify the functionality of the system and the validation process used to obtain reliable results. Finally, the description of the conducted experiments of this research is presented; each description contains the objective of the experiment and its general explanation.

3.1 General Workflow of the Proposed Biometric System

Figure 17 shows the general workflow of the proposed system. The description of each part of the workflow is explained later.

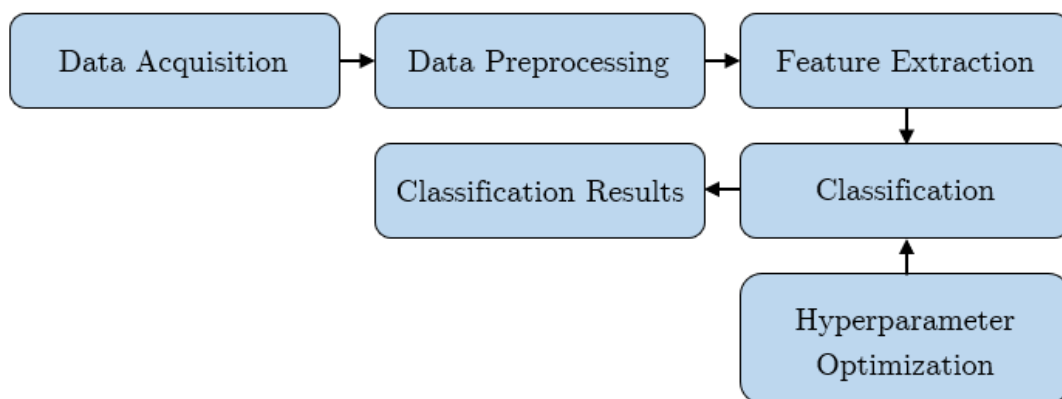


Figure 17: Workflow of the proposed biometric system.

3.2 Data Acquisition

The EEG signals used in this study corresponds to two different datasets. The first one is the open-access “DEAP dataset” [148], and the second one is a private dataset recorded in the “Instituto Nacional de Astrofísica, Óptica y Electrónica” (INAOE). The aim of working with two different datasets is to validate the proposed methodology.

3.2.1 DEAP Dataset

This dataset is available at <https://www.eecs.qmul.ac.uk/mmv/datasets/deap/index.html>. The authors of this dataset describe it as “a multimodal dataset for the analysis of human affective states” [148]. There are two versions of the dataset, one contains the original data, and the other corresponds to the preprocessed data.

The original data folder contains 32 .bdf files, each with 48 recorded channels at 512Hz. The channels correspond to 32 EEG channels, 12 peripheral channels, 3 unused channels, and 1 status channel. Specific toolkits such as EEGLAB for Matlab or MNE for Python allow reading the data. On the other hand, the preprocessed version of the dataset contains 32 .dat files, each with 40 recorded channels at 128Hz. This version still contains 32 EEG channels and 8 peripheral channels, and the files can be read using the cPickle Python module. The authors of DEAP selected 40 one-minute videos to create this dataset. Each video intended to evoke specific emotions on the viewers. Then, they recorded the physiological signals of 32 healthy participants (50% female), aged between 19 and 37 (mean age 26.9), while they saw the 40 videos. After each video, the participants rate their level of valence, arousal, dominance, and liking [148].

On both versions of the dataset, each file contains the 40 recordings of one participant, where each recording corresponds to one video. In the original version, there are only the raw signals. Nevertheless, the signals of the preprocessed version are the result of blind source separation for removing the EOG artifacts and a bandpass frequency filter from 4 - 45Hz. Moreover, this version segmented all the recordings into 3-seconds pre-trial (baseline) and 60-seconds trials [148]. The present work uses the preprocessed version of the dataset because of the benefits that it provides.

3.2.2 INAOE Dataset

This dataset was elaborated to develop biometric systems and brain-computer interfaces. The dataset is composed of the EEG recordings, but it also has the audio and video recordings of all participants. All these signals were captured simultaneously for allowing to develop unimodal biometric systems based on any of these signals or multimodal biometric systems based on a combination of them.

For recording the EEG signals, this dataset used the Emotive Epop+ brainwear device. The internal sampling rate of this device is 2048Hz, but it was downsampled to 128Hz,

and it contains 14 EEG channels. During the recording of the signals, each participant pronounced 135 random numbers between 1 and 10. The order in which the participants pronounced the numbers were the same among all of them. Moreover, each recording had a duration of 2.5 seconds. This dataset contains the recordings of 51 healthy participants (49% female). There is only one version of this dataset that corresponds to the raw EEG signals without any preprocessing technique for removing EOG artifacts or bandpass frequency filtering. Because of the intention of this work, it only used the EEG signals regardless of having access to voice and video recordings.

3.3 Data Preprocessing

Generally, the preprocessing of EEG signals can be divided into [79, 81]: noise filtering, and decomposition of the signal into frequency sub-bands. This section focuses on the second type of preprocessing, whose objective is to facilitate signals analysis rather than cleaning them. The two most widely used techniques are Fourier Decomposition [93, 94, 149] and Discrete Wavelet Decomposition [8, 9, 150, 151]. Nonetheless, the DWT can reveal features related to the nature of the signals unobvious for the Fourier transform [152]. For this reason, this work applied a DWT to both datasets because though the preprocessed version of the DEAP dataset was used, it did not contain this type of preprocessing.

The fundamental idea of wavelet analysis is expressing a signal as a linear combination of a particular set of functions obtained by shifting and dilating one single function called mother wavelet [152]. This work uses Daubechies-4 (db4) as mother wavelet due to its smoothing feature, making it appropriate to detect changes in EEG signals [114]. The following equation defines the DWT of the function $f(t)$ [153]:

$$DWT_{\psi}(j, k) = \int_{-\infty}^{\infty} f(t) * \psi_{j,k}(t) dt \quad (4)$$

where $*$ denotes convolution and $\psi_{j,k}(t)$ is the scaled and shifted mother wavelet defined as:

$$\psi_{j,k}(t) = \frac{1}{\sqrt{j}} \psi\left(\frac{t-k}{j}\right) \quad (5)$$

where $\psi(t)$ is the mother wavelet, and the parameters j and k represent the scale and the shift, respectively. This transformation decomposes a signal into a set of sub-bands

through successively high-pass and low-pass filtering combined with downsampling by a factor of two. The high-pass filter (h) is the discrete mother wavelet, while the low-pass filter (l) is its mirror version. The outputs of the low-pass filters are called approximation coefficients (A_l), and the outputs of the high-pass filters are known as detail coefficients (D_l). The l sub-index in the DWT coefficients corresponds to the level of decomposition. The maximum level of decomposition can be computed as [8, 9, 150]:

$$\log_2(M) - 1, \quad (6)$$

where M represents the length of the signal. Regarding the levels of decomposition of DWT some authors propose to use five levels to obtain the following frequency bands: 32 - 64Hz (D_1, γ); 16 - 32Hz (D_2, β); 8 - 16Hz (D_3, α); 4 - 8Hz (D_4, θ); 2 - 4Hz (D_5, δ) and <2Hz (A_5) [86, 114]. Section 2.2 described these bands, which correspond to the five primary brain rhythms related to specific cognitive functions. Figure 18 illustrates these bands computed from an EEG signal.

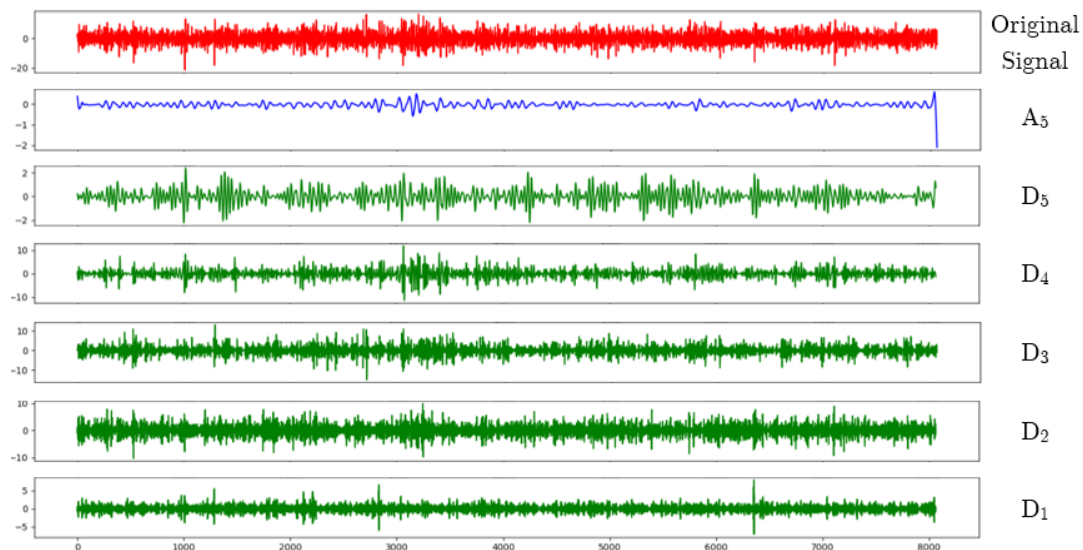


Figure 18: Example of discrete wavelet transform with five levels of decomposition.

Additionally, other authors suggest that four levels of decomposition are enough to achieve good results while reducing the computational cost of the process [8, 150, 151, 154]. This work made a comparison between the five levels DWT and the four levels DWT, but it also included two extra levels of decomposition: three and two. The objective for including these last two levels of decomposition in the comparison was to analyze this technique further.

3.4 Feature Extraction

The extracted wavelet coefficients show the energy distribution of EEG signals in time and frequency in a compact representation. However, the choice of the features represents a critical step in all classification systems because of its direct influence on classification performance. Some authors use the coefficients directly as their feature vectors [8, 147, 151]. Nevertheless, other authors try decreasing the dimensionality of the feature vectors extracting higher-level features such as the maximum, minimum, mean, standard deviation, entropy or relative energy of the wavelet coefficients in each sub-band [9, 114, 150, 152, 154]. For the present work chose the relative wavelet energy (RWE) as a feature because it has been proven to be very useful in classification tasks [146]. The energy (E) of each sub-band was computed using the following equations [155]:

$$E_{D_i} = \sum_{j=1}^N |D_{ij}|^2, i \in \{1, 2, 3, \dots, L\}, \quad (7)$$

$$E_{A_L} = \sum_{j=1}^N |A_{Lj}|^2, \quad (8)$$

where N is the length of the coefficient vector, L is the maximum level of decomposition, D_{ij} is the j th element of the detail coefficient vector D_i , and A_{Lj} is the j th element of the last (L) approximation coefficient vector A_L . Using equations (7) and (8), the total energy is defined as:

$$E_T = \left(\sum_{i=1}^L E_{D_i} \right) + E_{A_L}; \quad (9)$$

finally, the RWE was computed as follows:

$$RWE_i = \frac{E_i}{E_T}, \quad (10)$$

where E_i is an element of the set formed by the union of the energies of the detail coefficients with the energy of the last approximation coefficients ($\{E_{D_1}, E_{D_2}, \dots, E_{D_L}\} \cup \{E_{A_L}\}$). The length of the RWE vector depends on the level of decomposition ($L + 1$), and it is computed for each EEG channel. The final feature vector was the concatenation of all the RWE vectors. These vectors were scaled using min-max scaling to obtain values between zero and one. This scaling method is defined as follows:

$$x' = \frac{x - \min(x)}{\max(x) - \min(x)}, \quad (11)$$

where x is the original feature vector, and x' is the scaled feature vector.

3.5 Classification

This research tested six different classification algorithms to compare and choose the best one for this specific problem and datasets. The reason for choosing these classifiers was that each one is based on a different criterion to make the classification.

- Support Vector Machine (SVM) is known as a “large margin” classifier since it creates a large margin between the data points and its decision boundary. Moreover, this classifier is dependent on its kernel function [156].
- K-Nearest Neighbor (K-NN) is perhaps the most common distance-based classifier; regardless of its simplicity, it can achieve excellent results in lots of tasks [117].
- Random Forest (RF) is an ensemble algorithm based on decision trees. These kinds of algorithms follow the divide-and-conquer approach to improving the performance of its weak classifiers [157].
- Gaussian Naïve-Bayes (GNB) is a statistical classifier based on the Bayes’ Theorem. It is a very fast classification algorithm which performance is related to the independence assumption of the data [158].
- AdaBoost (AB) can be seen as an ensemble algorithm, but it is also known as a boosting classifier. The difference concerning Random Forest is that in the case of AdaBoost, the weak learners are tweaked in favor of those instances misclassified by previous classifiers [119].
- Multilayer Perceptron (MLP) is a biologically inspired classification algorithm. The basis of this algorithm is the connections among neurons represented with weights that are corrected during the training phase [116].

It is worth mentioning that this study just evaluated the closed set recognition, meaning that all testing classes were known at training time [159].

3.5.1 Hyperparameter Optimization

For selecting the hyperparameters of each classifier, this work employed a greedy search optimization. Greedy search optimizes only one hyperparameter at a time while keeping

other hyperparameters fixed [120]. It performs an exhaustive search through a manually specified subset of the hyperparameter space of the learning algorithm. In this work, ten-fold cross-validation was used to guide the performance of the greedy optimization. This optimization was made independently for each dataset. However, the subset of possible values for the hyperparameters was the same for both of them. Additionally, this study just used the five-level DWT for this optimization. Furthermore, in each dataset, 20% of the available data of each subject was selected randomly to perform this step. The subsequent phases did not use this data. Table 5 contains the set of values tested during the greedy search optimization process and the best value of each hyperparameter for each dataset.

Table 5: Set of values for hyperparameter optimization, and best value for each dataset.

Classifier	Hyperparameter	Tested Values	Best Value DEAP dataset	Best Value INAOE dataset
SVM	Penalty Parameter	0.5; 1; 10; 50; 100; 200; 300	300	300
	Kernel	linear; rbf; sigmoid	sigmoid	linear
	Tolerance	1e-7; 1e-6; 1e-5; 1e-3; 0.1; 1	1e-3	0.1
	Kernel coefficient	scale, auto	auto	scale
K-NN	Number of neighbors	1; 5; 10; 20; 50; 100	1	1
	Distance metric	Euclidean; Manhattan	Euclidean	Manhattan
	Leaf size	5; 10; 30; 50; 100	5	5
RF	Number of estimators	1; 10; 50; 100; 200; 500; 750; 1000	500	1000
	Min number of samples required to split an internal node	2; 5; 10; 50; 100	2	2
	Criterion	Gini; Entropy	Gini	Entropy

Classifier	Hyperparameter	Tested Values	Best Value DEAP dataset	Best Value INAOE dataset
GNB	Var smoothing	1e-9; 1e-8; 1e-7; 1e-6; 1e-5; 1e-4; 1e-3; 1e-2, 1e-1, 1, 10	0.1	1e-9
AB	Weak Classifier	SVM; RF	RF	RF
	Number of weak classifiers	5; 10; 50; 100; 500; 800	5	5
	Learning rate	0.1; 0.5; 1; 5	0.1	0.1
	Boosting algorithm	SAMME; SAMME.R	SAMME	SAMME
MLP	Neurons per hidden layer(s)	(106); (106,106); (106,106,106); (84,84); (127,127)	(106)	(127,127)
	Learning rate	1e-3; 5e-3; 0.01; 0.05; 0.1	1e-3	1e-3
	Batch normalization	True, False	True	False
	Dropout	True, False	True	True
	Dropout percentage	10; 20; 30; 40; 50	50	20
	L2 regularization	True, False	True	False
	L2 regularization value	0.01; 0.05; 0.1; 0.5	0.05	NA
Epochs	10; 100; 500	500	500	

3.6 Data Analysis

3.6.1 Performance Metrics

For measuring the performance of the classification algorithms in this multi-class scenario, this work computed the following metrics: Average accuracy (Acc), Macro-averaging Sensitivity (Se), and Macro-averaging Specificity (Sp). The average accuracy measures the effectiveness of a classifier. In contrast, the macro-averaging sensitivity represents the agreement of the data class labels with those predicted by the classifiers.

Finally, the macro-averaging specificity corresponds to the effectiveness of the classifier to identify the class labels [160]. These metrics were calculated with the following equations [161]:

$$Acc = \frac{\sum_{i=1}^l \frac{Tp_i + Tn_i}{Tp_i + Fn_i + Fp_i + Tn_i}}{l}, \quad (12)$$

$$Se = \frac{\sum_{i=1}^l \frac{Tp_i}{Tp_i + Fn_i}}{l}, \quad (13)$$

$$Sp = \frac{\sum_{i=1}^l \frac{Tn_i}{Tn_i + Fp_i}}{l} \quad (14)$$

where l is the number of participants (classes), Tp_i are the true-positive classifications, Tn_i are the true-negative classifications, Fp_i corresponds to the false-positive classifications, and Fn_i corresponds to the false-negative classifications; all of them of the i th participant. For illustrating better these concepts, if participant 1 is using the system, the following scenarios are examples for each of these measures:

- Tp_1 : Signal of participant 1 classified as participant 1.
- Tn_1 : Not signal of participant 1 classified as not participant 1.
- Fp_1 : Not signal of participant 1 classified as participant 1.
- Fn_1 : Signal of participant 1 classified as not participant 1.

The sensitivity and specificity measurements were also used to create a graphic representation of the performance of the classifiers through a Receiver Operating Characteristic (ROC) curve. This performance metric offers a more robust framework for evaluating classifier performance than the traditional accuracy measure. Additionally, it allows performing visual comparisons between the performance of the classifiers [162].

3.6.2 Validation of Experiments

This study executed ten-fold cross-validation with overlapping for validating the results of all the experiments shown in Chapter 4. The experiments used 80% of the available data because the hyperparameter optimization had already utilized the remaining 20%.

The train-test split of the datasets was performed by randomly selecting of 75% of the signals of each subject for training and 25% for testing. This way of splitting the datasets ensured that the same amount of information of each participant was used in the training

and testing phases. Moreover, the information contained in each fold was the same for all the classification algorithms. Figure 19 illustrates the general idea of this validation process.

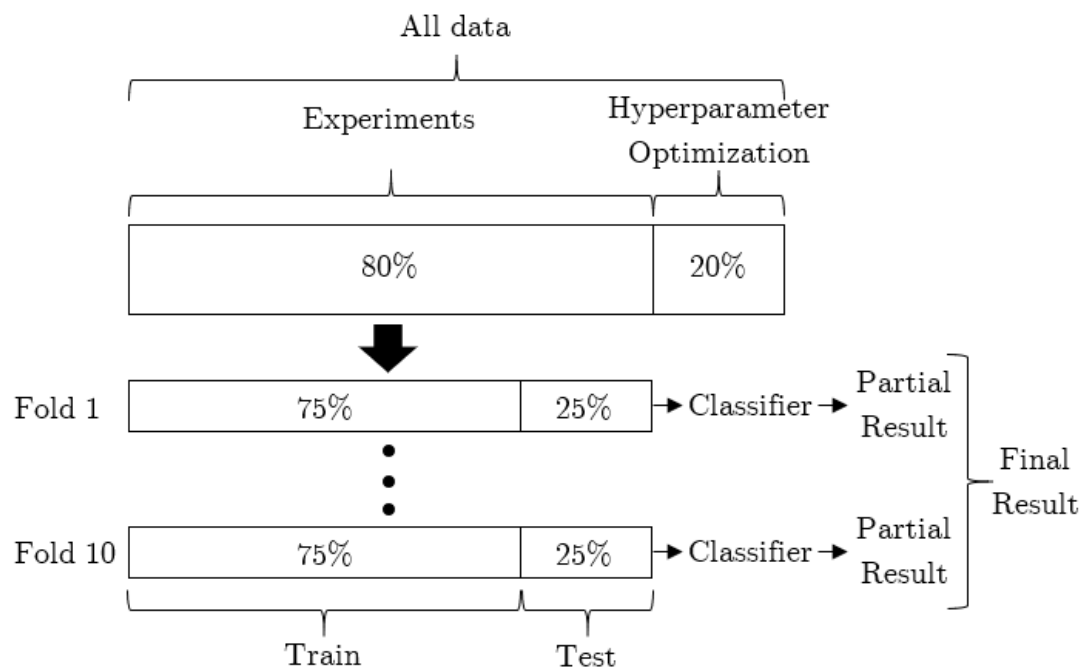


Figure 19: Validation process representation.

3.6.3 Experiments Description

This work conducted three experiments for evaluating the proposed method. Each experiment had the objective of assessing a specific feature of the process. A necessary clarification is that every experiment was performed separately in both datasets. Below is a detailed description of all the experiments.

3.6.3.1 Assessment of Levels of DWT

The objective of this experiment was to assess if there was any statistically significant difference between the decomposition levels of the DWT mentioned previously and select the best one for the following experiments. This experiment was performed using all available EEG recording time.

Each signal of the dataset was decomposed into sub-bands using DWT to calculate the RWE vector. Each feature vector corresponds to a row of the data matrix that was employed to train and test the different classifiers. Figure 20 represents this process. This process was repeated for all the different levels of decomposition. Finally, this work

compared the results obtained by each classifier for selecting the best decomposition level. Figure 21 shows the general workflow of the experiment.

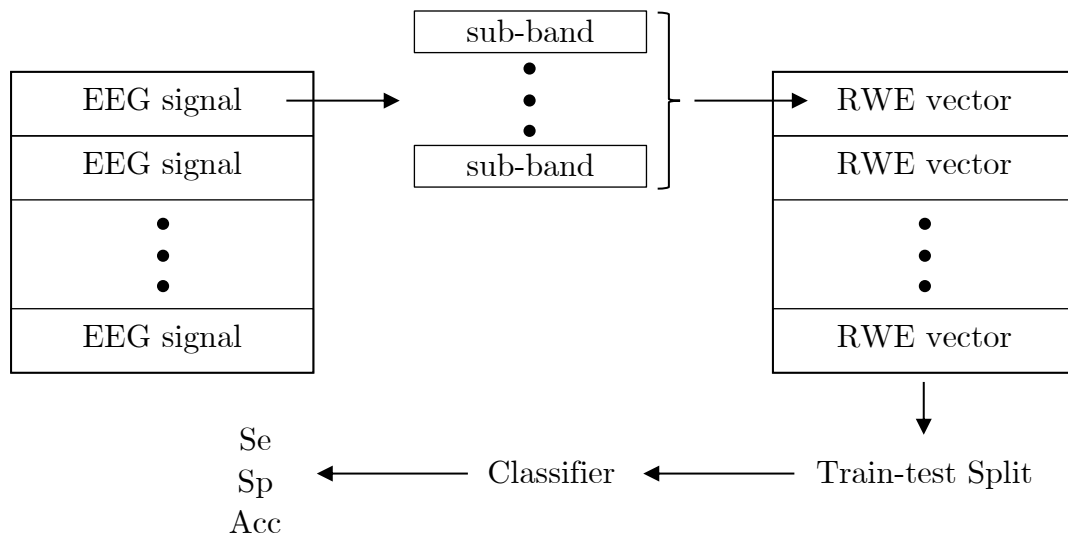


Figure 20: General classification process.

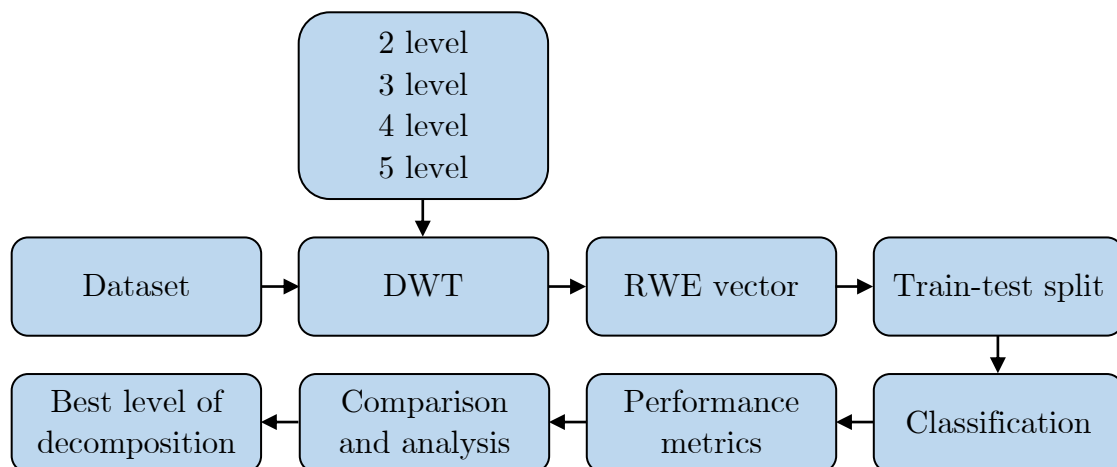


Figure 21: Flowchart for the assessment of levels of DWT.

3.6.3.2 Assessment of Different Recording Times Systematically Selected

The objective of this test was to study the impact that the duration of EEG recordings has on the performance of the system. This experiment only applied the best level of decomposition found in the previous experiment. There was a variation in the process between the two datasets because of the difference in the recording durations of the signals in each one, i.e., 60 seconds on the DEAP dataset and 2.5 seconds on the INAOE dataset.

In the case of DEAP dataset each signal was segmented in the following times: 0.25, 0.5, 1, 2, 4, 6, 8, 10, 20, 30, 40, 50 and 60 seconds. In contrast, the segments used in the INAOE dataset were: 0.25, 0.5, 0.75, 1, 1.25, 1.5, 1.75, 2, 2.25 and 2.5 seconds. In any case, all the segmentations were made from the beginning of each recording. Furthermore, the same preprocessing, feature extraction, and classification process mentioned above were applied to each time segment. Figure 22 shows the general flowchart of this experiment.

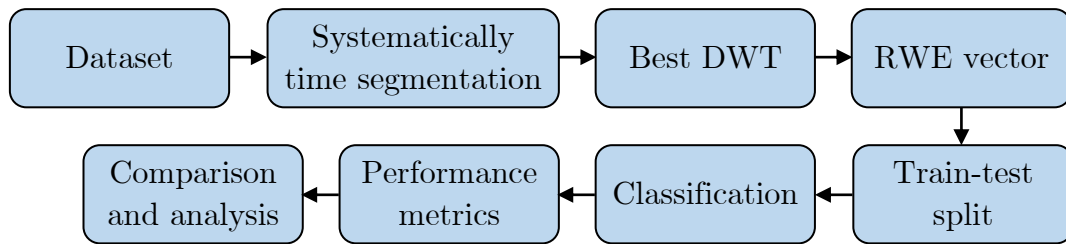


Figure 22: Flowchart for the assessment of different recording times systematically selected.

3.6.3.3 Assessment of Different Recording Times Randomly Selected

This last experiment had the purpose of testing the proposed method in a more realistic scenario since, in the previous experiment, the time segmentation always started from the beginning of the recording. However, in a more realistic scenario, the start of the segmentation should be taken randomly to successfully simulate the differences that may exist between the recordings. In general, this experiment was the same as the previous one, but changing the way the signals were segmented. That is why the only block that changes in Figure 23 concerning Figure 22 is the segmentation step.

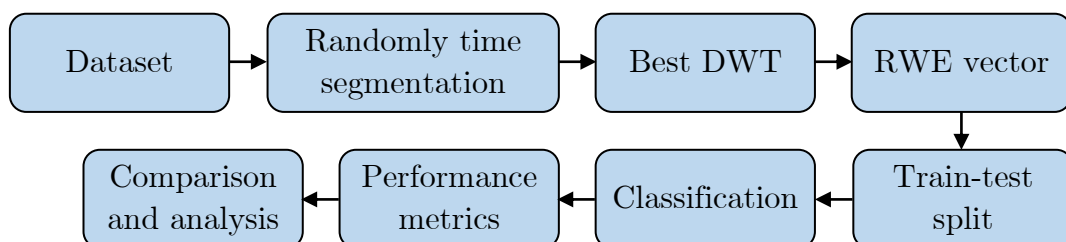


Figure 23: Flowchart for the assessment of different recording times randomly selected.

3.7 Summary

This chapter presented the details of the proposed method. Also, the datasets, preprocessing technique, feature extraction, and classification, including the hyperparameter optimization, were detailed. Likewise, this chapter introduced the performance measures computed in this work and the process for validating the results. Additionally, the goal and description of each experiment were also presented. The performance measures, validation process, and experiment description will be crucial to understand the results presented in Chapter 4.

4 Results

This chapter shows the results obtained in each of the experiments mentioned in Section 3.6.3. For each experiment, the results are presented separately for the two datasets used in this study. In the same way, the analysis of the results is presented independently. Finally, there is a comparison of the proposed system concerning previous works of this topic.

4.1 Assessment of Levels of DWT

4.1.1 Results with DEAP Dataset

Table 6 shows the performance of all classifiers using all available recording time (60 seconds). All the classifiers except for GNB obtained results above 95% in all the performance metrics. In the case of SVM and MLP, the results obtained were very close to 100%. Furthermore, based on these results, the decomposition level does not seem to have a significant impact on the classifiers.

For having a better perception of this impact, Figures 24, 25, and 26 show the performance of each classifier at each level of decomposition. When analyzing these boxplots, they seem to follow the same pattern in which the performance of the classifiers is very similar when using five, four, and three levels of decomposition. Nevertheless, when using two levels, the performance is affected. The results of GNB clearly show this difference between levels.

This work conducted a Multivariate Analysis of Variance (MANOVA) for checking if the difference in the performance of the classifiers caused by the variation in the level of decomposition of the DWT was significant. This analysis executed the Wilks, Pillai, Hotelling-Lawley, and Roy tests [163]. Although each of these tests is different, the p-value obtained in each one was the same, and it was 0.004. As this p-value is less than 0.05, it means that there was a significant difference between the performance of the classifiers and the level of decomposition used during the preprocessing.

Table 6: Results of the assessment of different levels of DWT using the DEAP dataset.

Level of Decomposition	Classifier	Sensitivity	Specificity	Accuracy
2	GNB	75,47±2,31	99,21±0,07	98,47±0,14
	RF	96,02±0,95	99,87±0,03	99,75±0,06
	AB	96,09±0,91	99,87±0,03	99,76±0,06
	KNN	98,01±0,66	99,94±0,02	99,88±0,04
	SVM	99,18±0,54	99,97±0,02	99,95±0,03
	MLP	98,44±0,86	99,95±0,03	99,90±0,05
3	GNB	88,24±1,50	99,62±0,05	99,27±0,09
	RF	98,05±0,58	99,94±0,02	99,88±0,04
	AB	98,05±0,68	99,94±0,02	99,88±0,04
	KNN	98,83±0,30	99,96±0,01	99,93±0,02
	SVM	99,57±0,48	99,99±0,02	99,97±0,03
	MLP	99,57±0,37	99,99±0,01	99,97±0,02
4	GNB	88,44±1,76	99,63±0,06	99,28±0,11
	RF	98,24±0,73	99,94±0,02	99,89±0,05
	AB	98,32±0,58	99,95±0,02	99,90±0,04
	KNN	98,67±0,47	99,96±0,02	99,92±0,03
	SVM	99,49±0,39	99,98±0,01	99,97±0,02
	MLP	99,26±0,51	99,98±0,02	99,95±0,03
5	GNB	87,85±1,70	99,61±0,05	99,24±0,11
	RF	98,28±0,70	99,94±0,02	99,89±0,04
	AB	98,16±0,78	99,94±0,03	99,89±0,05
	KNN	98,36±0,46	99,95±0,01	99,90±0,03
	SVM	99,45±0,43	99,98±0,01	99,97±0,03
	MLP	98,87±0,77	99,96±0,02	99,93±0,05

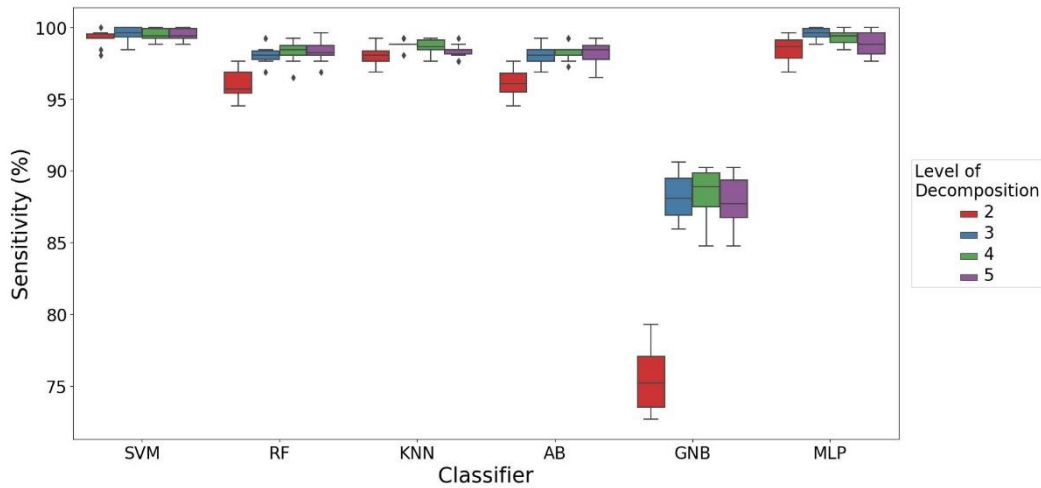


Figure 24: Sensitivity of the classifiers using different decomposition levels with the DEAP dataset.

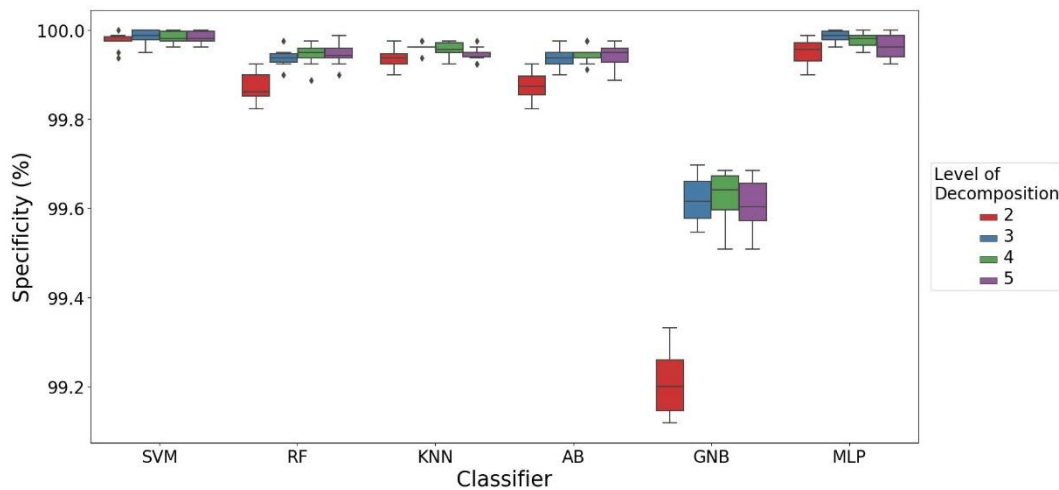


Figure 25: Specificity of the classifiers using different decomposition levels with the DEAP dataset.

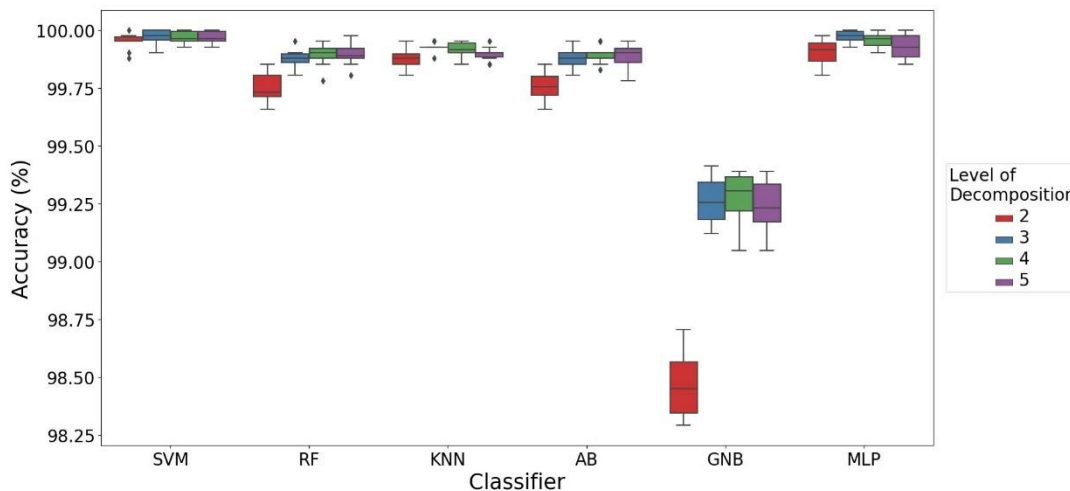


Figure 26: Accuracy of the classifiers using different decomposition levels with the DEAP dataset.

Additionally, a Hotelling's T^2 test was applied to all possible combinations of pairs between the decomposition levels (2-3, 2-4, 2-5, 3-4, 3-5, and 4-5). In each of the tests, the hypotheses were as follows:

- H_0 : The performance of all classifiers using decomposition level A is equal to the performance using decomposition level B.
- H_a : The performance of all classifiers using decomposition level A is different from the performance using decomposition level B.

The p-values obtained in each of the tests are in Table 7; this table shows that in the case of level three regarding levels four and five, the null hypothesis cannot be rejected. The same happens between level four and level five. Nevertheless, the p-value of any test that compares level two is less than or equal to 0.05, meaning that the null hypothesis is rejected. These results confirm the initial result obtained in the MANOVA and the trend observed in the boxplots.

Finally, another MANOVA was performed between the decomposition levels three, four, and five. This analysis resulted in a p-value of 0.484, which is greater than 0.05, indicating that there is no significant difference between these three levels. For this reason, for the following experiments with this dataset, only DWT with three decomposition levels was used since it is the least computationally expensive.

Table 7: Resulting p-values of Hotelling's T^2 tests between different levels of DWT using the DEAP dataset.

Level of decomposition	Level of decomposition			
	2	3	4	5
2	1	0.04	0.05	0.05
3		1	0.71	0.43
4			1	0.73
5				1

4.1.2 Results with INAOE Dataset

The process of extracting results using this dataset was the same as the one detailed for the DEAP dataset. Table 8 shows the performance of the classifiers using 2.5 seconds of

recording, i.e., the maximum time available. In this scenario, GNB was the classifier with the lowest performance; however, SVM had a similar performance. Using this dataset, the classifiers that stood out the most were AB and RF.

Figures 27, 28, and 29 show the boxplots for sensitivity, specificity, and accuracy, respectively. These figures provide a graphical representation of the impact of the different decomposition levels of DWT on the performance of the classifiers. As before, it seems that the only level of decomposition that affects performance is level two. However, when performing a MANOVA to verify said variation, the obtained p-value was 0.6318, indicating that the level of decomposition of DWT does not have any impact on the performance of the classifiers.

Despite the result of the MANOVA, this study applied the same Hotelling's T^2 tests described in Section 4.1.1. Table 9 shows the p-values obtained in each of the tests and, as can be seen, all are greater than 0.05. These p-values verified the result of the MANOVA since the hypothesis of equality of performance between the classifiers using different levels of decomposition could not be rejected. For this reason, the following experiments carried out with this dataset only used a discrete wavelet transform with two levels of decomposition.

Table 8: Results of the assessment of different levels of DWT using the INAOE dataset.

Level of Decomposition	Classifier	Sensitivity	Specificity	Accuracy
2	GNB	65,42±1,64	99,31±0,03	98,64±0,06
	RF	96,00±0,43	99,92±0,01	99,84±0,02
	AB	96,16±0,44	99,92±0,01	99,85±0,02
	KNN	94,09±0,45	99,88±0,01	99,77±0,02
	SVM	67,88±3,78	99,36±0,08	98,74±0,15
	MLP	87,59±2,03	99,75±0,04	99,51±0,08
3	GNB	67,04±1,66	99,34±0,03	98,71±0,07
	RF	97,13±0,60	99,94±0,01	99,89±0,02
	AB	97,16±0,43	99,94±0,01	99,89±0,02
	KNN	95,37±0,41	99,91±0,01	99,82±0,02

Level of Decomposition	Classifier	Sensitivity	Specificity	Accuracy
3	SVM	73,03±4,71	99,46±0,09	98,94±0,18
	MLP	92,01±1,01	99,84±0,02	99,69±0,04
4	GNB	66,59±1,43	99,33±0,03	98,69±0,06
	RF	97,37±0,45	99,95±0,01	99,90±0,02
	AB	97,41±0,46	99,95±0,01	99,90±0,02
	KNN	95,34±0,58	99,91±0,01	99,82±0,02
	SVM	74,05±4,78	99,48±0,10	98,98±0,19
	MLP	92,73±1,15	99,85±0,02	99,71±0,04
5	GNB	64,81±1,14	99,30±0,02	98,62±0,04
	RF	97,63±0,32	99,95±0,01	99,91±0,01
	AB	97,54±0,35	99,95±0,01	99,90±0,01
	KNN	95,25±0,62	99,91±0,01	99,81±0,02
	SVM	75,90±4,48	99,52±0,09	99,05±0,18
	MLP	93,85±0,90	99,88±0,02	99,76±0,04

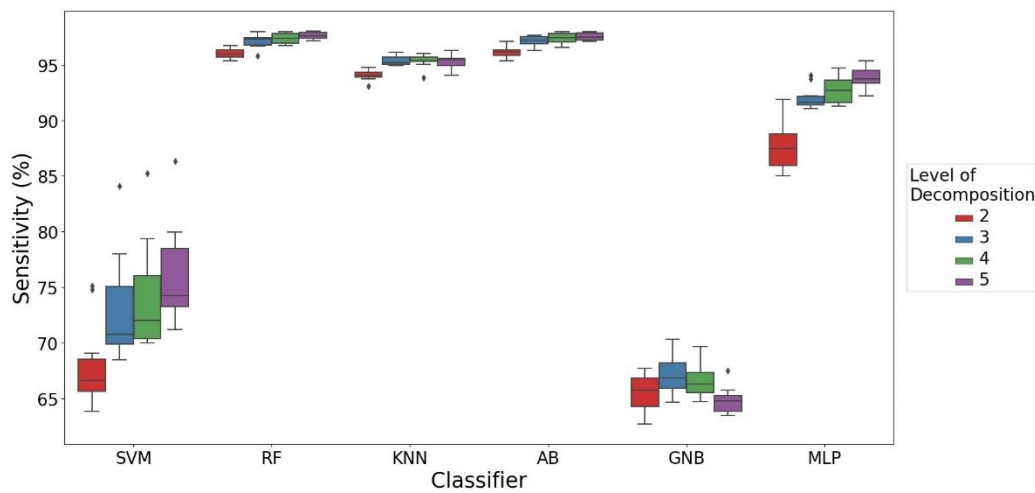


Figure 27: Sensitivity of the classifiers using different decomposition levels with the INAOE dataset.

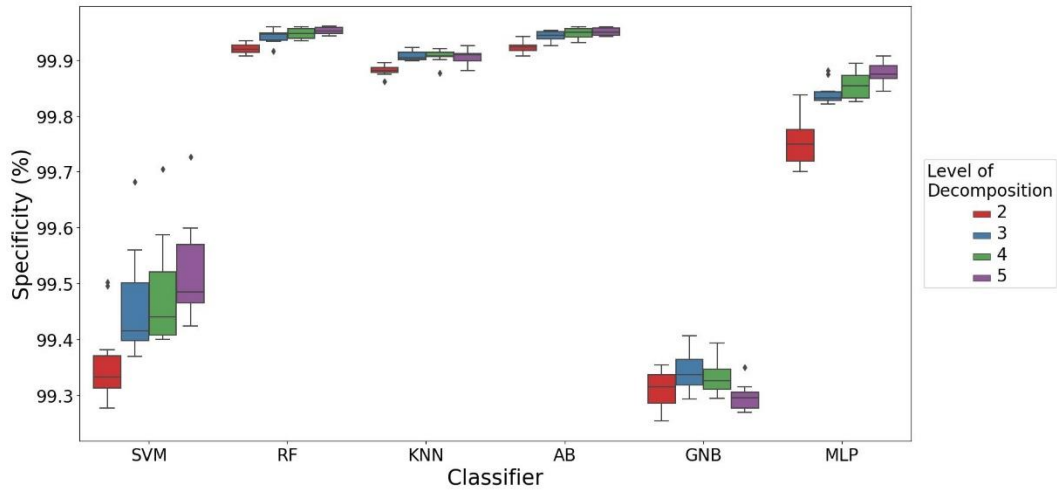


Figure 28: Specificity of the classifiers using different decomposition levels with the INAOE dataset.

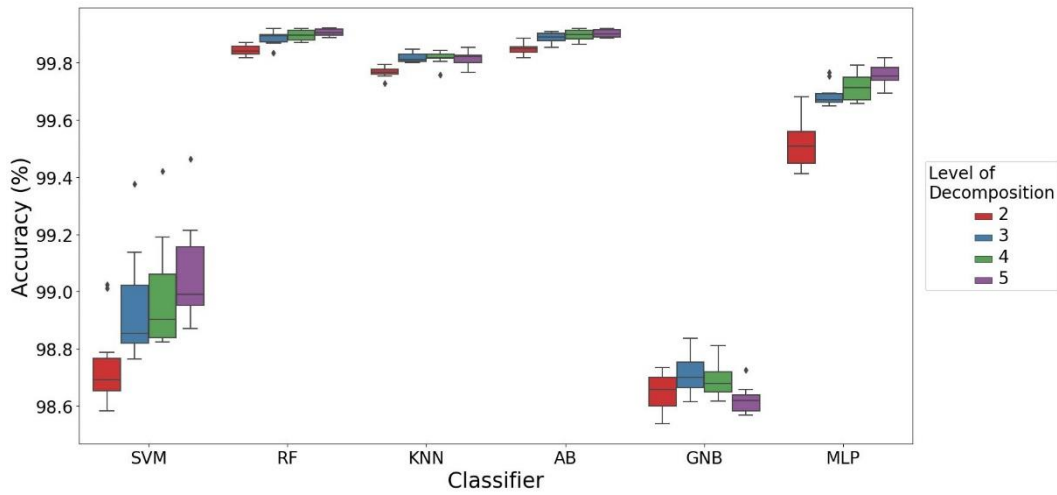


Figure 29: Accuracy of the classifiers using different decomposition levels with the INAOE dataset.

Table 9: Resulting p-values of Hotelling’s T² tests between different levels of DWT using the INAOE dataset.

Level of decomposition	Level of decomposition			
	2	3	4	5
2	1	0.51	0.45	0.61
3		1	0.99	0.58
4			1	0.53
5				1

4.2 Assessment of Different Recording Times Systematically Selected

4.2.1 Results with DEAP Dataset

Appendix A shows the performance of the classifiers using the time segments described in Section 3.6.3.2. This appendix reveals that with 4 seconds of recording, SVM and MLP reached a sensitivity, specificity, and accuracy greater than 90%. On the other hand, the rest of the classifiers, except for GNB, needed 8 seconds of recording to obtain similar results.

Figure 30 shows the initial section of a ROC curve using the time extremes of this experiment, i.e., 0.25 and 60 seconds. This figure allowed to visually checking the impact of the recording time on the performance of the classifiers. It is worth mentioning that the ROC curves are defined for binary classification problems. Therefore, the one-vs-all approach was used in this study, comparing the data of the first participant with all the others.

Additionally, to obtain better interpretability of the results of Appendix A, Figures 31, 32, and 33 show the boxplots of the performance of the classifiers grouped by time. These figures demonstrate that the performance obtained by GNB was below the rest of the classifiers. Also, the significant impact of the recording time over the results of the system was verified again. However, this impact seems to decrease with increasing time since the results obtained with 30, 40, 50, and 60 seconds do not show a significant difference between them as do the results obtained with 0.25, 0.5, 1, and 2 seconds of recording.

For this reason, a Hotelling's T^2 test was applied to the combination of each time segment concerning the total time (0.25-60, 0.5-60, 1-60, 2-60, 4-60, 6-60, 8-60, 10-60, 20-60, 30-60, 40-60, 50-60) to verify if there was a significant difference between using 60 seconds of recording or less. Table 10 shows the p-values obtained in these tests. In this table, using a 95% confidence level, there was no significant difference in the performance of the classifiers using 40, 50, or 60 seconds of recording.

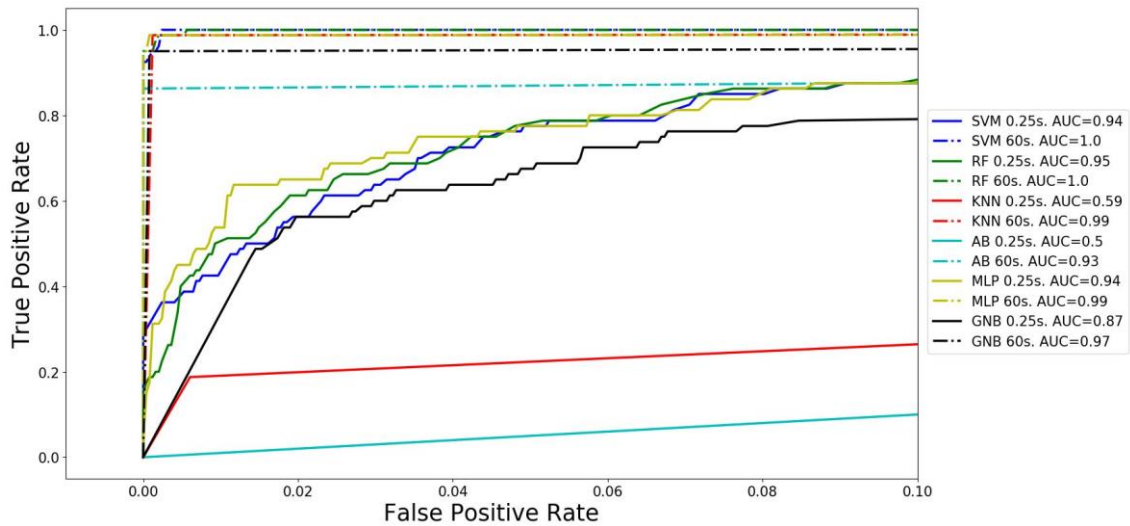


Figure 30: ROC curve of all classifiers using 0.25 and 60 seconds of recording time of the DEAP dataset.

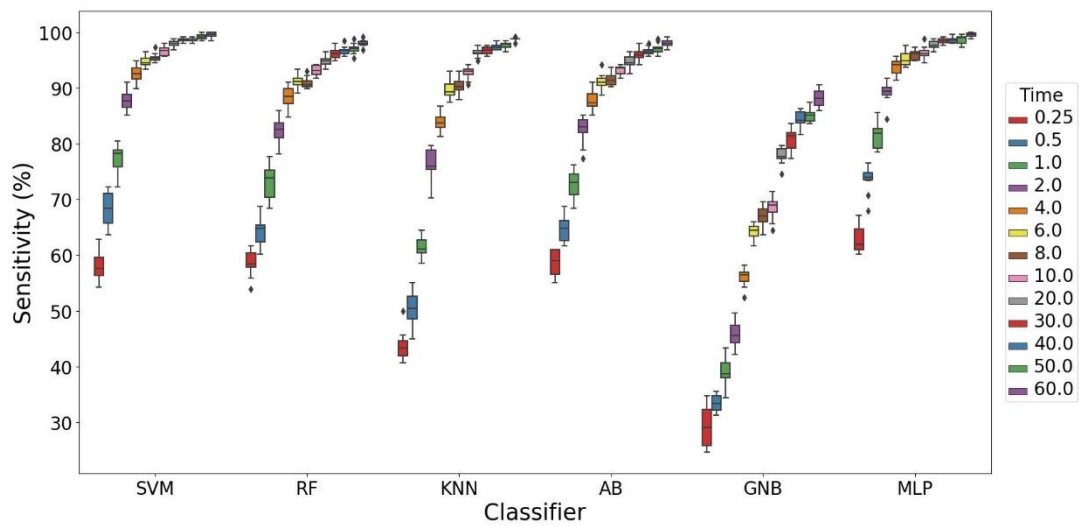


Figure 31: Sensitivity of the classifiers grouped by recording time using the DEAP dataset.

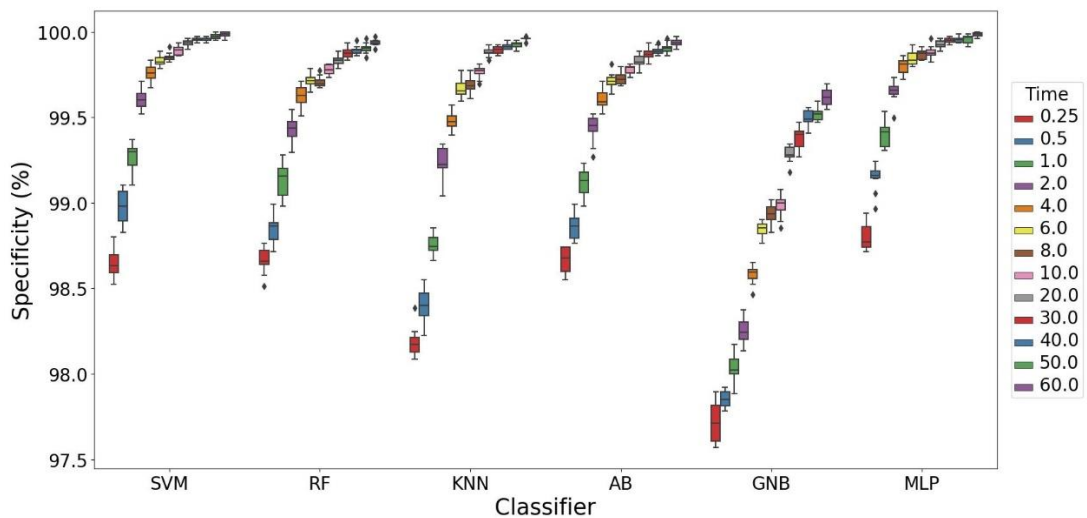


Figure 32: Specificity of the classifiers grouped by recording time using the DEAP dataset.

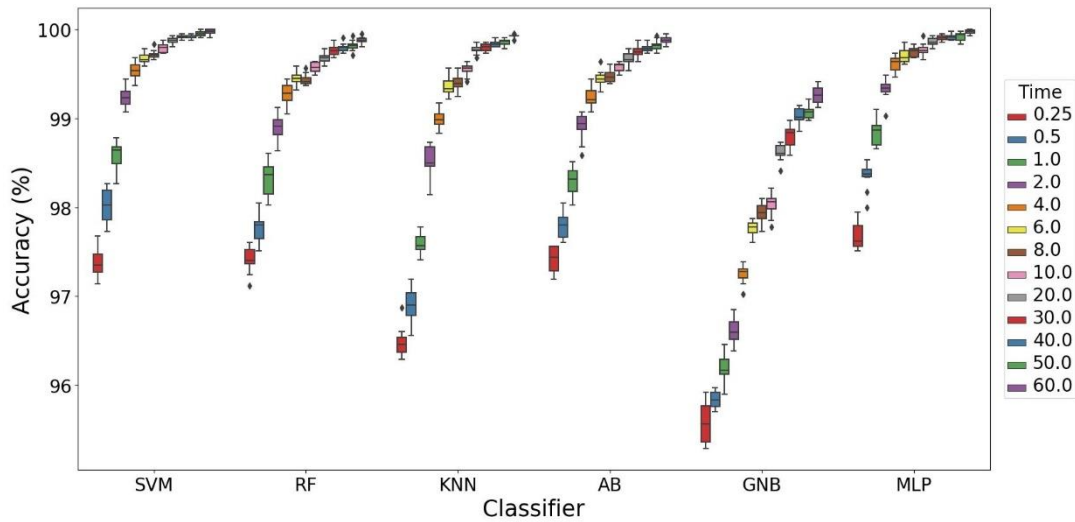


Figure 33: Accuracy of the classifiers grouped by recording time using the DEAP dataset.

Table 10: Resulting p-values of Hotelling’s T^2 tests between the results of each time segment and 60 seconds using the DEAP dataset.

Time segment	p-value
0.25	2.2e-16
0.5	2.2e-16
1	2.2e-16
2	2.2e-16
4	2.2e-16
6	8.6e-12
8	5.3e-11
10	3.1e-6
20	0
30	0.05
40	0.09
50	0.48

A MANOVA was performed with the data corresponding to the 40, 50, and 60 seconds segments to confirm the result mentioned above. The p-value obtained in this test was 0.08973 (> 0.05). This value established that when using this dataset is not necessary to have recordings longer than 40 seconds. Additionally, during this experiment, another

Hotelling's T^2 test was performed between each possible combination of classifier pairs using the data up to 40 seconds due to the previous results; Table 11 shows the p-values of each test. These results revealed that the performance of RF and AB was almost identical. This similarity is because the weak classifier of AB was RF. However, also, there was a high similarity between SVM and MLP. As SVM was the classifier that achieves higher results, it means that either SVM or MLP can be considered as the best one for developing a biometric system based on EEG signals using this dataset.

Table 11: Resulting p-values of Hotelling's T^2 tests between the performance of the classifiers with 40 seconds of recording using the DEAP dataset.

Classifier	Classifier					
	GNB	RF	AB	KNN	SVM	MLP
GNB	1	2.2e-16	2.2e-16	3.5e-13	2.2e-16	2.2e-16
RF		1	0.99	0.04	0.05	0
AB			1	0.02	0.1	0
KNN				1	6.6e-5	2.2e-6
SVM					1	0.8
MLP						1

4.2.2 Results with INAOE Dataset

The overall results of this experiment are presented in Appendix A. This appendix exhibits that with just 1 second of recording, RF and AB got values higher than 90% in all the performance metrics. At the same time, KNN needed 1.75 seconds to achieve similar results. On the other hand, GNB, SVM, and MLP never got sensitivities higher than 90%.

Figure 34 shows a graphical assessment of the performance of the classifiers. This figure corresponds to a ROC curve for all classifiers using 0.25 and 2.5 seconds of recording time. As in the case of the DEAP dataset, the one-vs-all approach was followed.

Figures 35, 36, and 37 analyze the sensitivity, specificity, and accuracy of the results contained in Appendix A. These figures show that SVM and MLP were the most unstable classifiers for this experiment because they have the highest standard deviation. Moreover, they represent the direct impact of the recording time on the performance of

the classifiers. Nevertheless, as in the results of the DEAP dataset, this impact seems to decrease when it is near to the maximum time.

This study applied a Hotelling's T^2 test to each of tested segments of time respecting to 2.5 seconds (0.25-2.5, 0.25-2.5, 0.75-2.5, 1-2.5, 1.25-2.5, 1.5-2.5, 1.5-2.5, 1.75-2.5, 2-2.5, 2.25-2.5) to check whether there was a time segment that produced results that were not statistically different from those of 2.5 seconds. Table 12 contains the resulting p-values of these tests. These values confirmed that the results obtained using 1.75 seconds are not statistically different from the results obtained using 2, 2.25, or 2.5 seconds of recording.

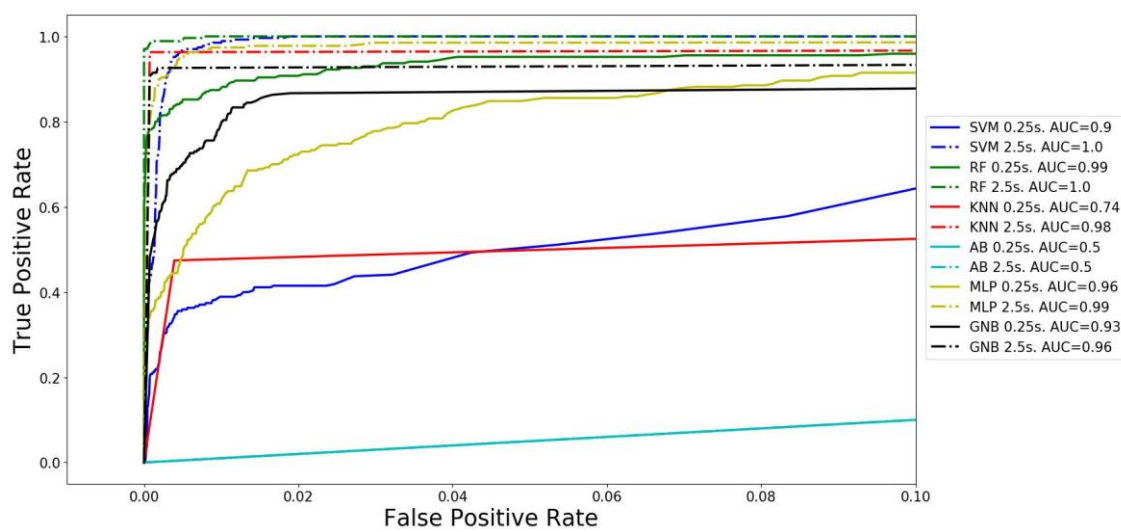


Figure 34: ROC curve of all classifiers using 0.25 and 2.5 seconds of recording time of the INAOE dataset.

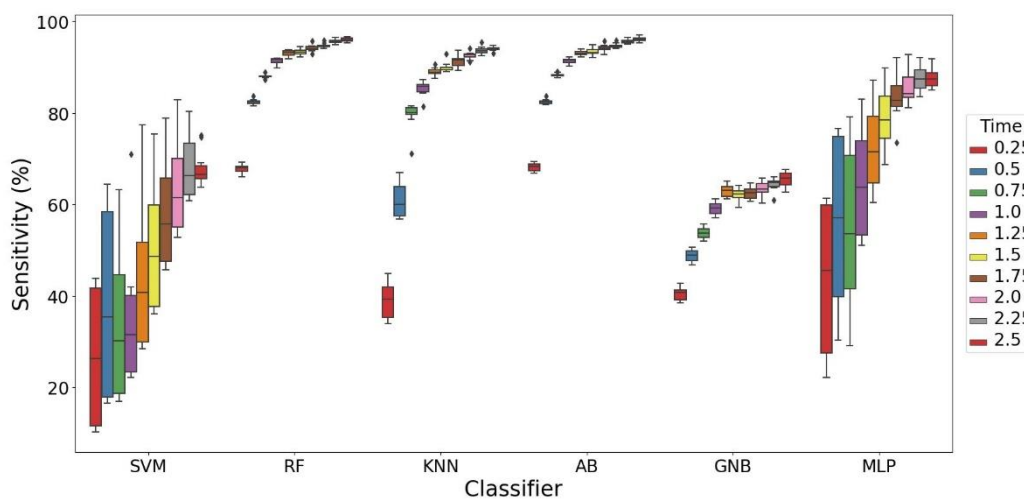


Figure 35: Sensitivity of the classifiers grouped by recording time using the INAOE dataset.

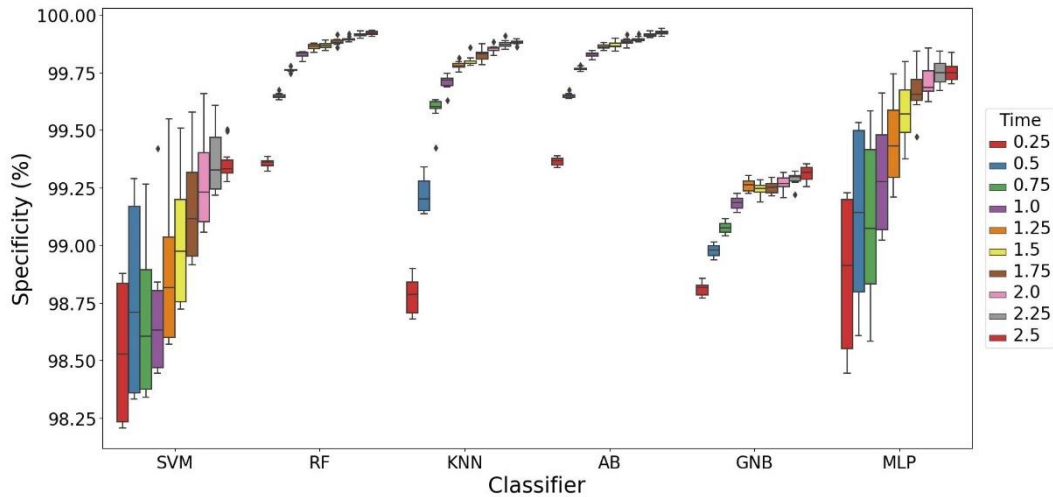


Figure 36: Specificity of the classifiers grouped by recording time using the INAOE dataset.

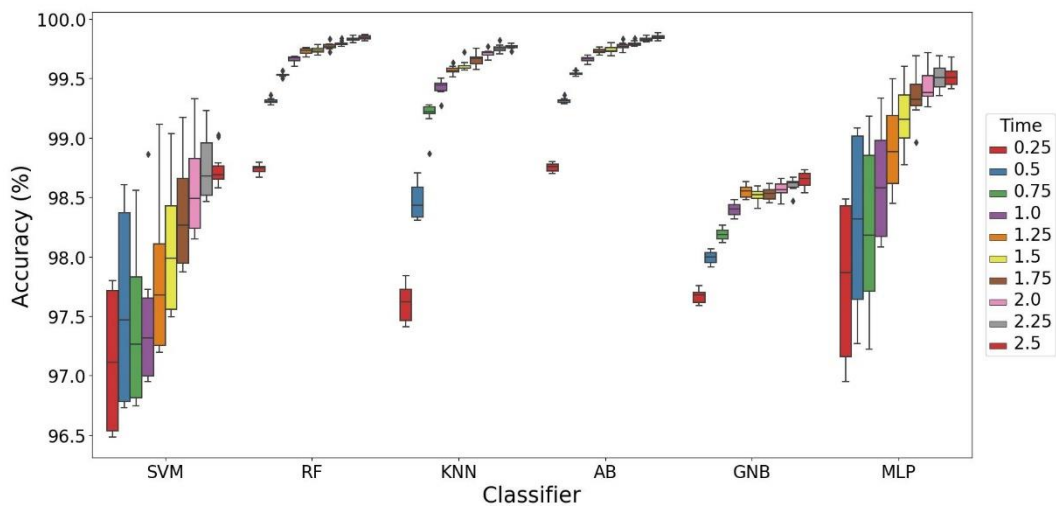


Figure 37: Accuracy of the classifiers grouped by recording time using the INAOE dataset.

Furthermore, a MANOVA was conducted with the classification results of the time segments: 1.75, 2, 2.25, and 2.5. The p-value for this test was 0.09799 (> 0.05), supporting that when using this dataset for developing biometric systems, it is not necessary to have recordings longer than 1.75 seconds.

Finally, Table 13 presents the resulting p-values of the Hotelling’s T^2 tests conducted with all the combinations of classifiers pairs omitting the results of more than 1.75 seconds of recording. These results show that there was no significant difference between the results of RF and AB, but this result was expected because the weak classifier of AB was RF. As AB was the classifier that achieves higher results, it means that either AB or

RF can be considered as the best one for developing a biometric system based on EEG signals using this dataset.

Table 12: Resulting p-values of Hotelling's T^2 tests between the results of each time segment and 2.5 seconds using the INAOE dataset.

Time segment	p-value
0.25	2.2e-16
0.5	8.5e-11
0.75	7.2e-6
1	0
1.25	0.02
1.5	0.05
1.75	0.21
2	0.16
2.25	0.16

Table 13: Resulting p-values of Hotelling's T^2 tests between the performance of the classifiers with 1.75 seconds of recording using the INAOE dataset.

Classifier	Classifier					
	GNB	RF	AB	KNN	SVM	MLP
GNB	1	2.2e-16	2.2e-16	1.1e-13	7.9e-8	0
RF		1	0.82	4.4e-5	2.2e-16	6.2e-14
AB			1	5.6e-6	2.2e-16	5.8e-14
KNN				1	2.2e-16	0
SVM					1	9.1e-11
MLP						1

4.3 Assessment of Different Recording Times Randomly Selected

4.3.1 Results with DEAP Dataset

The performance of the classification algorithms using the same time segments of the previous experiment, but randomly selecting the start of them, is shown in Appendix B. At first glance, the results obtained do not seem to show a significant difference between selecting the time segments from the start of the recording (previous experiment) and selecting the start of the segment randomly (current experiment). Nonetheless, a Hotelling's T^2 test was performed using all the results from all the classifiers obtained in both experiments for verifying this assumption. The p-value obtained in this test was 0.917, demonstrating that there was no significant difference between the performance of the system in a more controlled environment and a more realistic one.

4.3.2 Results with INAOE Dataset

The results of the assessment of different recording times randomly selected are shown in Appendix B. Even though there seems to be no difference between these results and the results of Section 4.2.2, a Hotelling's T^2 test was performed to validate it. The p-value obtained in this test was 0.09278, which is greater than 0.05. This value indicates that the difference between the performance of the classifiers in a more controlled environment (previous experiment) and a more realistic one (current experiment) is not significant.

4.4 Comparison of the Proposed System

Creating a fair comparison of the results obtained in this study with the previous researches in biometric systems based on EEG signals is complicated because of the variety of EEG datasets, features, the number of subjects, and cognitive tasks used [116, 142, 144–147, 164]. Despite these differences, Table 14 presents a short but detailed comparison with the previous related studies. In this table, the results of this work are the sensitivity using three levels of decomposition with 40 seconds in the case of the DEAP dataset and two levels of decomposition with 1.75 seconds in the case of the INAOE dataset.

This table shows that most of the previous studies used the multilayer perceptron as a classification algorithm. However, in the case of the DEAP dataset, the proposed MLP

performed better than previous works. Also, since it was proved that it does not have a significant difference with SVM, this classifier could be used instead due to its lower simplicity. On the other hand, in the results obtained with the INAOE dataset, MLP and SVM were not the best classifiers, but AB reached a sensitivity higher than most of the previous works.

An important fact to take into account while analyzing this comparison is the number of subjects in the datasets and the recording time used. Table 14 contains the number of subjects, but as most of the articles do not include the recording time, this parameter could not be included in this comparison. Nevertheless, in the case of this study, the difference between both databases is 38.25 seconds, which in terms of biometric systems, can be considered a huge difference.

Finally, despite some of the previous studies use the discrete wavelet transform, none of them uses the relative wavelet energy as a feature for the system. Instead, they calculate the mean, standard deviation, or entropy, which are common features for developing biometric systems.

Table 14: Comparison of the present study with previous works related to biometric systems based on EEG analysis.

Study	Year	Subjects	Feature	Classifier	Sensitivity (%)
Hu [164]	2010	3	AR coefficients	MLP	85,00
			Linear complexity		
			Energy spectrum density		
			Energy entropy		
			Phase locking value		
Hu [142]	2010	3	AR coefficients	MLP	92,80
Shedeed [144]	2011	3	DFT and Wavelet mean, std and entropy	MLP	93,00
Gui, Jin, & Xu [145]	2014	32	Wavelet mean, std and entropy	MLP	94,04

Study	Year	Subjects	Feature	Classifier	Sensitivity (%)
Koike-Akino et al. [146]	2016	25	PCA and PLS	QDA	96,70
Zhang, Zhou, & Zeng [116]	2017	20	Gamma-band spectral power ratio	RF	86,00
				MLP	85,10
				KNN	78,00
				AB	73,90
				Bagging	66,70
Saini et al. [147]	2018	70	Gamma-band features	HMM	95,65
This work using DEAP	2020	32	Relative wavelet energy	MLP	98,67
				SVM	98,67
				KNN	97,34
				RF	96,68
				AB	96,60
				GNB	84,45
This work using INAOE	2020	51	Relative wavelet energy	AB	94,22
				RF	94,15
				KNN	91,28
				MLP	83,40
				GNB	62,45
				SVM	57,47

4.5 Summary

This chapter presented the results obtained in each experiment. The first experiment revealed that the decomposition level of the discrete wavelet transform might not have a significant impact on the performance of the classifiers. Subsequently, the analysis performed using different time segments of EEG recording helped to verify that this time has a direct impact on the performance of the classifiers.

Furthermore, during this experiment, the best classifiers for each dataset could be recognized. SVM and MLP were the best in the case of the DEAP dataset, while AB and RF stood out when using the INAOE dataset. On the other hand, the last experiment tested

the proposed system in a more realistic environment. As no significant difference in the performance of the classifiers concerning the experiment with a more controlled environment was found, the efficacy of the proposed method was verified. Finally, this chapter also included a brief comparison between the proposed system in this work and some studies on biometric systems based on EEG signals previously developed.

5 Conclusions and Future Work

This work proposed a biometric system based on the analysis of electroencephalogram signals. The discrete wavelet transform (DWT) served as a preprocessing method for the system. The wavelet relative energy was extracted as a feature, and six different artificial intelligence models were tested to select the best one.

Due to this study used two different datasets, the experimental results showed that the best classifier was different for each of them. Support Vector Machine and Multilayer Perceptron were the best when using the DEAP dataset. On the other hand, when using the INAOE dataset, the best classifiers turned out to be Random Forest and AdaBoost. The difference in the nature of the experiments used during the collection of the EEG signals in each of the datasets might be related to the differences in the best classifiers. However, the proposed methodology managed to obtain classifiers with a sensitivity, specificity, and accuracy greater than 95% using both datasets.

This study was carried out to discover the potential of EEG signals to develop biometric systems because these signals can solve some of the problems of biometrics, such as the verification that the user is alive. The results obtained demonstrated that these bioelectrical signals could be used to create robust biometric systems. Besides, this work analyzed the impact of the level of decomposition of discrete wavelet transform and the recording time on the classifier performance. It is worth mentioning that neither of these analyses has been previously performed.

The experimental results obtained using different levels of decomposition showed that although the state-of-the-art recommends using five or four levels, fewer levels can be used and obtain significantly similar results. Nevertheless, this always depends on the dataset, since in the case of DEAP, only three levels of decomposition were necessary, while for the INAOE dataset, two levels of decomposition were enough.

Furthermore, the results obtained in this study allowed the observation of the effect that the recording time of EEG signals has on the overall performance of the system. A MANOVA and Hotelling's T^2 tests verified this effect. Additionally, these techniques

exhibited that there is a point from which it does not matter if the available time increases, the performance of the system does not vary significantly. Consequently, using 2 seconds of EEG recording can be proposed as a standard for future studies because of the high results achieved with this time.

Finally, thanks to the results of this study, EEG signals should be applied to the development of biometric systems in scenarios where high security is needed, and the portability of the system is not a problem. However, with the development of more portable EEG recording devices, these systems could begin to be used in more common scenarios and gradually replace traditional biometrics.

Some of the limitations found during the development of this study were the lack of public datasets of EEG signals and the lack of own equipment for recording these signals. Most studies in the area of biometric systems based on EEG signals use private datasets. Therefore, accessing datasets with more realistic scenarios or more participants is very difficult, forcing researchers to create their datasets. Even though this work could not create a private dataset due to the lack of necessary materials, it worked with a private dataset of the INAOE.

As future work, an analysis of EEG channels should be performed. The study of channels could reduce the amount of data that the system must process by selecting only the channels that provide valuable information. Also, it could improve the portability of the system. Additionally, thanks to the quick development of Deep Learning, these types of neural networks should be tested for having a more extensive comparison. Likewise, in this work, only the development of unimodal biometric systems based on EEG signals was studied. However, it would be interesting to study the development of multimodal systems using classical signals such as voice, face or fingerprint, and bioelectric signals such as electrocardiograms. These multimodal biometrics could help to decrease the required time of EEG recording and increase the security of the system.

References

- [1] S. Manzoor and A. Selwal, "An Analysis of Biometric Based Security Systems," in *Fifth International Conference on Parallel, Distributed and Grid Computing*, 2018, pp. 306–311.
- [2] P. Saralaya, R. Anjali, G. Shivaprasad, and N. Reddy, "Biometric authentication usage for internet banking," in *2nd IEEE International Conference on Recent Trends in Electronics, Information and Communication Technology*, 2017, pp. 1810–1814.
- [3] S. Prabhakar, S. Pankanti, and A. Jain, "Biometric recognition: Security and privacy concerns," *IEEE Secur. Priv.*, vol. 1, no. 3, pp. 33–42, 2003.
- [4] M. Gomez-Barrero, C. Rathgeb, U. Scherhag, and C. Busch, "Predicting the vulnerability of biometric systems to attacks based on morphed biometric information," *IET Biometrics*, vol. 7, no. 4, pp. 333–341, 2018.
- [5] Z. Rui and Z. Yan, "A Survey on Biometric Authentication: Toward Secure and Privacy-Preserving Identification," *IEEE Access*, vol. 7, pp. 5994–6009, 2018.
- [6] A. Pal, A. K. Gautam, and Y. N. Singh, "Evaluation of bioelectric signals for human recognition," *Procedia Comput. Sci.*, vol. 48, pp. 746–752, 2015.
- [7] A. Christopher, A. Garule, and J. Joy, "Feasibility Study on Building Practical Authentication Systems using Brain Biometrics," in *International Conference on Advances in Computing, Communication and Control*, 2019, pp. 1–5.
- [8] U. Orhan, M. Hekim, and M. Ozer, "EEG signals classification using the K-means clustering and a multilayer perceptron neural network model," *Expert Syst. Appl.*, vol. 38, no. 10, pp. 13475–13481, 2011.
- [9] H. Amin *et al.*, "Feature extraction and classification for EEG signals using wavelet transform and machine learning techniques," *Australas. Phys. Eng. Sci. Med.*, vol. 38, no. 1, pp. 139–149, 2015.
- [10] B. C. Armstrong, M. V. Ruiz-Blondet, N. Khalifian, K. J. Kurtz, Z. Jin, and S. Laszlo, "Brainprint: Assessing the uniqueness, collectability, and permanence of a

- novel method for ERP biometrics,” *Neurocomputing*, vol. 166, pp. 59–67, 2015.
- [11] R. Rao and R. Derakhshani, “A comparison of EEG preprocessing methods using time delay neural networks,” in *2nd International IEEE EMBS Conference on Neural Engineering*, 2005, pp. 262–264.
- [12] G. Kalogiannis, G. Kapsimanis, and G. Hassapis, “An EEG pre-processing technique for the fast recognition of motor imagery movements,” in *IEEE Biomedical Circuits and Systems Conference*, 2016, pp. 90–94.
- [13] D.-X. Zhang, X.-P. Wu, and X. Guo, “The EEG Signal Preprocessing Based on Empirical Mode Decomposition,” in *2nd International Conference on Bioinformatics and Biomedical Engineering*, 2008, pp. 2131–2134.
- [14] Z. Alyasseri, A. Khader, M. Al-Betar, J. Papa, and O. Alomari, “EEG Feature Extraction for Person Identification Using Wavelet Decomposition and Multi-Objective Flower Pollination Algorithm,” *IEEE Access*, vol. 6, pp. 76007–76024, 2018.
- [15] S. Mangalagowri and P. Prasanna, “EEG feature extraction and classification using feed forward backpropagation algorithm for emotion detection,” in *International Conference on Electrical, Electronics, Communication, Computer and Optimization Techniques*, 2017, pp. 183–187.
- [16] W. Azlan and Y. Low, “Feature extraction of electroencephalogram (EEG) signal - A review,” in *IEEE Conference on Biomedical Engineering and Sciences*, 2014, pp. 801–806.
- [17] B. Das, M. Talukdar, R. Sarma, and S. Hazarika, “Multiple Feature Extraction of Electroencephalograph Signal for Motor Imagery Classification through Bispectral Analysis,” *Procedia Comput. Sci.*, vol. 84, pp. 192–197, 2016.
- [18] H. Chan, P. Kuo, C. Cheng, and Y. Chen, “Challenges and Future Perspectives on Electroencephalogram-Based Biometrics in Person Recognition,” *Front. Neuroinform.*, vol. 12, no. October, pp. 1–15, 2018.
- [19] D. Carrion-Ojeda, H. Mejia-Vallejo, R. Fonseca-Delgado, P. Gomez-Gil, and M. Ramirez-Cortes, “A method for studying how much time of EEG recording is needed to have a good user identification,” in *IEEE Latin American Conference on*

- Computational Intelligence*, 2019, pp. 1–6.
- [20] A. K. Jain, A. Ross, and S. Prabhakar, “An Introduction to Biometric Recognition,” *IEEE Trans. Circuits Syst. Video Technol.*, vol. 14, no. 1, pp. 4–20, 2004.
- [21] A. Jain and A. Ross, “Introduction to Biometrics,” in *Handbook of Biometrics*, 1st ed., A. Jain, P. Flynn, and A. Ross, Eds. Springer US, 2008, pp. 1–22.
- [22] M. D. Femila and A. A. Irudhayaraj, “Biometric System,” in *3rd International Conference on Electronics Computer Technology*, 2011, pp. 152–156.
- [23] F. Golshani, “Digital Biometrics,” in *Encyclopedia of Multimedia*, 2nd ed., B. Furht, Ed. Springer, Boston, 2008, pp. 160–165.
- [24] V. Kakkad, M. Patel, and M. Shah, “Biometric authentication and image encryption for image security in cloud framework,” *Multiscale Multidiscip. Model. Exp. Des.*, vol. 2, no. 4, pp. 233–248, 2019.
- [25] A. Adler and S. Schuckers, “Security and Liveness,” in *Encyclopedia of Biometrics*, 1st ed., S. Li, Ed. Springer US, 2009, pp. 1146–1152.
- [26] M. V. N. K. Prasad, J. A. Reddy, and C. R. Rao, “Fingerprint Template Protection Using Multiple Spiral Curves,” in *3rd International Conference on Advanced Computing, Networking and Informatics, Smart Innovation, Systems and Technologies*, 2016, vol. 43, pp. 593–601.
- [27] M. M. H. Ali, V. H. Mahale, P. Yannawar, and A. T. Gaikwad, “Overview of fingerprint recognition system,” in *International Conference on Electrical, Electronics, and Optimization Techniques, ICEEOT 2016*, 2016, pp. 1334–1338.
- [28] M. Abdolahi, M. Mohamadi, and M. Jafari, “Multimodal Biometric System Fusion Using Fingerprint and Face with Fuzzy Logic,” *Int. J. Soft Comput. Eng.*, vol. 2, no. 6, pp. 504–510, 2013.
- [29] I. Mohamed and I. Alhamdani, “Biometric Identification by Fingerprint Image Based Minutiae Detection,” *J. Educ. Sci.*, vol. 22, no. 2, pp. 155–166, 2009.
- [30] C. Ding and D. Tao, “Robust Face Recognition via Multimodal Deep Face Representation,” *IEEE Trans. Multimed.*, vol. 17, no. 11, pp. 2049–2058, 2015.
- [31] Y. Wen, K. Zhang, Z. Li, and Y. Qiao, “A Discriminative Feature Learning

- Approach for Deep Face Recognition,” in *15th European Conference on Computer Vision*, 2016, vol. 9911, pp. 499–515.
- [32] O. M. Parkhi, A. Vedaldi, and A. Zisserman, “Deep Face Recognition,” in *British Machine Vision Conference (BMVC)*, 2015, pp. 41.1-41.12.
- [33] W. Liu, Y. Wen, Z. Yu, M. Li, B. Raj, and L. Song, “SphereFace: Deep Hypersphere Embedding for Face Recognition,” in *2017 IEEE Conference on Computer Vision and Pattern Recognition (CVPR)*, 2017, pp. 6738–6746.
- [34] K. Salton, “LBPH process,” *Face Recognition: Understanding LBPH Algorithm*, 2017. [Online]. Available: <https://towardsdatascience.com/face-recognition-how-lbph-works-90ec258c3d6b>.
- [35] M. Chihaoui, A. Elkefi, W. Bellil, and C. Ben Amar, “A Survey of 2D Face Recognition Techniques,” *Computers*, vol. 5, no. 9, 2016.
- [36] B. Jiang, J. Zhang, B. Deng, Y. Guo, and L. Liu, “Deep Face Feature for Face Alignment and Reconstruction,” pp. 1–11, 2017.
- [37] P. Reid, “Voice Biometric Technologies,” in *Biometrics for Network Security*, 1st ed., Prentice Hall PTR, 2003, pp. 165–176.
- [38] L. Muda, M. Begam, and I. Elamvazuthi, “Voice Recognition Algorithms using Mel Frequency Cepstral Coefficient (MFCC) and Dynamic Time Warping (DTW) Techniques,” *J. Comput.*, vol. 2, no. 3, pp. 138–143, 2010.
- [39] N. P. Patel and A. Kale, “Optimize Approach to Voice Recognition Using IoT,” in *2018 International Conference On Advances in Communication and Computing Technology, ICACCT 2018*, 2018, pp. 251–256.
- [40] K. Chakraborty, A. Talele, and S. Upadhyay, “Voice Recognition Using MFCC Algorithm,” *Int. J. Innov. Res. Adv. Eng.*, vol. 1, no. 10, pp. 2349–2163, 2014.
- [41] C. Estrebou, L. Lanzarini, and W. Hasperué, “Voice recognition based on probabilistic SOM,” in *XXXVI Conferencia Latinoamericana en Informática, At Asunción, Paraguay*, 2010.
- [42] H. Fayek, “Normalized MFCCs,” *Speech Processing for Machine Learning: Filter banks, Mel-Frequency Cepstral Coefficients (MFCCs) and What’s In-Between*,

2016. [Online]. Available: <https://haythamfayek.com/2016/04/21/speech-processing-for-machine-learning.html>.
- [43] S. H. Khan, Z. Khan, and F. Shafait, "Can signature biometrics address both identification and verification problems?," in *12th International Conference on Document Analysis and Recognition, ICDAR*, 2013, pp. 981–985.
- [44] D. R. Shashikumar, K. B. Raja, R. K. Chhotaray, and S. Pattanaik, "Biometric Security System Based on Signature Verification Using Neural Networks," in *IEEE International Conference on Computational Intelligence and Computing Research, ICCIC 2010*, 2010, pp. 88–93.
- [45] Kaggle, "Offline and Online Handwriting," *Predict the trajectory of a handwritten signature*, 2013. [Online]. Available: <https://www.kaggle.com/c/icdar2013-stroke-recovery-from-offline-data/overview/description>.
- [46] D. Bertolini, L. S. Oliveira, E. Justino, and R. Sabourin, "Reducing forgeries in writer-independent off-line signature verification through ensemble of classifiers," *Pattern Recognit.*, vol. 43, no. 1, pp. 387–396, 2010.
- [47] R. Kumar, L. Kundu, B. Chanda, and J. D. Sharma, "A writer-independent off-line signature verification system based on signature morphology," in *First International Conference on Intelligent Interactive Technologies and Multimedia*, 2010, pp. 261–265.
- [48] D. S. Guru and H. N. Prakash, "Online signature verification and recognition: An approach based on symbolic representation," *IEEE Trans. Pattern Anal. Mach. Intell.*, vol. 31, no. 6, pp. 1059–1073, 2008.
- [49] O. Ayurzana, B. Pumbuurei, and H. Kim, "A study of hand-geometry recognition system," in *8th International Forum on Strategic Technology 2013, IFOST 2013*, 2013, vol. 2, pp. 132–135.
- [50] M. Khaliluzzaman, M. Mahiuddin, and M. M. Islam, "Hand Geometry Based Person Verification System," in *International Conference on Innovations in Science, Engineering and Technology (ICISSET)*, 2018, no. 10, pp. 1–6.
- [51] R. Sanchez-Reillo, "Hand Geometry," in *Encyclopedia of Biometrics*, Springer US, 2009, pp. 607–682.

- [52] J. Hashemi and E. Fatemizadeh, "Biometric Identification through Hand Geometry," in *The International Conference on "Computer as a Tool", EUROCON*, 2005, vol. 2, pp. 1011–1014.
- [53] A. K. Singh, A. K. Agrawal, and C. B. Pal, "Hand geometry verification system: A review," in *International Conference on Ultra Modern Telecommunications and Workshops*, 2009, pp. 1–7.
- [54] R. H. Abiyev and K. Altunkaya, "Human iris recognition for biometric identification," in *10th International conference on computer and information technology*, 2007, pp. 1–5.
- [55] I. Sinharoy, "Complexity and uniqueness of human iris. Fine textures on the iris forms unique biometric patterns which are encoded by iris recognition systems," *Primer on iris recognition*, 2014. [Online]. Available: https://indranilsinharoy.com/2014/12/05/dissertation_series/.
- [56] N. Kaur and M. Juneja, "A review on Iris Recognition," in *2014 Recent Advances in Engineering and Computational Sciences, RA ECS 2014*, 2014, pp. 1–5.
- [57] T. Thomas, A. George, and K. P. I. Devi, "Effective Iris Recognition System," *Procedia Technol.*, vol. 25, no. Raerest, pp. 464–472, 2016.
- [58] M. J. Burge and K. W. Bowyer, *Handbook of Iris Recognition*, Second. Springer, 2016.
- [59] A. Harb, M. Abbas, A. Cherry, H. Jaber, and M. Ayache, "Palm print recognition," in *International Conference on Advances in Biomedical Engineering, ICABME 2015*, 2015, pp. 13–16.
- [60] K. Zhang, D. Huang, and D. Zhang, "An optimized palmprint recognition approach based on image sharpness," *Pattern Recognit. Lett.*, vol. 85, pp. 65–71, 2017.
- [61] M. Ali, P. Yannawar, and A. Gaikwad, "Study Of Edge Detection Methods Based On Palmprint lines," in *International Conference on Electrical, Electronics, and Optimization Techniques*, 2016, pp. 1344–1350.
- [62] W. Jia *et al.*, "Palmprint Recognition Based on Complete Direction Representation," *IEEE Trans. Image Process.*, vol. 26, no. 9, pp. 4483–4498, 2017.

- [63] W. Li, L. Zhang, and D. Zhang, "Three dimensional palmprint recognition," in *IEEE International Conference on Systems, Man and Cybernetics*, 2009, no. October, pp. 4847–4852.
- [64] A. S. Anwar, K. K. A. Ghany, and H. Elmahdy, "Human Ear Recognition Using Geometrical Features Extraction," *Procedia Comput. Sci.*, vol. 65, pp. 529–537, 2015.
- [65] M. De Marsico, M. Nappi, and R. Daniel, "HERO: Human Ear Recognition against Occlusions," in *IEEE Computer Society Conference on Computer Vision and Pattern Recognition - Workshops, CVPRW 2010*, 2010, pp. 178–183.
- [66] A. S. Anwar, K. K. A. Ghany, and H. Elmahdy, "Human ear recognition using SIFT features," in *Third World Conference on Complex Systems*, 2015, pp. 1–6.
- [67] L. Yuan and Z. Mu, "Ear recognition based on 2D images," in *First IEEE Conference on Biometrics: Theory, Applications and Systems, BTAS'07*, 2007, no. 1, pp. 1–5.
- [68] A. Pal, A. Gautam, and Y. Singh, "Evaluation of bioelectric signals for human recognition," *Procedia Comput. Sci.*, vol. 48, pp. 746–752, 2015.
- [69] M. Sharma, S. Kacker, and M. Sharma, "A Brief Introduction and Review on Galvanic Skin Response," *Int. J. Med. Res. Prof.*, vol. 2, no. 12, pp. 13–17, 2016.
- [70] N. M. Aleman-Soler, C. M. Travieso, E. Guerra-Segura, J. B. Alonso, M. K. Dutta, and A. Singh, "Biometric approach based on physiological human signals," in *3rd International Conference on Signal Processing and Integrated Networks, SPIN 2016*, 2016, pp. 681–686.
- [71] S. Lynn, C. Watkins, M. Wong, K. Balfany, and D. Feeney, "Validity and Reliability of Surface Electromyography Measurements from a Wearable Athlete Performance System," *J. Sport. Sci. Med.*, vol. 17, no. 2, pp. 205–215, 2018.
- [72] Ch Salud, "Intramuscular Electromyogram," *Qué es un electromiograma*, 2017. [Online]. Available: <https://chsalud.es/blog/electromiograma/que-es-un-electromiograma/>.
- [73] S. N. Abbas and M. Abo-Zahhad, "Eye Blinking EOG Signals as Biometrics," in *Biometric Security and Privacy*, R. Jian, S. Al-maadeed, A. Bouridane, D.

- Crookes, and A. Beghdadi, Eds. Springer, Cham, 2016, pp. 121–140.
- [74] A. Bulling and H. Gellersen, “Toward Mobile Eye-Based Human-Computer Interaction,” *IEEE Pervasive Comput.*, vol. 9, no. 4, pp. 8–12, 2010.
- [75] S. Keshishzadeh and S. Rashidi, “A system of biometric authentication based on ECG signal segmentation,” in *22nd Iranian Conference on Electrical Engineering, ICEE 2014*, 2014, pp. 1873–1877.
- [76] N. Saad, A. Abdullah, and Y. Low, “Detection of Heart Blocks in ECG Signals by Spectrum and Time-Frequency Analysis,” in *4th Student Conference on Research and Development*, 2006, pp. 61–65.
- [77] S. Dubal and V. Bharadi, “Comparative analysis of various approaches for different biometric traits,” in *International Conference & Workshop on Electronics & Telecommunication Engineering*, 2016, pp. 163–168.
- [78] A. Nawrocka and A. Kot, “Methods for EEG signal analysis,” in *12th International Carpathian Control Conference, ICC'2011*, 2011, pp. 266–269.
- [79] J. Kaur and A. Kaur, “A review on analysis of EEG signals,” in *International Conference on Advances in Computer Engineering and Applications, ICACEA 2015*, 2015, pp. 957–960.
- [80] G. Rojas, C. Alvarez, C. Montoya, M. de la Iglesia, J. Cisternas, and M. Gálvez, “Study of resting-state functional connectivity networks using EEG electrodes position as seed,” *Front. Neurosci.*, vol. 12, no. 3, pp. 1–12, 2018.
- [81] S. Vaid, P. Singh, and C. Kaur, “EEG signal analysis for BCI interface: A review,” in *International Conference on Advanced Computing and Communication Technologies, ACCT*, 2015, vol. 2015-April, pp. 143–147.
- [82] J. Li, S. Barma, P. Mak, S. Pun, and M. Vai, “Brain Rhythm Sequencing Using EEG Signals: A Case Study on Seizure Detection,” *IEEE Access*, vol. 7, pp. 160112–160124, 2019.
- [83] R. M. Rangayyan, “Biomedical Signal Analysis: A Case-Study Approach,” in *Biomedical Signal Analysis: A Case-Study Approach*, 1st ed., Wiley-IEEE Press, 2002, p. 552.

- [84] M. Kattke, “The Human Brainwave States,” *The Science of Meditation: A Quantum Crystallography Perspective*, 2020. [Online]. Available: <http://dx.doi.org/10.13140/RG.2.2.25989.09446>.
- [85] A. Ridouh, D. Boutana, and S. Bourenane, “EEG Signals Classification Based on Time Frequency Analysis,” *J. Circuits, Syst. Comput.*, vol. 26, no. 12, pp. 1–26, 2017.
- [86] E. Maiorana, D. La Rocca, and P. Campisi, “On the Permanence of EEG Signals for Biometric Recognition,” *IEEE Trans. Inf. Forensics Secur.*, vol. 11, no. 1, pp. 163–175, 2016.
- [87] S. Sanei and J. Chambers, “Fundamentals of EEG Signal Processing,” in *EEG Signal Processing*, John Wiley & Sons Ltd, 2007, pp. 35–125.
- [88] A. Vallabhaneni, T. Wang, and B. He, “Brain-Computer Interface,” in *Neural Engineering*, Boston: Springer, 2005, pp. 85–121.
- [89] G. Gratton, “Dealing with artifacts: The EOG contamination of the event-related brain potential,” *Behav. Res. Methods, Instruments, Comput.*, vol. 30, no. 1, pp. 44–53, 1998.
- [90] O. Lins, T. Picton, P. Berg, and M. Scherg, “Ocular artifacts in EEG and event-related potentials I: Scalp topography,” *Brain Topogr.*, vol. 6, no. 1, pp. 51–63, 1993.
- [91] W. Zhou and J. Gotman, “Automatic removal of eye movement artifacts from the EEG using ICA and the dipole model,” *Prog. Nat. Sci.*, vol. 19, no. 9, pp. 1165–1170, 2009.
- [92] C. Joyce, I. Gorodnitsky, and M. Kutas, “Automatic removal of eye movement and blink artifacts from EEG data using blind component separation,” *Psychophysiology*, vol. 41, pp. 313–325, 2004.
- [93] R. Azim, S. Amin, S. A. Haque, N. Ambia, and A. Shoeb, “Feature extraction of human sleep EEG signals using Wavelet Transform and Fourier Transform,” in *2nd International Conference on Signal Processing Systems*, 2010, vol. 3, pp. 701–705.
- [94] S. Swee and L. You, “Fast Fourier analysis and EEG classification brainwave

- controlled wheelchair,” in *2nd International Conference on Control Science and Systems Engineering*, 2016, pp. 20–23.
- [95] P. Sarma, P. Tripathi, M. Sarma, and K. Sarma, “Pre-processing and Feature Extraction Techniques for EEG- BCI Applications: A Review of Recent Research,” *ADBU-Journal Eng. Technol.*, vol. 5, pp. 1–8, 2016.
- [96] P. Kumar, R. Arumuganathan, K. Sivakumar, and C. Vimal, “Removal of artifacts from EEG signals using adaptive filter through wavelet transform,” in *9th International Conference on Signal Processing*, 2008, pp. 2138–2141.
- [97] K. Li, G. Sun, B. Zhang, S. Wu, and G. Wu, “Correlation between forehead EEG and sensorimotor area EEG in motor imagery task,” in *Eighth IEEE International Conference on Dependable, Autonomic and Secure Computing*, 2009, pp. 430–435.
- [98] C. Guerrero-Mosquera and A. Navia, “New approach in features extraction for EEG signal detection,” in *Annual International Conference of the IEEE Engineering in Medicine and Biology Society*, 2009, pp. 13–16.
- [99] Y. Wang and S. Makeig, “Predicting Intended Movement Direction Using EEG from Human Posterior Parietal Cortex,” in *International Conference on Foundations of Augmented Cognition*, 2009, no. 7, pp. 437–446.
- [100] C. Vidaurre, N. Krämer, B. Blankertz, and A. Schlögl, “Time Domain Parameters as a feature for EEG-based Brain-Computer Interfaces,” *Neural Networks*, vol. 22, no. 9, pp. 1313–1319, 2009.
- [101] T. Kameswara, M. Rajyalakshmi, and T. Prasad, “An Exploration on Brain Computer Interface and Its Recent Trends,” *Int. J. Adv. Res. Artif. Intell.*, vol. 1, no. 8, pp. 17–22, 2012.
- [102] S. Jirayucharoensak and P. Israsena, “Automatic Removal of EEG Artifacts Using ICA and Lifting Wavelet Transform,” in *International Computer Science and Engineering Conference*, 2013, pp. 136–139.
- [103] M. Kalaivani, V. Kalaivani, and V. Anusuya, “Analysis of EEG Signal for the Detection of Brain Abnormalities,” in *International Conference on Simulations in Computing Nexus*, 2014, pp. 1–6.

- [104] D. Oana and M. Anca, "Comparison of Classifiers and Statistical Analysis for EEG Signals Used in Brain Computer Interface Motor Task Paradigm," *Int. J. Adv. Res. Artif. Intell.*, vol. 4, no. 1, pp. 8–12, 2015.
- [105] H. Maki, T. Toda, S. Sakti, G. Neubig, and S. Nakamura, "EEG signal enhancement using multi-channel wiener filter with a spatial correlation prior," in *IEEE International Conference on Acoustics, Speech and Signal Processing (ICASSP)*, 2015, pp. 2639–2643.
- [106] S. Mason, A. Bashashati, M. Fatourech, K. Navarro, and G. Birch, "A comprehensive survey of brain interface technology designs," *Ann. Biomed. Eng.*, vol. 35, no. 2, pp. 137–169, 2006.
- [107] P. Campisi and D. Rocca, "Brain waves for automatic biometric-based user recognition," *IEEE Trans. Inf. Forensics Secur.*, vol. 9, no. 5, pp. 782–800, 2014.
- [108] M. Poulos, M. Rangoussi, V. Chrissikopoulos, and A. Evangelou, "Parametric person identification from the EEG using computational geometry," in *6th IEEE International Conference on Electronics, Circuits and Systems*, 1999, no. 2, pp. 1005–1008.
- [109] J. Pardey, S. Roberts, and L. Tarassenko, "A review of parametric modelling techniques for EEG analysis," *Med. Eng. Phys.*, vol. 18, no. 1, pp. 2–11, 1996.
- [110] P. Stoica and R. L. Moses, "Basic Concepts," in *Spectral Analysis of Signals*, Upper Saddle River: Pearson Prentice Hall, 2005, pp. 1–21.
- [111] P. Welch, "The use of fast Fourier transform for the estimation of power spectra: A method based on time averaging over short, modified periodograms," *IEEE Trans. Audio Electroacoust.*, vol. 15, no. 2, pp. 70–73, 1967.
- [112] M. Alomari, E. Awada, A. Samaha, and K. Alkamha, "Wavelet-Based Feature Extraction for the Analysis of EEG Signals Associated Wavelet-Based Feature Extraction for the Analysis of EEG Signals Associated with Imagined Fists and Feet Movements," *Comput. Inf. Sci.*, vol. 7, no. 2, pp. 17–27, 2014.
- [113] A. Alariki, A. Ibrahim, M. Wardak, and J. Wall, "A review study of brain activity-based biometric authentication," *Comput. Sci.*, vol. 14, no. 2, pp. 173–181, 2018.
- [114] G. Pressel, I. Gaeris, and L. Rufiner, "Open access database of EEG signals

- recorded during imagined speech,” in *12th International Symposium on Medical Information Processing and Analysis*, 2017, pp. 1–11.
- [115] C. Cortes and V. Vapnik, “Support-Vector Networks,” *Mach. Learn.*, vol. 20, no. 3, pp. 273–297, Sep. 1995.
- [116] Q. Zhang, D. Zhou, and X. Zeng, “Machine Learning-Empowered Biometric Methods for Biomedicine Applications,” *AIMS Med. Sci.*, vol. 4, no. 3, pp. 274–290, 2017.
- [117] U. I. Awan, U. H. Rajput, G. Syed, R. Iqbal, I. Sabat, and M. Mansoor, “Effective Classification of EEG Signals Using K-Nearest Neighbor Algorithm,” in *14th International Conference on Frontiers of Information Technology*, 2016, pp. 120–124.
- [118] L. Breiman, “Random Forests,” *Mach. Learn.*, vol. 45, no. 1, pp. 5–32, 2001.
- [119] H. Rajaguru and S. Prabhakar, “Analysis of adaboost classifier from compressed EEG features for epilepsy detection,” in *International Conference on Computing Methodologies and Communication*, 2017, pp. 981–984.
- [120] P. Matuszyk, R. Castillo, D. Kottke, and M. Spiliopoulou, “A Comparative Study on Hyperparameter Optimization for Recommender Systems,” in *Workshop on Recommender Systems and Big Data Analytics*, 2016, pp. 13–21.
- [121] M. Poulos, M. Rangoussi, V. Chrissikopoulos, and A. Evangelou, “Person identification based on parametric processing of the EEG,” in *6th IEEE International Conference on Electronics, Circuits and Systems*, 1999, vol. 1, pp. 283–286.
- [122] R. Paranjape, J. Mahovsky, L. Benedicenti, and Z. Koles, “The electroencephalogram as a biometric,” in *Canadian Conference on Electrical and Computer Engineering*, 2001, vol. 2, pp. 1363–1366.
- [123] M. Poulos, M. Rangoussi, N. Alexandris, and A. Evangelou, “On the use of EEG features towards person identification via neural networks,” *Med. Inform. Internet Med.*, vol. 26, no. 1, pp. 35–48, 2001.
- [124] R. Palaniappan and P. Raveendran, “Individual identification technique using visual evoked potential signals,” *Electron. Lett.*, vol. 38, no. 25, pp. 1634–1635,

2002.

- [125] R. Palaniappan and R. Paramesran, "Using genetic algorithm to identify the discriminatory subset of multi-channel spectral bands for visual response," *Appl. Soft Comput.*, vol. 2, no. 1, pp. 48–60, 2002.
- [126] R. Palaniappan, "Method of identifying individuals using VEP signals and neural network," *IEE Proc. - Sci. Meas. Technol.*, vol. 151, no. 1, pp. 16–20, 2004.
- [127] K. Ravi and R. Palaniappan, "Neural network classification of late gamma band electroencephalogram features," *Soft Comput.*, vol. 10, no. 1, pp. 163–169, 2005.
- [128] R. Palaniappan, "Electroencephalogram signals from imagined activities: A novel biometric identifier for a small population," *Lect. Notes Comput. Sci. (including Subser. Lect. Notes Artif. Intell. Lect. Notes Bioinformatics)*, vol. 4224, pp. 604–611, 2006.
- [129] G. Mohammadi, P. Shoushtari, B. Ardekani, and M. Shamsollahi, "Person Identification by Using AR Model for EEG Signals," *World Acad. Sci. Eng. Technol.*, vol. 11, no. 2, pp. 281–285, 2006.
- [130] R. Palaniappan and K. Ravi, "Improving visual evoked potential feature classification for person recognition using PCA and normalization," *Pattern Recognit. Lett.*, vol. 27, no. 7, pp. 726–733, 2006.
- [131] R. Palaniappan and D. Mandic, "EEG Based Biometric Framework for Automatic Identity Verification," *J. VLSI Signal Process. Syst. Signal Image. Video Technol.*, vol. 49, no. 11, pp. 243–250, 2007.
- [132] H. Touyama and M. Hirose, "Non-Target Photo Images in Oddball Paradigm Improve EEG-Based Personal Identification Rates," in *30th Annual International Conference of the IEEE Engineering in Medicine and Biology Society*, 2008, pp. 4118–4121.
- [133] R. Palaniappan, "Multiple Mental Thought Parametric Classification: A New Approach for Individual Identification," *World Acad. Sci. Eng. Technol.*, vol. 2, no. 8, pp. 303–306, 2008.
- [134] A. Yazdani, A. Roodaki, S. Rezatofghi, K. Misaghian, and S. Setarehdan, "Fisher Linear Discriminant based person identification using Visual Evoked potentials,"

- in *9th International Conference on Signal Processing*, 2008, pp. 1677–1680.
- [135] A. Riera, A. Soria-Frisch, M. Caparrini, C. Grau, and G. Ruffini, “Unobtrusive biometric system based on electroencephalogram analysis,” *EURASIP J. Adv. Signal Process.*, pp. 1–8, 2008.
- [136] K. Das, S. Zhang, B. Giesbrecht, and M. Eckstein, “Using rapid visually evoked EEG activity for person identification,” in *31st Annual International Conference of the IEEE Engineering in Medicine and Biology Society*, 2009, pp. 2490–2493.
- [137] R. Palaniappan and C. Eswaran, “Using genetic algorithm to select the presentation order of training patterns that improves simplified fuzzy ARTMAP classification performance,” *Appl. Soft Comput.*, vol. 9, no. 1, pp. 100–106, 2009.
- [138] C. Gupta, Y. Khan, R. Palaniappan, and F. Sepulveda, “Wavelet Framework for Improved Target Detection in Oddball Paradigms Using P300 and Gamma Band Analysis,” *Biomed. Soft Computing Hum. Sci.*, vol. 14, no. 2, pp. 63–69, 2009.
- [139] K. Brigham and B. Kumar, “Subject identification from electroencephalogram (EEG) signals during imagined speech,” in *Fourth IEEE International Conference on Biometrics: Theory, Applications and Systems (BTAS)*, 2010, pp. 1–8.
- [140] A. Zúquete, B. Quintela, and J. Silva, “Biometric authentication using electroencephalograms: a practical study using visual evoked potentials,” *Electrónica e Telecomunicações*, vol. 5, no. 2, pp. 185–194, 2010.
- [141] M. Abdullah, K. Subari, J. Loong, C. Loong, and N. Ahmad, “Analysis of the EEG Signal for a Practical Biometric System,” *Int. J. Medical, Heal. Biomed. Bioeng. Pharm. Eng.*, vol. 4, no. 8, pp. 364–369, 2010.
- [142] J. Hu, “Biometric system based on EEG signals: A nonlinear model approach,” in *International Conference on Machine Vision and Human-machine Interface*, 2010, pp. 48–51.
- [143] X. Yang *et al.*, “P300 Wave based Person Identification using LVQ Neural Network,” *J. Conver. Inf. Technol.*, vol. 6, no. 3, pp. 296–302, 2011.
- [144] H. Shedeed, “A new method for person identification in a biometric security system based on brain EEG signal processing,” in *World Congress on Information and Communication Technologies*, 2011, pp. 1205–1210.

- [145] Q. Gui, Z. Jin, and W. Xu, "Exploring EEG-based biometrics for user identification and authentication," in *IEEE Signal Processing in Medicine and Biology Symposium*, 2014, pp. 1–6.
- [146] T. Koike-Akino *et al.*, "High-accuracy user identification using EEG biometrics," in *Annual International Conference of the IEEE Engineering in Medicine and Biology Society (EMBC)*, 2016, pp. 854–858.
- [147] R. Saini *et al.*, "Don't just sign use brain too: A novel multimodal approach for user identification and verification," *Inf. Sci. (Ny)*, vol. 430–431, no. 2, pp. 163–178, 2018.
- [148] S. Koelstra *et al.*, "DEAP : A Database for Emotion Analysis using Physiological Signals," *IEEE Trans. Affect. Comput.*, vol. 3, no. 1, pp. 18–31, 2012.
- [149] A. Zabidi, W. Mansor, Y. Lee, and C. Fadzal, "Short-time Fourier Transform Analysis of EEG Signal Generated During Imagined Writing," in *International Conference on System Engineering and Technology (ICSET)*, 2012, pp. 1–4.
- [150] P. Jahankhani, V. Kodogiannis, and K. Revett, "EEG signal classification using wavelet feature extraction and neural networks," in *IEEE John Vincent Atanasoff 2006 International Symposium on Modern Computing*, 2006, pp. 120–124.
- [151] E. Übeyli, "Combined neural network model employing wavelet coefficients for EEG signals classification," *Digit. Signal Process.*, vol. 19, no. 2, pp. 297–308, 2009.
- [152] A. Subasi, "EEG signal classification using wavelet feature extraction and a mixture of expert model," *Expert Syst. Appl.*, vol. 32, no. 4, pp. 1084–1093, 2007.
- [153] Z. Golrizkhatami and A. Acan, "ECG classification using three-level fusion of different feature descriptors," *Expert Syst. Appl.*, vol. 114, pp. 54–64, 2018.
- [154] T. Gandhi, B. K. Panigrahi, and S. Anand, "A comparative study of wavelet families for EEG signal classification," *Neurocomputing*, vol. 74, no. 17, pp. 3051–3057, 2011.
- [155] A. Hamad, E. Houssein, A. Hassanien, and A. Fahmy, "Feature Extraction of Epilepsy EEG using Discrete Wavelet Transform," in *12th International Computer Engineering Conference*, 2016, pp. 190–195.

- [156] C. Burges, “A Tutorial on Support Vector Machines for Pattern Recognition,” *Data Min. Knowl. Discov.*, vol. 2, pp. 121–167, 1998.
- [157] M. Bicego, “K-Random Forests: A K-means style algorithm for Random Forest clustering,” in *International Joint Conference on Neural Networks*, 2019, pp. 1–8.
- [158] H. Kamel, D. Abdulah, and J. Al-Tuwaijari, “Cancer Classification Using Gaussian Naive Bayes Algorithm,” in *5th International Engineering Conference, IEC 2019*, 2019, pp. 165–170.
- [159] W. Scheirer, A. Rocha, A. Sapkota, and T. Boult, “Towards Open Set Recognition,” *IEEE Trans. Pattern Anal. Mach. Intell.*, vol. 35, no. 7, pp. 1757–1772, 2011.
- [160] G. Canbek, S. Sagiroglu, T. Temizel, and N. Baykal, “Binary Classification Performance Measures/Metrics : A comprehensive visualized roadmap to gain new insights,” in *International Conference on Computer Science and Engineering (UBMK)*, 2017, pp. 821–826.
- [161] M. Sokolova and G. Lapalme, “A systematic analysis of performance measures for classification tasks,” *Inf. Process. Manag.*, vol. 45, no. 4, pp. 427–437, 2009.
- [162] Z.-C. Qin, “ROC analysis for predictions made by probabilistic classifiers,” in *International Conference on Machine Learning and Cybernetics*, 2005, no. 5, pp. 3119–3124.
- [163] C. Ateş, Ö. Kaymaz, H. Kale, and M. Tekindal, “Comparison of Test Statistics of Nonnormal and Unbalanced Samples for Multivariate Analysis of Variance in terms of Type-I Error Rates,” *Comput. Math. Methods Med.*, vol. 2019, pp. 1–8, 2019.
- [164] J. Hu, “Biometric system based on EEG signals by feature combination,” in *International Conference on Measuring Technology and Mechatronics Automation*, 2010, vol. 1, pp. 752–755.

Appendices

A Results of the Assessment of Different Recording Times Systematically Selected

Tables 15 and 16 contain the results of using the DEAP dataset and INAOE dataset, respectively.

Table 15: Results of the assessment of different recording times systematically selected using DEAP dataset.

Time (s)	Classifier	Sensitivity (%)	Specificity (%)	Accuracy (%)
0,25	GNB	29,18±3,38	97,72±0,11	95,57±0,21
	RF	58,52±2,26	98,66±0,07	97,41±0,14
	AB	58,63±2,24	98,67±0,07	97,41±0,14
	KNN	43,75±2,55	98,19±0,08	96,48±0,16
	SVM	57,97±2,42	98,64±0,08	97,37±0,15
	MLP	62,81±2,30	98,80±0,07	97,68±0,14
0,5	GNB	33,52±1,51	97,86±0,05	95,84±0,09
	RF	64,41±2,66	98,85±0,09	97,78±0,17
	AB	64,65±2,20	98,86±0,07	97,79±0,14
	KNN	50,39±2,82	98,40±0,09	96,90±0,18
	SVM	68,12±3,15	98,97±0,10	98,01±0,20
	MLP	73,59±2,42	99,15±0,08	98,35±0,15
1	GNB	38,87±2,45	98,03±0,08	96,18±0,15
	RF	73,01±2,97	99,13±0,10	98,31±0,19
	AB	72,89±2,45	99,13±0,08	98,31±0,15
	KNN	61,33±1,73	98,75±0,06	97,58±0,11
	SVM	77,30±2,27	99,27±0,07	98,58±0,14
	MLP	81,33±2,17	99,40±0,07	98,83±0,14
2	GNB	45,66±2,13	98,25±0,07	96,60±0,13
	RF	82,27±2,34	99,43±0,08	98,89±0,15
	AB	82,50±2,46	99,44±0,08	98,91±0,15

Time (s)	Classifier	Sensitivity (%)	Specificity (%)	Accuracy (%)
2	KNN	76,45±2,80	99,24±0,09	98,53±0,18
	SVM	87,85±1,77	99,61±0,06	99,24±0,11
	MLP	89,14±1,84	99,65±0,06	99,32±0,11
4	GNB	56,02±1,65	98,58±0,05	97,25±0,10
	RF	88,40±1,85	99,63±0,06	99,27±0,12
	AB	87,73±1,70	99,60±0,05	99,23±0,11
	KNN	83,83±1,52	99,48±0,05	98,99±0,10
	SVM	92,58±1,47	99,76±0,05	99,54±0,09
	MLP	93,67±1,35	99,80±0,04	99,60±0,08
6	GNB	64,3±1,31	98,85±0,04	97,77±0,08
	RF	91,17±1,38	99,72±0,04	99,45±0,09
	AB	91,05±1,48	99,71±0,05	99,44±0,09
	KNN	89,69±1,59	99,67±0,05	99,36±0,10
	SVM	94,73±0,84	99,83±0,03	99,67±0,05
	MLP	95,20±1,31	99,85±0,04	99,70±0,08
8	GNB	67,03±1,70	98,94±0,05	97,94±0,11
	RF	90,09±0,97	99,71±0,03	99,43±0,06
	AB	91,48±1,07	99,73±0,03	99,47±0,07
	KNN	90,39±1,30	99,69±0,04	99,40±0,08
	SVM	95,47±0,72	99,85±0,02	99,72±0,05
	MLP	95,98±0,89	99,87±0,03	99,75±0,06
10	GNB	68,44±1,97	98,98±0,06	98,03±0,12
	RF	93,16±0,84	99,78±0,03	99,57±0,05
	AB	93,16±0,77	99,78±0,02	99,57±0,05
	KNN	92,73±1,08	99,77±0,03	99,55±0,07
	SVM	96,64±0,80	99,89±0,03	99,79±0,05
	MLP	96,37±1,08	99,88±0,03	99,77±0,07
20	GNB	77,85±1,48	99,29±0,05	98,62±0,09
	RF	94,88±0,83	99,83±0,03	99,68±0,05
	AB	94,65±1,12	99,83±0,04	99,67±0,07
	KNN	96,37±0,84	99,88±0,03	99,77±0,05
	SVM	97,97±0,52	99,93±0,02	99,87±0,03

Time (s)	Classifier	Sensitivity (%)	Specificity (%)	Accuracy (%)
20	MLP	97,73±0,69	99,93±0,02	99,86±0,04
30	GNB	80,82±1,97	99,38±0,06	98,80±0,12
	RF	96,25±1,01	99,88±0,03	99,77±0,06
	AB	96,05±1,23	99,87±0,04	99,75±0,08
	KNN	96,72±0,66	99,89±0,02	99,79±0,04
	SVM	98,63±0,31	99,96±0,01	99,91±0,02
	MLP	98,48±0,54	99,95±0,02	99,90±0,03
40	GNB	84,45±1,35	99,50±0,04	99,03±0,08
	RF	96,68±0,77	99,89±0,02	99,79±0,05
	AB	96,60±0,74	99,89±0,02	99,79±0,05
	KNN	97,34±0,49	99,91±0,02	99,83±0,03
	SVM	98,67±0,31	99,96±0,01	99,92±0,02
	MLP	98,67±0,56	99,96±0,02	99,92±0,03
50	GNB	85,20±1,24	99,52±0,04	99,07±0,08
	RF	97,03±0,93	99,90±0,03	99,81±0,06
	AB	97,03±0,98	99,90±0,03	99,81±0,06
	KNN	97,70±0,62	99,93±0,02	99,86±0,04
	SVM	99,18±0,44	99,97±0,01	99,95±0,03
	MLP	98,63±0,77	99,96±0,02	99,91±0,05
60	GNB	88,24±1,50	99,62±0,05	99,27±0,09
	RF	98,05±0,58	99,94±0,02	99,88±0,04
	AB	98,05±0,68	99,94±0,02	99,88±0,04
	KNN	98,83±0,30	99,96±0,01	99,93±0,02
	SVM	99,57±0,48	99,99±0,02	99,97±0,03
	MLP	99,57±0,37	99,99±0,01	99,97±0,02

Table 16: Results of the assessment of different recording times systematically selected using INAOE dataset.

Time (s)	Classifier	Sensitivity (%)	Specificity (%)	Accuracy (%)
0,25	GNB	40,49±1,46	98,81±0,03	97,67±0,06
	RF	67,80±0,90	99,36±0,02	98,74±0,04
	AB	68,17±0,84	99,36±0,02	98,75±0,03
	KNN	38,98±3,73	98,78±0,07	97,61±0,15
	SVM	26,84±15,32	98,54±0,31	97,13±0,60
	MLP	43,59±16,68	98,87±0,33	97,79±0,65
0,5	GNB	48,77±1,28	98,98±0,03	97,99±0,05
	RF	82,43±0,55	99,65±0,01	99,31±0,02
	AB	82,51±0,51	99,65±0,01	99,31±0,02
	KNN	60,93±3,75	99,22±0,07	98,47±0,15
	SVM	37,98±20,41	98,76±0,41	97,57±0,80
	MLP	56,23±18,56	99,12±0,37	98,28±0,73
0,75	GNB	53,73±1,19	99,07±0,02	98,19±0,05
	RF	88,02±0,38	99,76±0,01	99,53±0,01
	AB	88,29±0,40	99,77±0,01	99,54±0,02
	KNN	79,43±2,89	99,59±0,06	99,19±0,11
	SVM	33,14±15,80	98,66±0,32	97,38±0,62
	MLP	55,53±16,86	99,11±0,34	98,26±0,66
1	GNB	59,11±1,31	99,18±0,03	98,40±0,05
	RF	91,35±0,72	99,83±0,01	99,66±0,03
	AB	91,37±0,63	99,83±0,01	99,66±0,02
	KNN	85,29±1,52	99,71±0,03	99,42±0,06
	SVM	34,81±14,49	98,70±0,29	97,44±0,57
	MLP	64,38±11,72	99,29±0,23	98,60±0,46
1,25	GNB	63,03±1,28	99,26±0,03	98,55±0,05
	RF	93,04±0,63	99,86±0,01	99,73±0,02
	AB	93,15±0,56	99,86±0,01	99,73±0,02
	KNN	89,04±0,80	99,78±0,02	99,57±0,03
	SVM	43,27±15,26	98,87±0,31	97,78±0,60

Time (s)	Classifier	Sensitivity (%)	Specificity (%)	Accuracy (%)
1,25	MLP	72,36±9,16	99,45±0,18	98,92±0,36
1,5	GNB	62,16±1,34	99,24±0,03	98,52±0,05
	RF	93,35±0,68	99,87±0,01	99,74±0,03
	AB	93,41±0,77	99,87±0,02	99,74±0,03
	KNN	89,92±1,10	99,80±0,02	99,60±0,04
	SVM	50,28±13,30	99,01±0,27	98,05±0,52
	MLP	78,52±6,48	99,57±0,13	99,16±0,25
1,75	GNB	62,45±1,33	99,25±0,03	98,53±0,05
	RF	94,15±0,70	99,88±0,01	99,77±0,03
	AB	94,22±0,73	99,88±0,01	99,77±0,03
	KNN	91,28±1,18	99,83±0,02	99,66±0,05
	SVM	57,47±11,15	99,15±0,22	98,33±0,44
	MLP	83,40±4,66	99,67±0,09	99,35±0,18
2	GNB	63,41±1,70	99,27±0,03	98,57±0,07
	RF	94,76±0,50	99,90±0,01	99,79±0,02
	AB	94,79±0,49	99,90±0,01	99,80±0,02
	KNN	92,59±0,80	99,85±0,02	99,71±0,03
	SVM	63,27±9,71	99,27±0,19	98,56±0,38
	MLP	85,57±3,29	99,71±0,07	99,43±0,13
2,25	GNB	64,40±1,36	99,29±0,03	98,60±0,05
	RF	95,71±0,43	99,91±0,01	99,83±0,02
	AB	95,63±0,44	99,91±0,01	99,83±0,02
	KNN	93,63±0,83	99,87±0,02	99,75±0,03
	SVM	67,89±6,73	99,36±0,13	98,74±0,26
	MLP	87,45±2,69	99,75±0,05	99,51±0,11
2,5	GNB	65,42±1,64	99,31±0,03	98,64±0,06
	RF	96,00±0,43	99,92±0,01	99,84±0,02
	AB	96,16±0,44	99,92±0,01	99,85±0,02
	KNN	94,09±0,45	99,88±0,01	99,77±0,02
	SVM	67,88±3,78	99,36±0,08	98,74±0,15
	MLP	87,59±2,03	99,75±0,04	99,51±0,08

B Results of the Assessment of Different Recording Times Randomly Selected

Tables 17 and 18 contain the results of using the DEAP dataset and INAOE dataset, respectively.

Table 17: Results of the assessment of different recording times randomly selected using DEAP dataset.

Time (s)	Classifier	Sensitivity (%)	Specificity (%)	Accuracy (%)
0,25	GNB	25,90±2,68	97,61±0,09	95,37±0,17
	RF	50,12±2,44	98,39±0,08	96,88±0,15
	AB	48,79±3,21	98,35±0,10	96,80±0,20
	KNN	38,87±1,79	98,03±0,06	96,18±0,11
	SVM	51,68±2,44	98,44±0,08	96,98±0,15
	MLP	59,10±1,85	98,68±0,06	97,44±0,12
0,5	GNB	35,12±2,82	97,91±0,09	95,94±0,18
	RF	63,98±1,30	98,84±0,04	97,75±0,08
	AB	64,26±1,63	98,85±0,05	97,77±0,10
	KNN	50,20±1,87	98,39±0,06	96,89±0,12
	SVM	69,38±3,41	99,01±0,11	98,09±0,21
	MLP	74,02±2,72	99,16±0,09	98,38±0,17
1	GNB	40,23±1,89	98,07±0,06	96,26±0,12
	RF	74,22±2,26	99,17±0,07	98,39±0,14
	AB	74,53±1,89	99,18±0,06	98,41±0,12
	KNN	63,52±1,48	98,82±0,05	97,72±0,09
	SVM	79,73±1,63	99,35±0,05	98,73±0,10
	MLP	82,38±1,56	99,43±0,05	98,90±0,10
2	GNB	48,44±2,20	98,34±0,07	96,78±0,14
	RF	80,51±1,93	99,37±0,06	98,78±0,12
	AB	80,66±1,50	99,38±0,05	98,79±0,09
	KNN	78,55±1,69	99,31±0,05	98,66±0,11
	SVM	88,63±2,19	99,63±0,07	99,29±0,14
	MLP	90,82±0,81	99,70±0,03	99,43±0,05

Time (s)	Classifier	Sensitivity (%)	Specificity (%)	Accuracy (%)
4	GNB	56,76±2,75	98,61±0,09	97,30±0,17
	RF	89,65±1,92	99,67±0,06	99,35±0,12
	AB	89,26±1,86	99,65±0,06	99,33±0,12
	KNN	88,44±1,33	99,63±0,04	99,28±0,08
	SVM	94,10±1,07	99,81±0,03	99,63±0,07
	MLP	94,41±1,25	99,82±0,04	99,65±0,08
6	GNB	61,91±2,45	98,77±0,08	97,62±0,15
	RF	91,17±1,04	99,72±0,03	99,45±0,06
	AB	91,05±1,43	99,71±0,05	99,44±0,09
	KNN	90,23±1,49	99,68±0,05	99,39±0,09
	SVM	94,96±1,63	99,84±0,05	99,69±0,10
	MLP	96,45±1,57	99,89±0,05	99,78±0,10
8	GNB	65,70±1,75	98,89±0,06	97,86±0,11
	RF	91,45±1,77	99,72±0,06	99,47±0,11
	AB	91,64±1,73	99,73±0,06	99,48±0,11
	KNN	92,15±1,61	99,75±0,05	99,51±0,10
	SVM	96,95±1,07	99,90±0,03	99,81±0,07
	MLP	96,91±1,03	99,90±0,03	99,81±0,06
10	GNB	70,86±2,41	99,06±0,08	98,18±0,15
	RF	92,73±1,15	99,77±0,04	99,55±0,07
	AB	92,85±1,22	99,77±0,04	99,55±0,08
	KNN	93,63±1,43	99,79±0,05	99,60±0,09
	SVM	97,27±0,96	99,91±0,03	99,83±0,06
	MLP	97,15±1,09	99,91±0,04	99,82±0,07
20	GNB	78,67±2,24	99,31±0,07	98,67±0,14
	RF	94,65±1,43	99,83±0,05	99,67±0,09
	AB	94,69±1,58	99,83±0,05	99,67±0,10
	KNN	95,78±1,12	99,86±0,04	99,74±0,07
	SVM	97,70±0,88	99,93±0,03	99,86±0,06
	MLP	97,85±0,91	99,93±0,03	99,87±0,06
30	GNB	81,88±1,75	99,42±0,06	98,87±0,11
	RF	95,66±1,25	99,86±0,04	99,73±0,08

Time (s)	Classifier	Sensitivity (%)	Specificity (%)	Accuracy (%)
30	AB	95,98±0,94	99,87±0,03	99,75±0,06
	KNN	97,03±0,99	99,90±0,03	99,81±0,06
	SVM	99,22±0,52	99,97±0,02	99,95±0,03
	MLP	98,09±0,95	99,94±0,03	99,88±0,06
40	GNB	84,69±1,64	99,51±0,05	99,04±0,10
	RF	96,02±1,09	99,87±0,04	99,75±0,07
	AB	95,98±1,08	99,87±0,03	99,75±0,07
	KNN	97,27±0,84	99,91±0,03	99,83±0,05
	SVM	99,26±0,37	99,98±0,01	99,95±0,02
	MLP	98,36±0,67	99,95±0,02	99,90±0,04
50	GNB	87,50±1,25	99,60±0,04	99,22±0,08
	RF	97,34±1,13	99,91±0,04	99,83±0,07
	AB	97,03±0,84	99,90±0,03	99,81±0,05
	KNN	97,73±0,78	99,93±0,03	99,86±0,05
	SVM	99,18±0,56	99,97±0,02	99,95±0,04
	MLP	98,79±0,71	99,96±0,02	99,92±0,04
60	GNB	88,32±1,67	99,62±0,05	99,27±0,10
	RF	97,46±0,77	99,92±0,02	99,84±0,05
	AB	97,46±0,84	99,92±0,03	99,84±0,05
	KNN	98,36±0,78	99,95±0,03	99,90±0,05
	SVM	99,26±0,56	99,98±0,02	99,95±0,04
	MLP	99,06±0,84	99,97±0,03	99,94±0,05

Table 18: Results of the assessment of different recording times randomly selected using INAOE dataset.

Time (s)	Classifier	Sensitivity (%)	Specificity (%)	Accuracy (%)
0,25	GNB	37,39±1,08	98,75±0,02	97,54±0,04
	RF	66,17±1,16	99,32±0,02	98,67±0,05
	AB	66,12±1,42	99,32±0,03	98,67±0,06
	KNN	39,90±2,93	98,80±0,06	97,64±0,11
	SVM	55,72±2,13	99,11±0,04	98,26±0,08
	MLP	66,87±1,57	99,34±0,03	98,70±0,06
0,5	GNB	47,82±1,39	98,96±0,03	97,95±0,05
	RF	80,38±1,05	99,61±0,02	99,23±0,04
	AB	80,27±1,10	99,61±0,02	99,23±0,04
	KNN	65,98±2,48	99,32±0,05	98,67±0,10
	SVM	36,78±6,05	98,74±0,12	97,52±0,24
	MLP	63,25±3,62	99,27±0,07	98,56±0,14
0,75	GNB	52,10±1,71	99,04±0,03	98,12±0,07
	RF	86,33±0,84	99,73±0,02	99,46±0,03
	AB	86,31±0,98	99,73±0,02	99,46±0,04
	KNN	71,50±4,76	99,43±0,10	98,88±0,19
	SVM	54,56±10,04	99,09±0,20	98,22±0,39
	MLP	72,48±5,44	99,45±0,11	98,92±0,21
1	GNB	54,10±1,26	99,08±0,03	98,20±0,05
	RF	89,45±0,56	99,79±0,01	99,59±0,02
	AB	89,56±0,49	99,79±0,01	99,59±0,02
	KNN	81,47±3,65	99,63±0,07	99,27±0,14
	SVM	49,03±6,98	98,98±0,14	98,00±0,27
	MLP	75,40±3,66	99,51±0,07	99,04±0,14
1,25	GNB	58,34±1,82	99,17±0,04	98,37±0,07
	RF	92,08±0,48	99,84±0,01	99,69±0,02
	AB	92,06±0,53	99,84±0,01	99,69±0,02
	KNN	84,98±2,65	99,70±0,05	99,41±0,10
	SVM	61,66±6,79	99,23±0,14	98,50±0,27

Time (s)	Classifier	Sensitivity (%)	Specificity (%)	Accuracy (%)
1,25	MLP	80,46±2,49	99,61±0,05	99,23±0,10
1,5	GNB	60,52±0,99	99,21±0,02	98,45±0,04
	RF	93,88±0,46	99,88±0,01	99,76±0,02
	AB	93,85±0,40	99,88±0,01	99,76±0,02
	KNN	90,28±0,97	99,81±0,02	99,62±0,04
	SVM	62,72±2,30	99,25±0,05	98,54±0,09
	MLP	82,90±2,74	99,66±0,05	99,33±0,11
1,75	GNB	62,29±1,36	99,25±0,03	98,52±0,05
	RF	94,73±0,28	99,89±0,01	99,79±0,01
	AB	94,78±0,34	99,90±0,01	99,80±0,01
	KNN	90,47±2,19	99,81±0,04	99,63±0,09
	SVM	68,49±3,90	99,37±0,08	98,76±0,15
	MLP	85,58±1,39	99,71±0,03	99,43±0,05
2	GNB	64,20±1,39	99,28±0,03	98,60±0,05
	RF	95,57±0,30	99,91±0,01	99,83±0,01
	AB	95,48±0,39	99,91±0,01	99,82±0,02
	KNN	92,27±0,86	99,85±0,02	99,70±0,03
	SVM	73,50±3,41	99,47±0,07	98,96±0,13
	MLP	88,14±1,69	99,76±0,03	99,53±0,07
2,25	GNB	66,09±1,08	99,32±0,02	98,67±0,04
	RF	95,56±0,42	99,91±0,01	99,83±0,02
	AB	95,55±0,40	99,91±0,01	99,83±0,02
	KNN	93,45±0,89	99,87±0,02	99,74±0,04
	SVM	74,24±2,87	99,48±0,06	98,99±0,11
	MLP	89,06±1,28	99,78±0,03	99,57±0,05
2,5	GNB	65,19±1,51	99,30±0,03	98,63±0,06
	RF	95,90±0,38	99,92±0,01	99,84±0,01
	AB	95,85±0,21	99,92±0,00	99,84±0,01
	KNN	94,02±0,71	99,88±0,01	99,77±0,03
	SVM	71,33±3,90	99,43±0,08	98,88±0,15
	MLP	88,97±1,39	99,78±0,03	99,57±0,05